UNIVERSIDADE ESTADUAL DE CAMPINAS

FACULDADE DE ODONTOLOGIA DE PIRACICABA

RAPHAEL CAVALCANTE COSTA

NOVAS ESTRATÉGIAS PARA APRIMORAR AS PROPRIEDADES DE SUPERFÍCIE DO TITÂNIO E CONTROLE DE BIOFILMES RELACIONADOS COM INFECÇÕES PERI-IMPLANTARES

NEWLY STRATEGIES TO ENHANCE TITANIUM SURFACE PROPERTIES AND TO CONTROL BIOFILM-RELATED PERI-IMPLANT INFECTIONS

Piracicaba

2020

RAPHAEL CAVALCANTE COSTA

NOVAS ESTRATÉGIAS PARA APRIMORAR AS PROPRIEDADES DE SUPERFÍCIE DO TITÂNIO E CONTROLE DE BIOFILMES RELACIONADOS COM INFECÇÕES PERI-IMPLANTARES

NEWLY STRATEGIES TO ENHANCE TITANIUM SURFACE PROPERTIES AND TO CONTROL BIOFILM-RELATED PERI-IMPLANT INFECTIONS

Dissertação apresentada à Faculdade de Odontologia de Piracicaba da Universidade Estadual de Campinas como parte dos requisitos exigidos para a obtenção do título de Mestre em Clínica Odontológica, na Área de Prótese Dental.

Dissertation presented to the Piracicaba Dental School of the University of Campinas in partial fulfillment of the requirements for the degree of Master in Dental Clinic, in Prosthodontics area.

Orientador: Prof. Dr. Valentim Adelino Ricardo Barão

ESTE EXEMPLAR CORRESPONDE À VERSÃO FINAL DA DISSERTAÇÃO DEFENDIDO PELO ALUNO RAPHAEL CAVALCANTE COSTA, E ORIENTADA PELO Prof. Dr. VALENTIM ADELINO RICARDO BARÃO.

Piracicaba

2020

Ficha catalográfica
Universidade Estadual de Campinas
Biblioteca da Faculdade de Odontologia de Piracicaba
Marilene Girello - CRB 8/6159

C823n

Costa, Raphael Cavalcante, 1994-
Novas estratégias para aprimorar as propriedades de superfície do titânio e controle de biofilmes relacionados à infecções peri-implantares / Raphael Cavalcante Costa. – Piracicaba, SP : [s.n.], 2020.

Orientador: Valentim Adelino Ricardo Barão.
Dissertação (mestrado) – Universidade Estadual de Campinas, Faculdade de Odontologia de Piracicaba.

1. Biofilmes. 2. Titânio. 3. Osseointegração. I. Barão, Valentim Adelino Ricardo, 1983-. II. Universidade Estadual de Campinas. Faculdade de Odontologia de Piracicaba. III. Título.

Informações para Biblioteca Digital

Título em outro idioma: Newly strategies to enhance titanium surface properties and to control biofilm-related peri-implant infections
Palavras-chave em inglês:
Biofilms
Titanium
Osseointegration
Área de concentração: Prótese Dental
Titulação: Mestre em Clínica Odontológica
Banca examinadora:
Valentim Adelino Ricardo Barão [Orientador]
Cinthia Pereira Machado Tabchory
Carolina Patrícia Aires
Data de defesa: 28-02-2020
Programa de Pós-Graduação: Clínica Odontológica

Identificação e informações acadêmicas do(a) aluno(a)
- ORCID do autor: https://orcid.org/0000-0002-2684-5488
- Currículo Lattes do autor: http://lattes.cnpq.br/5227412843129808

UNIVERSIDADE ESTADUAL DE CAMPINAS
Faculdade de Odontologia de Piracicaba

A Comissão Julgadora dos trabalhos de Defesa de Dissertação de Mestrado, em sessão pública realizada em 28 de fevereiro de 2020, considerou o candidato RAPHAEL CAVALCANTE COSTA aprovado.

PROF. DR. VALENTIM ADELINO RICARDO BARÃO

PROFª. DRª. CAROLINA PATRÍCIA AIRES

PROFª. DRª. CINTHIA PEREIRA MACHADO TABCHOURY

A Ata da defesa, assinada pelos membros da Comissão Examinadora, consta no SIGA/Sistema de Fluxo de Dissertação/Tese e na Secretaria do Programa da Unidade.

DEDICATÓRIA

A **Deus**, pela dádiva da vida, pela saúde, e por me permitir conquistar mais uma etapa. Agradeço pelo seu imenso amor que me faz persistir e perseverar, por mostrar-me que sou capaz de vencer e ultrapassar os obstáculos da vida.

Aos meus pais, **Ednaldo de Sousa Costa** e **Maria das Graças Cavalcante Araújo de Sousa**, pelas inúmeras vezes que abriram mão de seus sonhos para que os meus pudessem ser realizados. Além disso, por suprirem minha vida com amor, cuidado, paciência e ensinamentos. Agradeço ainda pelo incentivo, compreensão e força neste período distante de graduação e pós-graduação. Vocês são meu alicerce e palavras jamais serão capazes de traduzir o meu sentimento, se estou concretizando este sonho é porque tive o apoio de vocês, muito obrigado por tudo. Amo vocês!

Aos meus irmãos, **Ricardo Cavalcante Costa e Renata Cavalcante Costa**, pelo amor, motivação, carinho e por nossa amizade.

AGRADECIMENTOS

À **Universidade Estadual de Campinas – UNICAMP**, na pessoa do Magnífico Reitor, **Prof. Dr. Marcelo Knobel**, pelo meu mestrado nesta instituição.

À **Faculdade de Odontologia de Piracicaba – UNICAMP**, na pessoa do seu Diretor, **Prof. Dr. Francisco Haiter Neto**, pela oportunidade da realização do Programa de Pós-Graduação em Clínica Odontológica.

À Coordenadora Geral da Pós-Graduação **Profa. Dra. Karina Gonzales Silvério Ruiz** e ao Coordenador do Programa de Pós-Graduação em Clínica Odontológica **Prof. Dr. Valentim Adelino Ricardo Barão.**

À **Coordenação de Aperfeiçoamento de Pessoal de Nível Superior – Brasil (CAPES) - Código de Financiamento 001**, pela possibilidade de realizar este curso de pós-graduação.

À **Fundação de Amparo à Pesquisa do Estado de São Paulo (FAPESP)**, pela concessão de bolsa de estudo no período de setembro de 2018 a agosto de 2020, **processo nº 2018/04630-2**, fundamental para o desenvolvimento desta pesquisa.

Ao meu orientador, **Prof. Dr. Valentim Adelino Ricardo Barão**, pela oportunidade de ser um dos seus orientandos e por todo apoio e entusiasmo com que me recebeu. Muito obrigado por estar sempre presente, atuando de forma resolutiva e crítica, sendo um verdadeiro exemplo de professor, pesquisador e orientador. Agradeço também pela compreensão diante das minhas limitações e por sempre me incentivar a crescer cada vez mais. As oportunidades proporcionadas foram únicas e acredito que dificilmente serei capaz de retribuir toda essa confiança, por esse motivo deixo expressa a minha sincera gratidão.

Ao **Laboratório de Plasmas Tecnológicos da Universidade Estadual Paulista "Júlio de Mesquita Filho" – UNESP (Campus de Sorocaba)**, representado pelo **Prof. Dr. Nilson Cristino da Cruz** e pela **Profa. Dra. Elidiane Cipriano Rangel** pela parceria no desenvolvimento da superfície experimental avaliada neste estudo.

Ao **Laboratório de Bioquímica Oral da FOP – UNICAMP**, representado pelo **Prof. Dr. Jaime Aparecido Cury** pela disponibilização da área de microbiologia para realização dos ensaios microbiológicos.

Ao **Centro de Microscopia e Imagens da FOP-UNICAMP**, representado pelo **Prof. Pedro Duarte Novaes** pela disponibilização dos microscópios eletrônico de varredura (MEV) e microscópio confocal de varredura a laser (CLSM).

Ao **Laboratório de Pesquisa Clínica em Odontologia da UnG**, representado pela **profa. Magda Feres** pela disponibilidade e contribuições nas análises de Checkerboard DNA-DNA hybridization.

Ao **Brazilian Nanotechnology National Laboratory – LNNano do Centro Nacional de Pesquisa em Energia e Materiais - CNPEM**, pela contribuição no desenvolvimento das análises de CLSM deste trabalho.

Ao **Centro de Energia Nuclear na Agricultura (CENA) – Laboratório de Química Analítica**, pela contribuição nas análises de ICP-OES realizadas neste trabalho.

Ao **Laboratório de Tribologia e Compósitos da USP São Carlos**, representado pelo **Prof. Dr. Carlos Alberto Fortulan** pela contribuição nas análises tribológicas realizadas neste trabalho.

Ao **Instituto de Física Gleb Wataghi da UNICAMP**, representado pelo **Prof. Dr. Richard Landers**, pela contribuição com as análises de XPS.

Aos docentes **Profa. Dra. Altair Del Bel Cury, Prof. Dra. Renata Cunha Matheus Rodrigues Garcia, Prof. Marcelo Ferraz Mesquita, Prof. Dr. Wander José da Silva** e **Prof. Dr. Antônio Pedro Ricomini Filho** por todo o conhecimento compartilhado.

Aos técnicos **Eduardo Pinez - Laboratório de Prótese Total da FOP-UNICAMP**, **Alfredo José da Silva – Laboratório Bioquímica Oral da FOP-UNICAMP**, **Gislaine Regina Alves Piton – Laboratório de Prótese Parcial Removível**

da FOP-UNICAMP, Adriano Luis Martins – Laboratório de Microscopia, Lidiane e Fátima – Laboratório de Química Analítica CENA/USP e ao Lucas, Gustavo e Larissa- Laboratório de Plasmas Tecnológicos da UNESP/Sorocaba pela solicitude e prontidão em ajudar sempre que necessário.

À secretária do **Departamento de Prótese e Periodontia da FOP - UNICAMP**, **Sra. Eliete Aparecida Ferreira Marin**, pela atenção, solicitude e gentileza.

Aos professores **Dra. Vanessa Cavalli Gobbo, Dra. Érica Dorigatti de Avila e Dr. João Gabriel Silva Sousa** pela disponibilidade em participar da banca de qualificação e as professoras **Dra. Cinthia Pereira Machado Tabchoury** e **Dra. Carolina Patrícia Aires** pela participação na banca de defesa, contribuindo grandiosamente com este trabalho de dissertação de mestrado.

A todos os meus amigos do **Laboratório de Prótese Total** B**runa Egumi Nagay**, **Carolini Dini, Jairo Matozinho Cordeiro, João Gabriel Silva Souza**, **Guilherme Almeida Borges, Letícia Del Rio**, **Daniele Valente Veloso, Thaís Barbin , Heloísa Navarro Pantaroto**, **Thamara Beline e Anna Gabriella Camacho Presotto** pela convivência, amizade e conhecimentos compartilhados.

Em especial à **Jairo Matozinho Cordeiro, Bruna Egumi Nagay, Guilherme Almeida Borges, Caroline Dini e João Gabriel Silva Souza** pelo carinho e por dividirem comigo mais que um grupo de pesquisa, momentos de felicidade e aprendizado. O tempo nos transformou em uma equipe da qual me orgulho imensamente de fazer parte. Vocês fizeram essa trajetória mais suave, sendo modelo de amizade e companheirismo. Levarei nossas memórias (e do "PEU com U") com muito amor em meu coração.

Aos meus amigos do Laboratório de Bioquímica Oral, em especial à **Juliana Campos, Débora Rocha, Bárbara Oliveira, Aline Soares, Luis Fernando e Robson Silva** por dividirem comigo grande parte das etapas realizadas neste trabalho. Guardarei carinhosamente todos os nossos momentos vividos.

Aos amigos conquistados durante a pós-graduação, em especial **Rodrigo Barros Estevans Lins, Mariana Barbosa Arruda Câmara, Olivia Maria Costa de**

Figueiredo, Mayara Abreu Pinheiro, Catharina Marques Sacramento, Tamires Pereira Dutra e Thayane Cerquiare Businari. Obrigado pela amizade, apoio e bons momentos.

As minhas "rommates" do apt. 53, **Mariana Marinho Davino de Medeiros** e **Loyse Martorano Fernandes** e ao **Fábio Oliveira Furlan** por serem a minha família longe de casa. Vocês estavam comigo em cada etapa, feliz ou triste, e se mantiveram sempre de braços abertos. Levarei cada lembrança com muito carinho!

As minhas queridas amigas da UFPB, **Karla Lorene França Leit**e, **Priscila Sarmento Pinto e Lays Nóbrega Gomes**, por acreditarem no meu potencial e sempre me incentivarem durante todo o processo de pós-graduação. Agradeço por todos os bons momentos compartilhados em cada retorno à Paraíba.

À minha família e a todos que, direta ou indiretamente, contribuíram para a realização desse trabalho.

Muito obrigado!

RESUMO

A osseointegração deficiente na interface osso/implante e as infecções peri-implantares são as principais causas relacionadas com as falhas das reabilitações com implantes dentários a base de titânio (Ti). Considerando estes fatores etiológicos, estratégicas terapêuticas estão sendo desenvolvidas visando aumentar as taxas de sucesso das reabilitações orais com implantes. Dentre estas abordagens, os tratamentos de superfície têm um papel promissor para aplicações biomédicas por tornar a superfície do Ti mais bioativa e aprimorar o processo de osseointegração. Portanto, (1) o primeiro estudo objetivou desenvolver um tratamento de superfície experimental (PEO-BG) baseado em 45S5-bioglass (45% SiO_2, 245% CaO, 24.5% NaO e 6% P_2O_5) utilizando o plasma eletrolítico de oxidação (PEO) como nova via para incorporação no Ti. As propriedades de superfície, mecânicas, tribológicas, eletroquímicas, microbiológicas e biológicas foram avaliadas. O recém-desenvolvido PEO-BG mostrou alta rugosidade e área de superfície determinando uma topografia de superfície complexa, status super-hidrofílico, composição química e camada de óxido mimética ao 45S5-BG. O revestimento experimental aprimorou as propriedades mecânicas e tribológicas ($p<0,05$) e melhorou a resistência à corrosão após degradação simulada *in vitro* (28 dias) ($p<0,05$). O revestimento PEO-BG também foi capaz de modular a adesão microbiana (2 h) e a formação de biofilme oral (24 h) alterando o perfil bacteriano e reduzindo o potencial patogênico ($p<0,05$). Além disso, o novo revestimento pode ser considerado bioativo devido a capacidade de induzir a formação de hidroxiapatita partir da liberação progressiva de íons com consequente aumento do pH. Em adição, PEO-BG favoreceu a maior adsorção de proteínas plasmáticas do sangue humano sem apresentar toxicidade para fibroblastos, o que sugere efeitos biológicos promissores *in vivo*. Além das falhas da osseointegração, superfícies de implantes também são suceptíveis ao acúmulo crônico de biofilmes poli-microbianos que são imersos em uma matriz extracelular (ME). A ME atua como uma barreira protetora e torna dificil o controle do biofilme e tratamento das infecções peri-implantares. Desta forma, (2) o segundo estudo avaliou por um modelo *in vitro* que simula o processo de transição da peri-implantite (biofilme supragengival para subgengival) o papel da ME na patogenicidade do biofilme oral e na resistência contra antimicrobianos na superfície do Ti. Além disso, foi testada uma estratégia terapêutica combinada utilizando um emergente agente de desestruturação da matriz (iodo povidine)

associado com antibióticos em biofilmes formados *in situ* na cavidade oral. Identificou-se que ME leva a disbiose do biofilme oral, aumentando a virulência bacteriana e o dano as células do hospedeiro ($p<0,05$). Adicionalmente, a ME também aumentou a resistência antimicrobiana de biofilmes na superfície do Ti ($p<0,05$). Assim, a abordagem de duplo direcionamento reduziu a formação de biofilme oral aumentando a eficácia de antimicrobianos direcionados para peri-implantite ($p<0,05$). Conclui-se que, tratamentos de superfícies bioativos, como o recém desenvolvido PEO-BG que melhora as propriedades de superfície do Ti, buscando aprimorar a osseointegração e aumentar a longevidade dos tratamentos com implantes dentários, assim como, a recente estratégia combinada visando a degradação da ME é uma estratégia eficaz e promissora para controle do biofilme e tratamento não-cirúrgico da peri-implantite.

Palavras-chave: Biofilme, Titânio, Osseointegração, Modificações de superfície, Bioglass

ABSTRACT

The decreases osseointegration at the bone/implant interface and peri-implant infections are the main causes related to failures in rehabilitation with titanium (Ti) based dental implants. Considering these etiological factors, therapeutic strategies have been developed recently aiming to increase the success rates of implant rehabilitation. Among these approaches, surface treatments have a promising role for biomedical applications due to the ability to able the Ti surface more bioactive and improve the osseointegration. Thus, (1) the first study aimed to develop a surface treatment (PEO-BG) based on 45S5-bioglass (45% SiO2, 245% CaO, 24.5% NaO and 6% P2O5) using plasma electrolytic oxidation (PEO) as a new route for incorporation on Ti. The surface, mechanical, tribological, electrochemical, microbiological and biological properties were evaluated. The newly developed PEO-BG showed high roughness and surface area determining a complex surface topography, super-hydrophilic status, chemical composition and oxide layer mimetic to the 45S5-BG. Experimental coating improved the mechanical and tribological properties ($p<0.05$) and enhanced the corrosion resistance after simulated in vitro degradation (28 days) ($p<0.05$). The PEO-BG coating was also able to modulate microbial adhesion (2 h) and the formation of oral biofilm (24 h), changing the bacterial profile and reducing the pathogenic potential ($p<0.05$). Furthermore, developed coating can be considered bioactive due to hydroxyapatite-inducing ability with progressive release of bioactive ions and increase of pH. In addition, PEO-BG favored greater adsorption of plasma proteins from human blood without presenting toxicity to fibroblasts, which suggests promising biological effects in vivo. Another relevant point is that implant surfaces are also susceptible to the chronic accumulation of microorganisms immersed in biofilm extracellular matrix (ME). ME acts as a protective barrier and to able it difficult to control biofilm and peri-implant infections treatment. Then, (2) the secondy study evaluated the role of ECM in the pathogenicity of oral biofilm and resistance against antimicrobials on Ti surface using an *in vitro* model that simulates the transition process to peri-implantitis (from supragingival to subgingival biofilm). Additionally, a dual-targeting therapeutic approach was tested using an emerging matrix disrupting agent (iodo povidone) in biofilms formed *in situ* in the oral environment. ECM biofilm leads to oral biofilm dysbiosis, increasing virulence and damage to host cells ($p<0.05$). In addition, ECM biofilm also increased the antimicrobial resistance of Ti surface

biofilms ($p<0.05$). Hence, dual-targeting therapeutic approach reduced oral biofilm formation enhanced the efficacy of peri-implant targeted antimicrobials ($p<0.05$). In conclusion, bioactive surface treatments such as the newly developed PEO-BG coating, which improves the surface properties of Ti aiming to enhance osseointegration and increase the longevity of treatments with dental implants as well as the recent combined strategy for ECM degradation is an effective and promising strategy for biofilm control and non-surgical treatment of peri-implantitis.

Keyword: Biofilm, Titanium, Osseointegration, Surface modifications, Bioglass

SUMÁRIO

1. INTRODUÇÃO

As reabilitações orais com implantes dentários são atualmente a principal opção terapêutica para substituição parcial (Kern et al., 2018) ou total dos dentes perdidos (Chiapasco; Gatti, 2003). De fato, estudos clínicos de longos períodos de acompanhamento têm demonstrado considerável melhora na função mastigatória (Cardoso et al., 2016; Lam vo et al., 2019), aumentando a satisfação dos pacientes (Mishra; Chowdhary, 2019) e impactando diretamente na qualidade de vida (Bakker et al., 2019; Jawad et al., 2017; Marra et al., 2017) de adultos e idosos reabilitados com implantes. Além disso, revisões sistemáticas recentes (Chen et al., 2019; Gallardo et al., 2019; Hu et al., 2019) têm evidenciado altas taxas de sucesso e longevidade dos tratamentos com diferentes sistemas de implantes e protocolos de carregamento. Com base nisto, os implantes dentários podem ser considerados alternativas de tratamento bem estabelecidas, seguras, previsíveis e com prognóstico favorável em diferentes condições clínicas.

Desde 1980, implantes de titânio (Ti) começaram a ser produzidos com base nos estudos prévios de Brånemark que descreveu pela primeira vez as habilidades específicas de osseointegração do Ti com tecidos vivos (Brånemark et al., 1983). Fisiologicamente, ocorre uma forte ligação do Ti com moléculas de O_2 promovendo a imediata formação de uma camada de dióxido de titânio (TiO_2) com reconhecido papel no aprimoramento das propriedades biológicas deste metal (Pantaroto et al., 2018). A camada amorfa de TiO_2 fornece aos implantes a energia de superfície necessária para osseointegração, biocompatibilidade, melhora as propriedades mecânica e proporciona resistência à corrosão (Barão et al., 2012; Marques et al., 2016; Spriano et al., 2018). Por esta razão, Ti e suas são

os principais biomateriais utilizados na confecção de implantes biomédicos (CORDEIRO; BARÃO, 2017). Contudo, esta camada de TiO_2 é muito instável e suceptível a processos degradativos de natureza física, química e microbiológica com a exposição da superfície de Ti ao ambiente corrosivo dos fluidos corpóreos (Chrcanovic et al., 2016; Mathew et al., 2012).

Nesta perspectiva, abordagens que tem por objetivo melhorar a estabilidade eletroquímica do Ti e as respostas biológicas,favorecendo uma osseointegração mais rápida e efetiva são consideradas importantes no campo da implantodontia (Song; Koo; Ren, 2015; Spriano et al., 2018). Desta forma, os tratamentos de superfície são técnicas consagradas de modificações morfológicas, físicas e químicas da superfície do Ti (Song; Koo; Ren, 2015), tornando-a bioativa e favorecendo uma ligação química ao invéz de apenas mecânica do implante ao osso (Beline et al., 2019; Marques et al., 2016). Atualmente, tratamentos como SLA® (Straumann), TICER® (Microdent) e TiUnite (Nobel Biocare) são disponibilizados comercialmente para implantes dentários (Shi et al., 2016). Embora estes tratamentos promovam resultados biológicos satisfatórios, seus efeitos são limitados em promover um forte contato osso-implante nos períodos iniciais de osseointegração e acelerar a cinética de biomineralização (Spriano et al., 2018). Portanto, em condições clínicas que demandem de maior dependência da fixação mecânica primária, como em casos de implantes de diâmetro reduzido, instalados em áreas de baixa densidade óssea ou submetidos a carregamento imediato, os tratamentos de superfície são fatores chaves para o sucesso das reabilitações (Nicolau et al., 2019; Shi et al., 2016).

Nesta perspectiva, a incorporação de biomateriais com propriedades osteogênicas comprovadas pode ser uma estratégia promissora para aprimorar os resultados clínicos de

implantes a base de Ti (Soares et al., 2018). Dentre eles, o 45S5-Bioglass® (45% SiO_2, 24.5 % CaO, 24.5% Na_2O e 6% P_2O_5) tem ganhado atenção na área biomédica devido sua alta bioatividade e habilidades osteoindutivas e osteocondutivas (Baino; Hamzehlou; Kargozar, 2018; Hench, 2006; Jones, 2015). Previamente, inúmeras tecnologias já foram utilizadas para deposição de partículas de vidros bioativos na superfície de metais (Abushahba et al., 2019; Asif et al., 2014; Barros et al., 2019; Popa et al., 2015; Rohr et al., 2019; Xue et al., 2017). Entretanto, a diferença de propriedades mecânicas entre as partículas de biovidro e o metal produz revestimentos que dificilmente aderem à superfície que promovem rachaduras ou delaminação e reduzem os efeitos biológicos dos biovidros na cavidade oral (Popa et al., 2015).

Para superar este problema, o plasma eletrolítico de oxidação (PEO) pode ser considerado uma nova via para síntese de revestimentos de vidro bioativo na superfície do Ti (Rizwan et al., 2018). Como o PEO permite a incorporação de elementos bioativos no substrato e não apenas a deposição de biomateriais na superfície, isso pode ser interessante para evitar o descolamento de partículas de BG e potencializar os efeitos biológicos. Adicionalmente, as modificações químicas e topográficas derivadas do tratamento com PEO tem sido amplamente associadas na melhoria de propriedades de superfície, mecânica, eletroquímica, microbiológica e biológica do Ti e suas ligas (Beline et al., 2016; Cordeiro et al., 2018; Marques et al., 2016; Matos et al., 2017; Nagay et al., 2019; Santos-Coquillat et al., 2019). Assim, foi hipotetizado que o PEO poderia ser utilizado para produzir revestimentos aderentes, bioativos e bio-inspirados na composição química do 45S5-bioglass, buscando manter as suas propriedades biológicas e aperfeiçoar a biomineralização de implantes dentários.

Outro ponto relevante é que além dos problemas relacionados com a osseointegração deficiente, que podem ser minimizados por meio de tratamento de superfície biofuncionais, a complexa geometria dos implantes e a anatomia dos tecidos peri-implantares favorecem a adesão microbiana e o acúmulo de biofilmes (Bowen et al., 2018; Marsh; Devine, 2011). Os biofilmes peri-implantares são bem aderidos e difíceis de serem erradicados, podendo progredir de uma condição clínica de inflamação (mucosite) para infecção (peri-implantite) e promover danos aos tecidos duros e moles de suporte (Mombelli; Décaillet, 2011; Spriano et al., 2018). Portanto, perda da osseointegração e infecções dos tecidos peri-implantes são as principais causas relacionados com falhas precoces (Chrcanovic et al., 2016) e redução das taxas de sucesso (Derks; Tomasi, 2015) dos tratamentos com implantes dentários, sendo um desafio ainda não superado na prática clínica.

Atualmente, as terapias utilizadas no controle do biofilme peri-implantar são baseadas em métodos mecânicos, químicos, antibioticoterapia e associação de métodos (Al-Hashedi et al., 2017; Dostie et al., 2017). Contudo, o desbridamento causa danos irreversíveis a superfície do implante, enquanto que os antibióticos não são capazes de remover totalmente os microrganismos (Louropoulou; Slot; Van Der Weijden, 2014). Desta forma, a intervenção terapêutica mais eficaz para as doenças peri-implantares ainda não está bem estabelecida (Esposito; Grusovin; Worthington, 2012; Graziani; Figuero; Herrera, 2012). Oefeito reduzido de agentes antimicrobianos tópicos e sistêmicos vem sendo associado a complexa estrutura, a natureza polimicrobiana dos biofilmes orais e das respostas reduzidas do hospedeiro (Arciola; Campoccia; Montanaro, 2018; Bowen et al., 2018).

De forma geral, sabe-se que os biofilmes orais são comunidades bacterianas imersas em uma matriz extra-celular tridimensional polimérica (Flemming; Wingender, 2010; Koo; Yamada, 2016). Esta matriz extracelular (ME) é produzida por meio da síntese de α-glucanos,por exoenzimas bacterianas (glicosiltransferases - Gtf), que representam o principal componente da matriz do biofilme (Bowen; Koo, 2011; Costa Oliveira; Cury; Ricomini-Filho, 2017). Dentre as suas principais funções, a matriz exerce um importante papel protetor à medida que cria uma barreira mecânica, espessa e bem aderida em superfícies bióticas (Klein et al., 2015) e abióticas (Matos et al., 2017). Essa barreira "biológica" proporciona a criação de microambientes com diferentes níveis de pH, metabólitos e reduzidos níveis de O_2 que favorece a dinâmica de sucessão microbiológica de biofilmes supragengivais para subgengivais (Flemming; Wingender, 2010). Em adição, a matriz também dificultada a difusão de fluidos como saliva e antimicrobianos, reduzindo os efeitos imunológicos do hospedeiro e terapêuticos, respectivamente (Koo; Falsetta; Klein, 2013). Diante dos mecanismos expostos, tem sido evidenciado que a matriz extracelular é um fator relevante na transição de um biofilme comensal para mais agressivo e multi-resistente na superfície dentária (Klein et al., 2015; Ren et al., 2019) e de resina acrílica (Hwang et al., 2017), porém, ainda é limitado o conhecimento do papel da matriz na modulação e virulência de biofilmes orais formados na superfície de Ti.

O estado da arte a cerca das terapias para controle do biofilme peri-implantar tem direcionado as pesquisas para o desenvolvimento de novas estratégias focadas na desestruturação da matriz do biofilme visando potencializar o efeito de agentes antimicrobianos (Kim et al., 2018; Ren et al., 2019; Weldrick; Hardman; Paunov, 2019).. Recentemente, foi descrito que o iodopovidona [$(C6H9NO)_nI$], antimicrobiano de baixo

custo e estabilidade molecular, é um potencial agente direcionado para degradação da matriz. Este agente antimicrobiano a base de iodo age inibindo a síntese de α-glucanos pela exoenzima de *S. mutans* (GtfB), apresentando resultados promissores no controle de biofilmes mistos (*Candida albicans* e *S. mutans*) (Kim et al., 2018). Embora estas terapias apresentem resultados promissores, o efeito desta abordagem terapêutica combinada (agente degradante da matriz e antibióticos) ainda não foi testado experimentalmente em biofilmes polimicrobianos simulando uma condição de doença peri-implantar.

Em síntese, tratamentos de superfície que possam induzir osseointegração de maneira mais rápida, assim como, abordagens terapêuticas para aumentar a eficácia de antimicrobianos contra biofilmes orais podem ser consideradas novas estratégias para melhorar as propriedades de superfície do Ti e controle das infecções peri-implantares, respectivamente. Portanto, está dissertação tem como objetivos: (1) desenvolver uma nova superfície experimental com composição química ao 45S5-bioglass por PEO para melhorar as propriedades de superfície, mecânica, tribológica, eletroquímica, microbiológica e biológicas do Ti, e (2) avaliar o papel da ME na patogênese do biofilme oral desenvolvido na superfície do Ti, analisando o efeito de uma estratégia combinada direcionada para degradação da matriz do biofilme, visando aumentar a eficácia de antibióticos direcionadas para o tratamento não-cirúrgico da peri-implantite.

2 ARTIGOS

2.1 ARTIGO[#]: Synthesis of bioactive glass-based coating by plasma electrolytic oxidation: untangling a new deposition pathway toward titanium implant surface

Raphael C. Costa[†], João G. S. Souza[†], Jairo M. Cordeiro[†], Martinna Bertolini[§], Érica D.de Avila[‖], Richard Landers[£], Elidiane C. Rangel[#], Nilson C da Cruz[#], Carlos A. Fortulan[€], Belén Retamal-Valdes[‡], Magda Feres[‡], Valentim A. R. Barão[†*]

[†] Department of Prosthodontics and Periodontology, Piracicaba Dental School, University of Campinas (UNICAMP), Av. Limeira, 901, Piracicaba, São Paulo 13414-903, Brazil.

[§] Oral Health and Diagnostic Sciences Department, Division of Periodontology, University of Connecticut, School of Dental Medicine, 263 Farmington Avenue, Farmington, CT 06030, USA.

[‖] Department of Dental Materials and Prosthodontics, School of Dentistry at Araraquara, São Paulo State University (UNESP), R. Humaitá, 1680, Araraquara, São Paulo 14801-903, Brazil.

[£] Institute of Physics Gleb Wataghin, University of Campinas (UNICAMP), Cidade Universitária Zeferino Vaz, Barão Geraldo, Campinas, São Paulo 13083-859, Brazil.

[#] Laboratory of Technological Plasmas, Institute of Science and Technology, São Paulo State University (UNESP), Av. Três de Março, 511, Sorocaba, São Paulo 18087-180, Brazil.

[€] Department of Mechanical Engineering, University of São Paulo (USP), Trabalhador São Carlense, 400, São Carlos, São Paulo, 13566-590, Brazil.

[‡] Department of Periodontology, Dental Research Division, Guarulhos University, Eng Prestes Maia, 88, Guarulhos, São Paulo, 07023-070 Brazil.

***Corresponding author:**

Valentim A.R. Barão, Departamento of Prosthodontics and Periodontology, Piracicaba Dental School, Univeristy of Campinas, Av. Limeira, 901, Piracicaba, SP, Brazil 13414-903, Tel.: + 55-19-2106 5719. E-mail: vbarao@unicamp.br

O artigo foi submetido para o periódico ACS Applied Materials & Interfaces (IF = 8.456)

ABSTRACT

Bioactive glasses (BG) have attracted attention for dental implant coatings applications as a consequence of their bioactivity and osteogenic properties in biological systems. Although BG particles coatings were previously developed by different methods, poor particle adhesion on surfaces and reduced microbiological and biological properties because of glass crystallization are factors that limit their clinical application. To overcome this problem, we untangled, for the first time, the plasma electrolytic oxidation (PEO) as a new pathway for the synthesis of bioactive glass-based coating (PEO-BG) on titanium (Ti) substrate. Instead of BG particles, we used bioactive elements in electrolyte solution inspired into the 45S5-BG. Hence, the newly developed PEO-BG coating was investigated with respect to the surface, mechanical, tribological, electrochemical, microbiological and biological properties compared to machined and sandblasted/acid-etched control surfaces. Characterizations analyses showed that PEO treatment was able to successfully synthesize a coating with higher roughness and surface area, resulting in a complex surface topography, superhydrophilic status, chemical composition and oxide layer mimetic to 45S5-BG (~ 45.0 Si, 24.5 Ca, 24.5 Na, 6.0 P w/v%). Additionally, PEO-BG enhanced mechanical properties and promoted good substrate adherence with increased resistance to tribological wear and higher corrosion resistance after *in vitro* degradation simulation (28 days). Furthermore, PEO-BG modulated microbial adhesion (2 h) and oral biofilm formation (24 h), which changed the bacterial profile reducing periodontal pathogenic bacterial associated with peri-implant disease. Interestingly, PEO-BG revealed similar biological mechanisms as the 45S5-bioglass (bioactive ion release, higher pH fluctuations and hydroxyapatite-inducing ability). For biological analyses, PEO-BG showed higher adsorption of blood plasma proteins and did not present cytotoxic effect on fibroblasts. Thus, PEO-BG coating was synthesized by PEO with enhanced biomechanical properties and may be considered a promising approach for dental implants applications due to biocompatibility, reduction of the peri-implant biofilm pathogenicity and probable improved response to of osseointegration.

KEYWORDS: Surface Modification; Bioactive Glass; Plasma Electrolytic Oxidation, Titanium, Dental Implant.

1. INTRODUCTION

Titanium (Ti) and titanium-based alloys are well-established biomaterials for dental and orthopedic implants because of their proper biocompatibility, corrosion resistance and mechanical properties[1]. Although oral treatment with Ti-based implants exhibits high long-term success rate[2,3], Ti material does not present suitable bioactive properties and is susceptible to degradation in the oral environment [4]. In addition, the mechanical bonding rather than chemical bonding of the Ti with the human bone can favor osteolysis, bone resorption and peri-implant infections [5,6]. Consequently, such harmful effects influence the biomedical rehabilitation lifetime, increasing the loosening and premature fracture of the implants[7,8].To overcome such drawbacks, surface optimization have been proposed for Ti-based materials[9]. Morphological, physical and chemical modifications are strategies indicated to achieve greater osseointegration, improved bioactivity and implant treatment success[10,11]. Hence, protective and multifunctional bioactive surfaces have been designed in recent years to better biomineralization kinetics and strong bone-implant contact in the initial periods of osseointegration[12].

Larry Hench's 45S5-bioglass® (45 wt% SiO_2, 24.5 wt% CaO, 24.5 wt% Na_2O, and 6 wt% P_2O_5)[13] was discovered in 1969 and has gained attention in bone tissue engineering due to their bioactivity and osteogenic properties[14,15]. In fact, 45S5-bioglass is synthetic silica-based bioactive material with higher bioactivity indexes ($I_B > 8$) among bioactive glasses and glass-ceramics[16]. Furthermore, osteoinductive and osteoconductive abilities are related to a complex mechanism based on ion leaching and controlled dissolution of glass when in contact with body fluids[17,18]. This process triggers precipitation of an apatite layer on implant surfaces that also acts as a template for newly bone formation and even bonding soft tissues[15,19]. Additionally, bioactive glasses (BG) are able to induce antimicrobial activity by changes in the environmental pH, leading to increased osmotic pressure and bacterial cell damage[20–22]. For this reason, BG are used for a wide range of applications including toothpastes, bone grafting, scaffolding, drug delivery, soft tissue engineering

and coatings on biomaterials [16,23].

BG particles have been also incorporated on Ti alloys[24–30] and zirconia substrate[17,25,31,32] aiming application in dental implants. For this, different methods such as dip-coating[28], air abrasion[33], vitreous enamelling[34], plasma spraying[35], flame spraying[26], sputtering[27,36], laser deposition[24,29], and electrophoretic deposition[30,37] were employed for particle incorporation on metal surfaces. However, some strategies have been unsuccessful as they may decrease mechanical behavior[15] or limit biological performance[17]. The main problem is the mismatch in thermal expansion coefficients of these classical BG systems (~15– 17x10^{-6} ºC^{-1}) and Ti substrate (~9.2x10^{-6} ºC^{-1}), which difficulty its adherence on the surface and promotes cracks or delamination of the coating[27]. Another unsuccessful strategy also described was the direct incorporation of BG particles into the metal alloy matrix due to the mechanical weakening of the substrate observed after heat treatment[38]. In this context, alternative Si-based glass compositions have been also investigated to address these issues[31]. Nevertheless, changes in chemical composition increases bioactive glass crystallization that difficult surface reactions and reduce bioactivity.

To overcome this problem, plasma electrolytic oxidation (PEO) can be considered a promising approach with relatively simple and effective technique[19]. Since PEO treatment allows the incorporation of bioactive elements into substrate and not only the deposition of biomaterials on surface, this would be highly interesting to avoid detachment of BG powders and particles related to the failure of other methods[22,38]. PEO treatment is an electrochemical technique based on anodizing at high voltages exceeding the dielectric breakdown voltage of the oxide layer and gas envelope[12]. As a result, short-lived numerous plasma microdischarges are generated on the substrate, which promotes rapid growth of the coating and incorporation of bioactive elements with good interfacial adhesion to Ti substrate[39]. Notably, experimental bioactive surfaces by PEO with calcium phosphate compounds (e.g. hydroxyapatite HA) and another chemical elements (Ca, P, Zn, Cu, Mg, Ag, Sr, Si) have been previously developed[12,40–44]. In agreement, our previous studies[45–50] also

showed that bioactive elements incorporated on Ti surface improve mechanical, electrochemical and biological properties.

The physiological mechanisms of BGs are known to be related to their chemical composition and stoichiometric ratio of biological elements similar to human bone[16,18]. Hence, we hypothesized that PEO would enable effortlessly to create adherent and bioactive glass coatings mimicking the composition of the classical 45S5-bioglass promoting good biological responses. To our best knowledge, this study is the first one to test PEO as a new pathway to develop an adherent and resistant coating with chemical and oxides composition similar to 45S5-bioglass to circumvent the currently limitations of other BG-coatings. Thus, the newly developed coating bio-inspired on 45S5-bioglass synthetized via PEO is investigated and discussed in detail in this paper.

2. EXPERIMENTAL SECTION

2.1. Experimental Design

The experimental design of this study can be seen in Fig. 1. Commercially pure titanium (cpTi; ø=10mm x 2 mm) discs were polished and randomized in each group. Two surface conditions were considered as controls: machine (cpTi) and sandblasted and acid-etched (SLA). PEO treatment was used for synthesis of mimetic bioactive glass-based coating to create the experimental group (PEO-BG). Electrolyte solution containing silica (Si), calcium (Ca), sodium (Na) and phosphorus (P) reagents allowed to obtain a stoichiometric proportion of 45S5-bioglass (gold standard bioactivity) on Ti surface. Wide range of surface, electrochemical, mechanical, tribological, microbiological and biological properties were assessed.

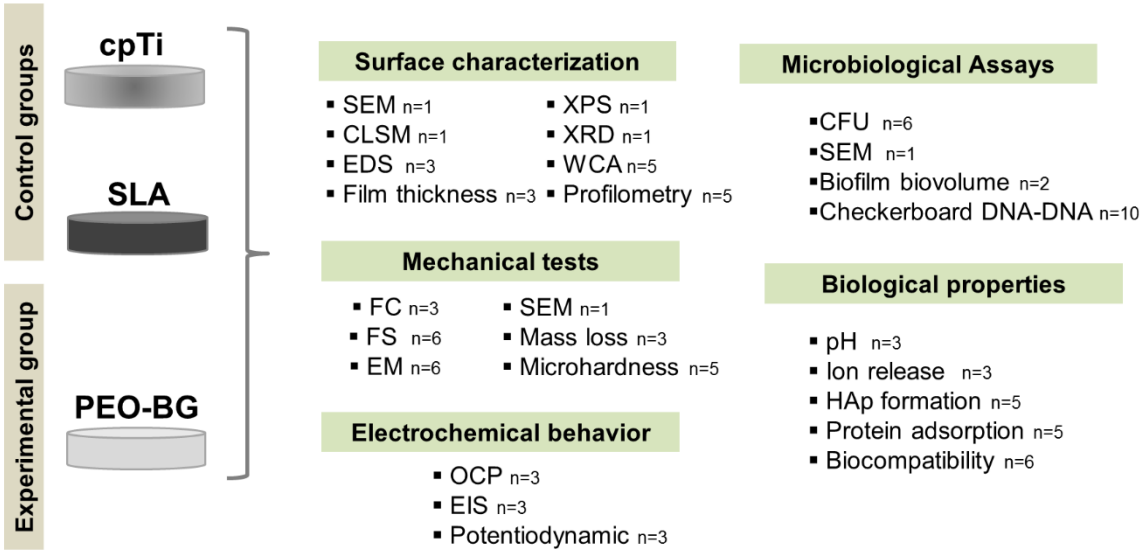

Figure 1. Schematic diagram of the experimental design. SEM = scanning electron microscopy; CLSM = confocal laser scanning microscopy; XPS= X-ray photoelectron spectroscopy; EDS = energy-dispersive spectroscopy; XRD = X-ray diffractometry; WCA = water contact angle, FC = friction coefficient, FS = flexural strength, EM = elasticity modulus, OCP = open circuit potential, EIS = electrochemical impedance spectroscopy, CFU = colony-forming units, HAp formation = hydroxyapatite formation.

2.2 Surfaces preparation

CpTi discs grade II (Realum Industria e Comércio de Metais Puros e Ligas Ltd., São Paulo, SP, Brazil) were polished with #320 and #400 grit SiC abrasive papers (Carbimet 2, Buehler, Lake Bluff, IL, USA) in an automatic polisher (EcoMet 300 Pro with AutoMet 250; Buehler, Lake Bluff, IL, USA) to standardize the surface condition (Ra = 0.20 ±0.06 µm)[50]. All samples were ultrasonically cleaned with deionized water (10 min), degreased with 70% propanol (10 min) and hot-air dried (250 °C)[51]. Afterwards, polished cpTi discs were used as control (machined surface). SLA surface was obtained from sandblasting with 150 µm particles of Al_2O_3 (Polidental Indústria Comércio Ltd., Cotia, São Paulo, Brazil)

deposited at 50 mm of distance with 90° of angulation using 0.45 MPa pressure during 30 s and chemically treated with an aqueous solution containing 18% HCl (v/v) (Sigma-Aldrich, St. Louis, MO, USA) and 49% H_2SO_4 (v/v) (Sigma-Aldrich, St. Louis, MO, USA) at 60°C for 1 h, according to standard procedures[52,53].

The plasma electrolytic oxidation treatment was carried out using a pulsed direct current (DC) power supply (Plasma Technology Ltd., Kowloon, Hong Kong, China). Briefly, cpTi discs were used as the anode, while a steel tank with a cooling system (23 ±1.5 ºC) was the cathode. Samples were completely submerged in the electrolytic solution prepared using 0.014 M sodium metasilicate (Na_2SiO_3-$5H_2O$), 0.20 M calcium acetate ($C_4H_6O_4Ca$), 0.50 sodium nitrate ($NaNO_3$) and 0.0010M sodium glycerolphosphate ($C_3H_7Na_2O_6P$) (Dinâmica Química Contemporânea, Diadema, SP, Brazil) as precursor sources for main bioactive elements of the 45S5-bioglass®[16]. 0.025 M $Na_2EDTA{\cdot}2H_2O$ (Dinâmica Química Contemporânea, Diadema, SP, Brazil) was used as chelating agent in all electrolyte solutions[12]. PEO working parameters were adapted according to our previous protocol described elsewhere[50]. The treatment was conducted with the pulse voltage anodic (500 V), unipolar frequency (1000 Hz), alternate duty cycle [10% (+) and 70 (-)] for 420 s. Subsequently, the PEO-BG discs were rinsed in distilled water and air-dried (For more details see supporting information, Fig. S1A).

2.3 Coating characterizations

2.3.1 Structural morphology/topography

To evaluate the surface morphology, top-view and cross-section scanning electron micrographs were acquired in SEM (JEOL JSM-6010LA, Peabody, MA, USA) using electron beams with low accelerating voltages (3 kV) of 5.0 and 10.0 keV[46]. Coatings topography were

analyzed by noncontact 3D CLSM (VK-X200 series, Keyence, Osaka, Japan), and VK-Analyzer software (Keyence v3.3.0.0, Osaka, Japan) was used for image processing[49]. The surface area was estimated in cropped images of 100 × 100 μm that were obtained at the magnification of 50×. Besides, a portable eddy current meter (MCT-401 model, Minipa do Brasil, São Paulo, Brazil) was used to measure the thickness of the coatings with an average of 10 measurements in randomly chosen regions of the sample surface (each 5 μm^3) according to the standard ISO 21968[54].

2.3.2 Chemical composition based on 45S5-Bioglass

The 45S5-bioglass basic elements (% atomic) and stoichiometric proportion [45% Si, 24.5% Ca, 24.5% Na and 6% P (w/v%), 5:2:2:1 biological ratio] related to bioactivity[16] were checked by energy-dispersive spectroscopy. Three random regions on surface, and cross-sectioned outer and inner coatings were selected to verified these individual bioactive elements distribution (in the order of 1 μm^3). Titanium (Ti) and oxygen (O_2) elements were excluded from the stoichiometric calculation because they do not represent the coating composition. The chemical states of the outermost oxide layer were determined by X-ray photoelectron spectroscopy (Vaccuum Scientific, VSW HA100, Macclesfield, UK) operated at 12 kV and 120 W, 90º take-off angle with 15Å maximum sampling depth. The spectra were referenced to adventitious carbon (C) at 284.6 eV binding energy and 44 eV pass energies. Atomic proportions of Ti, O, Al, Si, Ca, Na and P were determined from the Gaussian deconvolution of the peaks. The reference binding energy was acquired from the National Institute of Standards and Technology XPS Online Database[1]. Then, chemical and oxide composition was also used to determine the bioactivity of the coating by Hench's ternary diagram[16].

2.3.3 Crystalline phases characterization

The crystalline structure of the coatings was determined by XRD (PANalytical, X'Pert3 Powder, Almelo, Netherlands) using Cu Kα radiation (λ = 1.540598 Å), operating at 45 kV and 40 mA, using 2θ configuration in the 25° to 65° range with 0.02° step size [6].

2.3.4 Roughness and wettability

The surface roughness (Ra – arithmetic mean, Rt – maximum height, Rz – average peak-to-valley height and Rq – root mean square average) was measured using a profilometer (Dektak 150-d; Veeco, Plainview, NY, USA). Three measurements (in the right, center, and left regions of the disc) were taken with a 500-μm cutoff and speed of 0.05 mm/s for 12 s[49]. The difference in roughness line profile between surfaces tested was also acquired by CLSM. For wettability, deionized water contact angle measurements were performed on an automated goniometer (Ramé-Hart 100-00; Ramé-Hart Instrument Co., Succasunna, NJ, USA) using the sessile drop (10 μL) method and analyzed with specific software (DROPimage Standard, Rame-Hart Instrument Co., Succasunna, NJ) based on the Young equation[55]. Representative micrographs of contact angle from each surface were obtained.

2.4 Mechanical tests

2.4.1 Microhardness

The Vickers microhardness (VHS) was measured by means of an indenter (Shimadzu, HMV-2 Micro Hardness Tester, Shimadzu Corporation, Kyoto, Japan). The applied load was 0.5 kgf for 15 s. The test was performed at four randomly distributed points in each sample. The values of microhardness were calculated according to the following formula: $HV = 1.8544P/d^2$, where P = applied load and d = length of the diagonals of indentations[56].

2.4.2 Flexural Strength and elastic modulus

Flexural strength and elasticity modulus tests were conducted on rectangular bar cpTi samples (2 mm wide × 2 mm thick × 25 mm long) standardized according to ISO 4049 protocol[57] and surface treated as mentioned above. Samples were evaluated for three-point bending test with crosshead speed of 0.5 mm/min in a universal testing machine (Instron Model 4411, Instron Corp., Canton, MA, USA)[58]. The test was graphically recorded and considered completed when any failure or permanent deformation was detected by an abrupt load change. Flexural strength value (MPa) was determined according to the formula: [$fs = 8FL = \pi D^3$], where *fs* = flexural strength value (MPa), *F* = fracture strength or elastic limit (N), *L* = distance between the supports and *D* = diameter of the specimen (mm). Elastic modulus (GPa) was automatically monitored and calculated by the software Bluehill 2 (Instron Corporation, High Wycombe, UK).

2.4.3 Friction coefficient and mass loss

A custom made tribological system was used to determine the friction coefficient of surfaces[59]. The custom-made pin-on-disk tribometer (Faculty of Mechanical Engineering: University of São Paulo, São Carlos, SP, Brazil) consisted of an counter body of Zr ball (Y-TPZ; ø=5mm) articulates against the face Ti disc immersed in simulated body fluid solution (SBF)[60]. A total of 100 mL of SBF (37 °C) at pH 7.4 was used in each test to mimic the blood plasma. At the beginning of each test, the ball surface was cleaned and the surface checked for any damage. The test was carried out with vertical normal load (5 N), track diameter (5.8 mm), sliding velocity (0.01 m/s), sliding duration (1100 s) determined in the pilot study (data not shown). During the tribological test, the evolution of surface wear was graphically monitored by LabViews software (National Instruments, São Paulo, SP, Brazil) and friction coefficient average determined (μ). In parallel, discs were weighed on a precision scale (AUY-UNIBLOC Analytical Balance, Shimadzu

Corporation, Kyoto, Japan) before (baseline) and after tribological tests to determine mass loss (μg)[61].

2.4.4 Wear track characterization

After tribological tests, the morphological of the features wear scars were investigated by SEM (JEOL JSM-6010LA, Peabody, MA, USA). To calculate the wear volume of the samples, optical microscope with 1.0 μm precision and ×120 magnification (VMM-100-BT; Walter UHL, Asslar, Germany) equipped with digital camera (KC-512NT; Kodo BR Eletrônica Ltda., São Paulo, SP) and analyzer unit (QC 220-HH Quadra-Check 200; Metronics Inc., Bedford, USA) was used. Total surface area was calculated by measuring the ends of the disc. Wear tracks width was calculated in 4 different regions (top, bottom, right and left) and wear track diameter was considered. Final surface damage was analyzed through the wear track length in relation to the total surface area. All measurements were performed by a previously calibrated examiner (intraclass correlation coefficient .834; $p<.0001$).

2.5 Eletrochemical behavior

The electrochemical assessment was used to investigate the corrosion behavior of cpTi, SLA and PEO-BG surfaces in SBF for 28 days[62,63]. A three-electrode cell associated with a potentiostat (Interface 1000, Gamry Instruments, Warminster, PA, USA) was used to carry out three tests: the open circuit potential (OCP), the electrochemical impedance spectroscopy (EIS) and the potentiodynamic polarization following our previous protocol[49,53,56,64]. SBF at 37 ±1 °C (pH 7.4) was adopted as the electrolytic solution (10 mL) for all tests[60].

For each corrosion experiment, a cathodic potential (-0.9 V vs. SCE) was applied for 10 min to standardize the oxide layer. Afterward, OCP was carried out for 3600 s to obtain the free corrosion potential of the material. EIS was acquired at frequencies between 100 kHz and 5 MHz [64]. Then, EIS data were analyzed by Echem Analyst software (Gamry Instruments) using an

appropriated circuit to each surface and used to construct Nyquist, Bode (|Z|), and phase angle plots considering the real (Z') and imaginary (Z'') components of impedance. Hence, polarization resistance (R_p) and capacitance (Q) parameters were acquired. Samples were polarized from -0.8 to 1.8 V (scan rate of 2 mV/s) to draw the potentiodynamic polarization curves, which was possible by the Tafel extrapolation method (Echem Analyst Software, Gamry Instruments) with the following parameters: E_{corr} (corrosion potential), i_{corr} (corrosion current density), Tafel slopes (βc, βa), passivation current density (i_{pass}) and corrosion rate. For data analyses, the exposed area (in cm^2) of each surface (cpTi = 1.19, SLA = 1.44 and PEO-BG = 2.72) was considered.

2.6 Microbiological assay

2.6.1 In vitro biofilm model

The microcosm biofilm model[65] was used to test the effect of PEO-BG surface on microbial adhesion and polymicrobial biofilm formation. Briefly, samples were cleaned by UV-light (4 W, λ=280 nm, Osram Ltd., Berlin, Germany) for 20 min each side and coated with filtered saliva (0.22 μm membrane filter), for 30 min at 37°C to simulate salivary pellicle formation[66]. For biofilm growth, stimulated human saliva (unfiltered) was used as a bacterial inoculum (~10^7 cell/mL) to mimic oral microbiological composition[65]. Then, saliva-coated discs were incubated with BHI medium (1:90 v/v) (Becton-Dickinson, Sparks, MD, USA) and saliva (1:10 v/v) to promote initial microbial adhesion (2 h) and biofilm formation (24 h) under static conditions (37 °C, 10% CO_2). For salivary pellicle and biofilm inoculum, fresh stimulated human saliva was collected from 5 healthy volunteers (approved by local Research and Ethics Committee, number: 86638918.0.0000.5418) based on inclusion and exclusion criteria described elsewhere[67].

2.6.2 Viability of bacteria cells

After biofilm growth, discs were transferred to microcentrifuge tubes containing 1 mL 0.9% NaCl vigorously vortexed and sonicated at 7W for 30 s (Branson, Sonifer 50, Danbury, CT, USA)

to detach the biofilms[68]. A 100-µL volume of the sonicated bacteria cell suspension was six-fold serially diluted in 0.9% NaCl ($1:10^7$). The suspensions were inoculated using the drop-counting technique in Columbia blood agar (CBA) medium supplemented with 5% (v/v) defibrinated sheep blood for quantification of total viable bacteria[50]. Subsequently, the plates were incubated with 10% CO_2 at 37 °C for 48 h. Colony-forming units (CFUs) were counted by stereomicroscopy, and the results were expressed as the logarithm of CFU per milliliter (log10 CFU/mL).

2.6.3 Biofilm structure and morphology

Confocal laser scanning microscopy (CLSM) was used for biovolume measurements and 3D structure analyses of biofilms. Live bacterial cells were stained with 1 µM SYTO-9 green fluorescent nucleic acid (485-498 nm; Thermo Scientific, USA) under protection from light for 20 min[69]. Images were obtained in a DMI 6000 CS inverted microscope coupled to a TCS SP5 computer-operated confocal laser scanning system (Leica Microsystems CMS, Mannheim, Germany) with a 40× oil immersion objective (numeric aperture 1.25) and Ar-ion laser tuned at 488 nm for excitation[50]. Stacks of z-plane images from at least 3 different fields of view per sample were acquired and then reconstructed into 3-D images using the IMARIS software (Bitplane, Inc., Saint Paul, MN, USA). Surface reconstructions using the surpass mode were used to calculate the biovolumes (in μm^3) of biofilms. Additionally, biofilm morphology was also visualized by SEM. For this, biofilms on samples were fixed for 2 h in Karnovsky solution (2.5% glutaraldehyde, 2% formaldehyde, 0.1 M sodium phosphate buffer; pH 7.2), followed by dehydration in a series of ethanol washes, dried, and sputter-coated with gold[65].

2.6.4 Biofilm composition

Since bioglass-based coatings can modulate microbiological growth, bacterial species related to peri-implant diseases were assessed by checkerboard DNA–DNA hybridization technique[70,71]. The biofilms developed on Ti surfaces were collected by means of a modified cell

scraper (length, 240mm) (TPP, Trasadingen, Switzerland) in one movement from a central area of each disc. Samples were inserted into a tube containing 150 µL of TE solution (Tris HCl 10 mM + ethylenediaminetetraacetic acid 1 mM, pH 7.6), and 100-µL of 0.5 M NaOH, boiled for 10 min and the final solution was neutralized with 0.8 mL of 5 M ammonium. DNA samples were digoxigenin labeled with DNA probes of the genome of the bacterial species, hybridized in a Miniblotter 45 (Immunetics), and DNA probes were detected using a specific antibody against digoxigenin conjugated to phosphatase alkaline. Signals were detected using AttoPhos substrate (Amersham Life Sciences, Arlington Heights, IL, USA) and results were obtained using Typhoon Trio Plus (Molecular Dynamics, Sunnyvale, CA, USA). Data were expressed as levels and proportions of 40 periodontal pathogens [65,72].

2.7 Biological property

2.7.1 Hydroxyapatite formation

Surface bioactivity was evaluated based on hydroxyapatite (HAp)-inducing ability. Samples were fixed in custom-made plastic vials containing SBF[73] and were kept under static conditions inside a biological thermostat at 37 ±0.5 °C remaining for 7, 14 and 28 days. The amount of SBF was determined according to surface area (cpTi = 11.4 mL, SLA = 14.1 mL and PEO-BG = 27.2 mL) and replaced by newly prepared SBF every two days[62,73]. To perform the HAp analysis, discs were removed from the SBF, rinsed with distilled water and air dried in a desiccator without heating for 24 h. To confirm the formation and morphology of hydroxyapatite on surfaces XRD and SEM analyses were conducted, respectively.

2.7.2 Ion release and pH measurement

The kinetic of ion dissolution from the coating was assessed by inductively coupled plasma optical emission spectrometer (ICP-OES)(iCAP model, 7000 series, Thermo Scientific, MA, USA) operating at RF power of 1.3 kW, with a plasma flow of 1 L min^{-1}, sample flow rate of 0.8 mL min^{-1}

and argon flow of 0.8 L min^{-1} [43]. Samples were immersed in plastic tubes containing 5 mL of ultrapure deionized water (≥18.2 MΩ cm) obtained from an Advance A10 Milli-Q system (Millipore, Bedford, MA, USA) and maintained at 37 ±1 °C. After various time points (1, 2, 4, 6, 8, 10, 12, 24, 48, and 72 h) samples were acidified with 65% nitric acid (Sigma-Aldrich, St. Louis, MO, USA) and analyzed for ionic release of Si^{4+}, Ca^{2+}, Na^{+}, P^{+}, Ti^{4+} (PEO-BG), Ti^{4+} and Al^{3+} (SLA) and Ti^{4+} (cpTi). During the immersion period, solutions were agitated twice. Blank solution (ultrapure deionized water) was included into the batch measurements as a reference. The detection of the technique was estimated to ppm as an average of three replica measurements. Simultaneously, pH measurement was performed using a pH microelectrode (Accumet; Cole-Parmer, USA) coupled to a pHmeter (Procyon SA-720, Olímpia, Brazil) calibrated with pH standards of 4.0 and 7.0[69].

2.7.3 Protein adsorption

Human blood plasma (approved by the Local Research and Ethics Committee 60177416.4.0000.5418) was used as the protein model, and the adsorption was measured by the bicinchoninic acid method (BCA Kit, Sigma-Aldrich, St. Louis, MO, USA)[74]. Firstly, discs were incubated with 1 mL of human blood plasma under horizontal stirring (75 rpm) at 37 °C. After 2 h, samples were washed three times (to remove non-adherent proteins), transferred to cryogenic tubes with 1 mL of 0.9% NaCl and sonicated in a Cup Horn (5.5 in. cup, Q500, Qsonica, Newtown, Connecticut, USA) at an amplitude of 80% for 60 s. The solution was diluted 100-fold and introduced into 96-well plates. Finally, protein concentration was calculated based on a standard curve and absorbance read at a wavelength of 562 nm in a microplate spectrophotometer (Multiskan, Thermo Scientific, Vantaa, Finland).

2.7.4 Biocompatibility assay

Human gingival fibroblast cells (HGF - Rio de Janeiro Cell Bank Code 0089) were grown in low-glucose Dulbecco's modified Eagle medium (DMEM, Sigma Chemical Co., St. Louis, MO) supplemented with 10% fetal bovine serum (FBS, Gibco, Grand Island, NY), 100 IU/ mL penicillin, 100 mg/mL streptomycin (Sigma-Aldrich, St. Louis, MO), and 2 mM L-glutamine (Gibco, Grand Island, NY) in a humidified incubator at 5% CO_2 atmosphere at 37 °C [50,74]. For all experiments, HGF cells were plated in duplicate at 1×10^5cells/mL in 24-well culture plates in Alpha MEM supplemented with 10% FBS and antibiotics for 24 h to allow cell adhesion on polished cpTi (gold standard of bioactivity) and the experimental coating (PEO-BG). Cells seeded onto 24-well polystyrene plates served as standard growth controls (positive control-C^+), and cells incubated with 40 μg/mL camptothecin (Sigma-Aldrich, St. Louis, MO) represented the negative control, with 100% cell death.

The effect of the PEO-BG coating on metabolically active HGF cells was determined by the alamarBlue assay[50]. Briefly, the culture medium was removed, and 500 μL of fresh medium containing 10% alamarBlue (Invitrogen,Carlsbad, CA) was added to each sample well. The plates were then incubated for 12 h at 37 °C for alamarBlue reagent conversion into a detectable fluorescent product, and 100 μL was transferred to a 96-well polystyrene black plate (TPP tissue culture plates, St. Louis,MO) for measurement. The quantitative fluorescence signals of viability and cytotoxicity were measured using a Fluoroskan (Fluoroskan Ascent FL, Thermo Scientific,Waltham, MA) at an excitation and emission wavelength of 544 and 590 nm, respectively. Additionally, cell morphology and viability was verified by CSLM analysis, confirmed by fluorescent indicators of live (green-488 nm) and dead (red-561 nm) cells. Samples were acquired through 10× dry (Plan NeoFluar NA 0.3 air) objective lens. Images were also taken through 5× and 10× as a stack for three-dimensional (3D) reconstruction. The experiment was performed in duplicate for each experimental and control group.

2.8 Statistical Analysis

The normality and homoscedasticity of all response variables were tested by the Shapiro–Wilk and Levene methods, respectively. One-way ANOVA was used to test the statistically significant differences among the cpTi, SLA and PEO-BG for surface, mechanical, electrochemical, microbiological and biological properties. Tukey's HSD test was used as a post hoc technique for multiple comparisons. A mean difference significant at the 0.05 level was used for all tests (IBM SPSS Statistics for Windows, v. 21.0., IBM Corp., Armonk, NY, USA).

3. RESULTS AND DISCUSSION

3.1 PEO treatment is a new approach for bioglass-based coating synthesis on Ti surface

It is known that PEO treatments display an important role for improvement of the surface characteristics of dental implants[1,19]. Here, we successfully use PEO treatment as a new pathway for synthesis of 45S5-bioglass-based coating on Ti surface. It ought to be mentioned that newly developed PEO-BG coating was obtained by adjusting the work process parameters and electrolyte solution (Fig. S1A) with bioactive glass precursor reagents, which based on electrical response (Fig. S1B and S1C) changed surface morphology/topography of Ti. Interestingly, PEO-BG created irregular blasted facets with nonuniform aggregates (which resembles the "glass grain-like") and presented craters characterized by evident circular pits. In contrast, machined surfaces presented longitudinal grooves and homogeneous surfaces as a result of the polishing process, whereas SLA experimental surface exhibited sandblasting holes with superposition of small pits produced by the acid-etching similar to commercial surfaces, such as SLA® and SLAactive® (Straumann AG, Basel, Switzerland). These characteristics of surface morphology and topography can be confirmed by SEM micrographs (Fig. 2A) and three-dimensional images obtained by CSLM (Fig. 2B), respectively.

PEO-BG surface modifications can be attributed to the electrolyte solution and the deposition parameters used. Our electrolyte design strategy explored the possibilities of

simultaneous combination of the bioactive elements, such as Si (Na_2SiO_3-$5H_2O$), Ca ($C_4H_6O_4Ca$), Na ($NaNO_3$) and P ($C_3H_7Na_2O_6P$) in stable solutions to simulate the bioglass composition. For this, different sources and their individual compatibility (i.e. the solubility) with base electrolyte was preliminary tested increasing gradually the concentration of the respective compounds (data not shown). The choice of base components for the electrolyte solution was due to their good solubility and low cost compared to 45S5-BG precursors (SiO_2, CaO, NaO, P_2O_6) targeting industrial applications. The pH of all electrolyte solutions were acidified to avoid the hydrolysis of Ca^{2+} and Na^+ with precipitation of Ca(OH) and Na(OH), respectively. Since Ca(OH) and Na(OH) can alkalize the solution and favor the precipitation of PO_4^3, Na2EDTA·$2H_2O$ was used to avoid this because forms a strong chelating complex with Ca, Na and Si. Hence, all elements of interest were completely dissolved into a homogeneous solution (i.e. maintained clear solutions) creating acid (pH = 4.38) and high conductivity (σ, $mS \cdot cm^{-1}$=137.5) electrolytes.

Although high concentration and conductivity solutions may favor the incorporation of the bioactive elements, they also influence the PEO electrical response[12]. During PEO process, the micro-discharges are responsible for melting the material, creating melted oxides, leading to the effective incorporation of bioactive elements into the porous surface[49]. Our electrolyte solution induced the formation of a thick oxide layer jointly changed the electrical characteristics and quality of micro-discharges (~178) and, consequently, the surface morphology[44]. Then, the scattered micro-discharges creates atypical PEO surface with craters instead of pores, as similarly described elsewhere[50,75]. In terms of bioglass mechanisms, surfaces with larger surface area (Fig. 2B) may play an important role for surface biological reactions in host tissues[38].

Regarding the chemical composition, PEO-BG showed the incorporation of all bioactive elements by EDS mapping (Fig. 2C) with homogeneous distribution on the surface, outer and inner layers of the coating (Fig. 2D). The stoichiometric ratio of 45S5-bioglass (5: 2: 2: 1 wt% for biological ratio of Si: Ca: Na: P concentration) and Ca/P atomic ratio above that required for hydroxyapatite (approximately 1.67)[60] were obtained. Altogether, the new PEO-BG can be

considered a bioactive glass mimetic coating based on its chemical composition and class A bioactivity with respect to Hench's ternary diagram (Fig 2E)[16]. The advantages of incorporating 45S5-bioglass precursors on Ti surface are the following: (i) Si acts in the formation and calcification of bone tissue, (ii) Ca and P are bone tissue components related to osteoblast activation in osteogenesis processes, and (iii) Na plays an important role in modulating metabolic reactions in body fluids[15,16,76]. Since PEO coatings doped with Si, Ca, Na and P have been recognized bioactive and biocompatible by *in vitro* [47,62] and animal models[77,78], the stoichiometric ratio between the bioactive elements that mimetic bioglass substrate it may be a possible way to further improve biological responses and the osseointegration behavior.

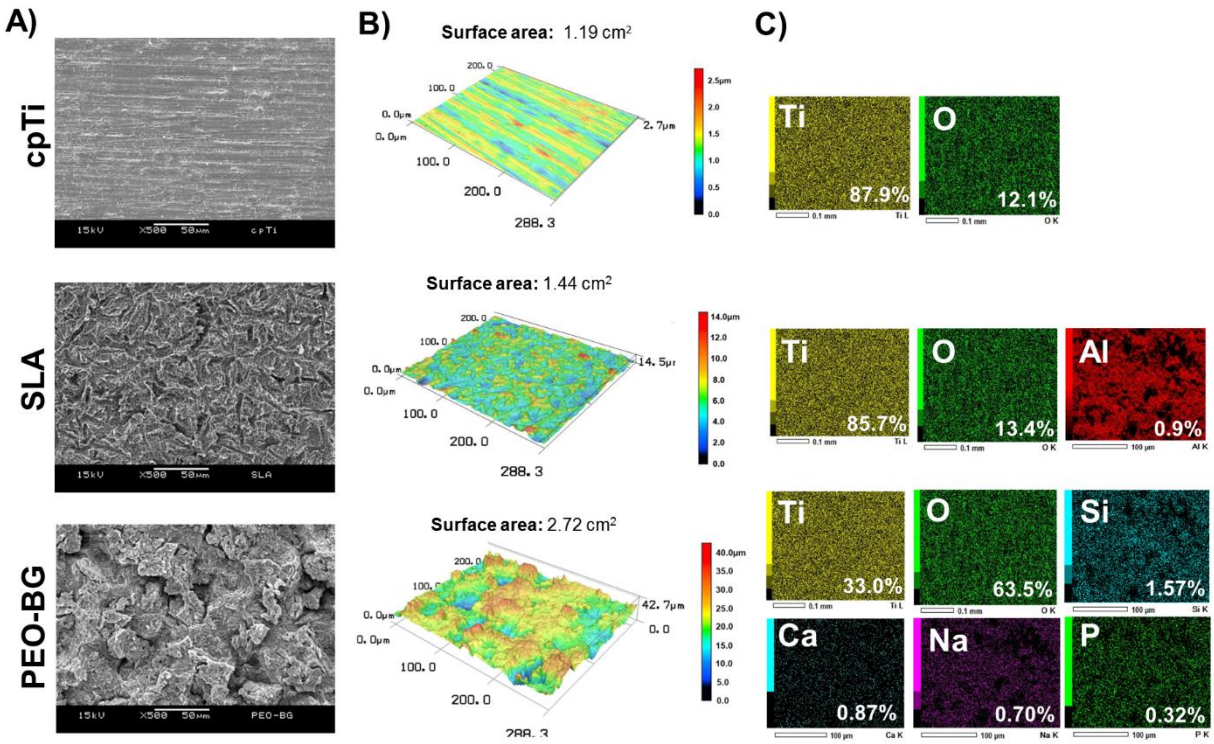

D)

% Atomic (PEO-BG)						
	Si	Ca	Na	P	Ti	O
Surface	1.57	0.87	0.70	0.32	33.0	63.5
Outer	1.34	0.61	0.60	0.20	45.1	52.1
Inner	1.04	0.43	0.46	0.18	67.3	30.5
Stoichiometric ratio (w/v%)					**Ratio**	
	Si	Ca	Na	P	Ca/P	Si/Ti
Surface	45.2	25.1	20.0	9.0	2.7	0.3
Outer	48.7	22.1	21.8	7.2	2.1	0.02
Inner	49.2	20.3	21.8	8.5	2.3	0.01

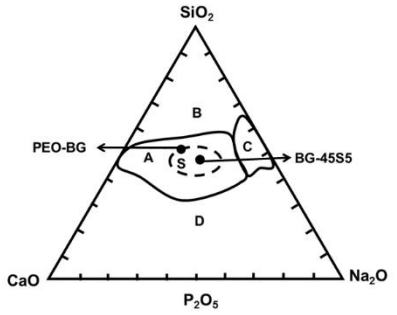

Figure 2. Surface morphology and chemical composition of the controls (cpTi and SLA) and experimental (PEO-BG) groups. **(A)** SEM micrographs top-view (500× magnification), **(B)** three-dimensional CLSM images (50× magnification) and **(C)** chemical mapping by EDS with element concentrations (wt%) on surfaces. Surface area was estimated in cropped images of 100 × 100 µm that were obtained at the magnification of 50×. **(D)** The distribution of bioactive elements on the surface, outer, inner layers of PEO-BG coating and respective stoichiometric proportion based on 45S5-BG are showed on bottom. **(E)** Ternary eutectic diagram showing the relationship between composition and bioactivity level, where regions: A = bone tissue binding, B = no binding to tissues

(low reactivity), C = no binding to tissues (high reactivity), D = no binding to tissues (does not form glass), D = connective tissue binding and S= connective tissue binding is also illustrated.

3.2 PEO-BG coating changes the Ti surface properties leading to mimetic oxide layer composition of the 45S5-bioglass

Cross-section SEM micrographs (Fig. 3A) demonstrated that PEO treatment performed led to an irregular and complex coating on Ti surface. In fact, line roughness profile (Fig. 3A, on top) between PEO-BG and control surfaces shows the difference between both. PEO-BG also showed greater coating thickness when compared to the control groups (Fig. 3B). Additionally, surface roughness (Fig. 3C) of the PEO-BG coating were higher than those observed for the control surfaces ($p < 0.001$), particularly when considering Rt and Rz, as a result of the microdischarges that occurred in the PEO treatment[50]. Interestingly, PEO-BG also revealed superhydrophilic status ($\Theta w = 0^{o}$) (Fig. 3D), where surface adsorbed the water droplet immediately after dripping, exhibiting evident difference with SLA and machined surfaces ($p < 0.001$) confirmed by micrographs (Fig. 3d'). Probably, the morphological structure promotes contact of Si^{4+} (unstable) with OH^{-} water radicals through electrostatic interaction, forming silanoic groups (Si-OH) that makes the surface more reactive and hydrophilic as reported in bioactive glasses scaffolds and bone graft in contact with body fluids [38,76].

Previous studies showed the beneficial synergistic effect of the roughness, hydrophilicity and chemical composition on favoring more protein adsorption, osteoblastic[12,47,79] and fibroblast[50] cell adhesion on PEO surfaces compared to non-treated substrates. Another relevant point is that rougher surface induces the osteoblasts differentiation and enhances the quality of bone formed surrounding dental implants[80]. In fact, anodized dental implant has demonstrated increased bone formation in the early stages of healing, with highest removal torque compared to machined surface due to the greater contact area at the bone/implant interface[55]. Therefore, these surface properties observed on PEO-BG can be a key factor to enhance the osseointegration.

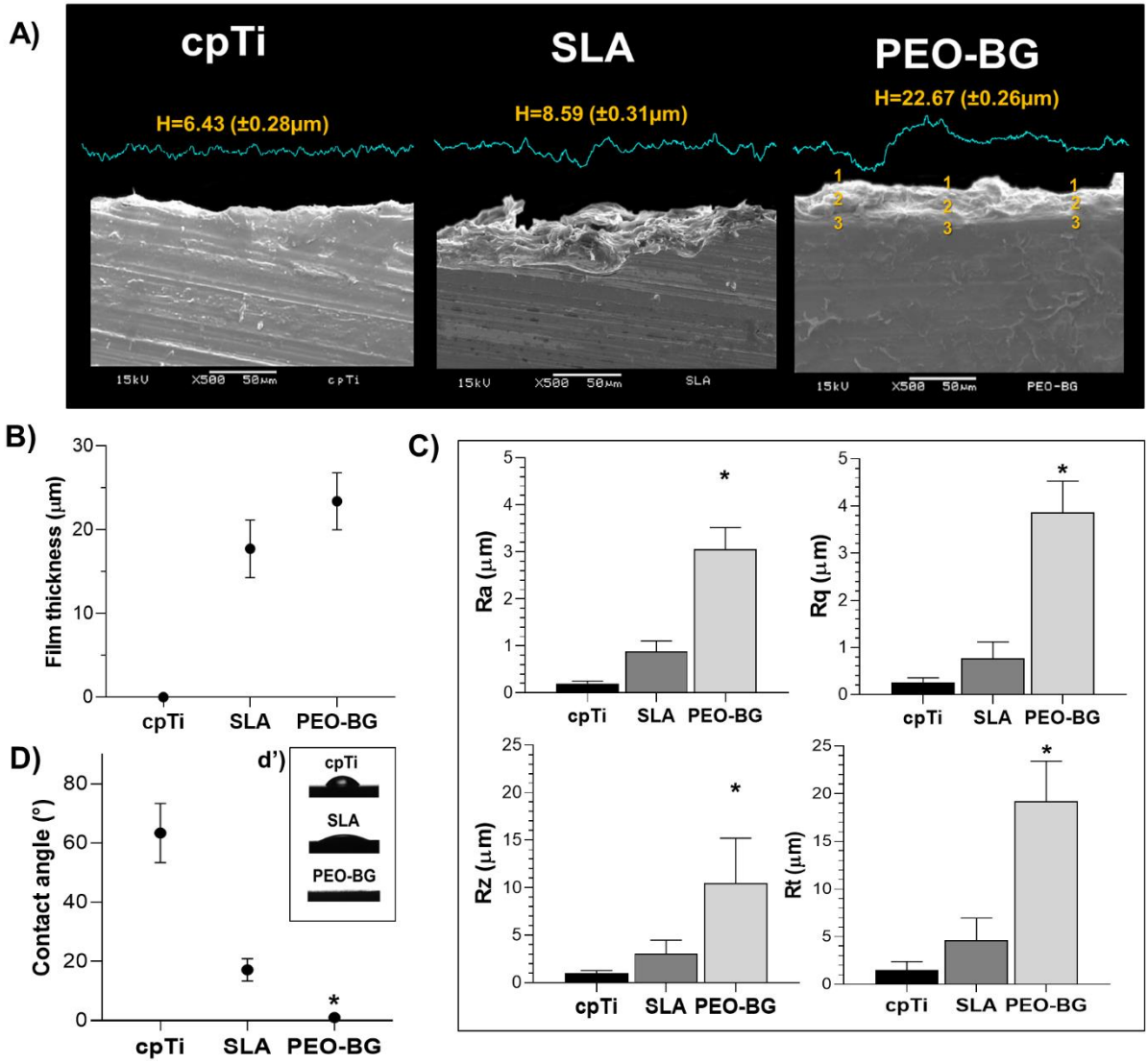

Figure 3. Surfaces characterization. **(A)** SEM micrograph cross-section (500× magnification) showing internal structure of coatings (bottom) as well as height (µm) and difference in profile of surface roughness line by CSLM (top). For PEO-BG coating (on the right), EDS analyzes (Fig. 2) were conducted in 3 different regions (1 = surface; 2 = outer and 3 = inner). **(B)** Coating thickness measured using eddy current method (µm). **(C)** Surface roughness parameters (Ra = arithmetic roughness, Rq = root mean square average, Rt = maximum height and Rz = average peak-to-valley height) by profilometer. **(D)** Water contact angle and (d') representative images of contact angle on

surfaces. *p<0.05, using the Tukey HSD test comparing PEO-BG and SLA surfaces. The error bars indicate standard deviations.

The XRD patterns (Fig. 4A) showed peaks of amorphous Ti (α phase) for all surfaces. In contrast, a mixture of TiO_2 crystalline phases, with characteristic peaks assigned to the anatase (~25°) and rutile (~27°) were obtained for the PEO-BG coating, while peaks assigned to Ti hydride (~22° and ~43º) was observed only for SLA surfaces. Since PEO treatment is considered an oxidation reaction, the micro-discharges trigger reactions involving Ti and O groups in the electrolytic solution, leading to the formation of crystalline structures on surface[44,81].

XPS analysis was performed to investigate the possible oxides states on the outermost Ti surface (Fig. 4B). XPS spectrum showed the expected compounds, including the presence of Ti2p (~455−467 eV) and O1s (~527-533 eV) for all groups, while Al2p (~72-78 eV) was found only on the SLA surface (Fig. 4b'), in agreement with XRD results. Interestingly, the absence of a Ti^0 metallic peak on the PEO surfaces suggests that this treatment generated an oxide coating that was thicker than the native oxide layer on the nontreated control[50]. The chemical composition observed in the EDS mapping (Fig. 2C) was in agreement with the elemental ratios determined by XPS (Fig. 4b''). PEO-BG presented spectrum for SiO_2 (~100-106 eV) , CaO(~345-349 eV) $CaCO_3$(~350-353 eV), Na_2O(~398-402 eV), P^+(~132-134 eV), PO_4^{-3}(~136-141 eV) and P_2O_5(~141-146 eV). The presence of the SiO_2, CaO, Na_2O and P_2O_5 clearly support the study hypothesis that PEO treatment was able to synthesize a mimetic coating in chemical composition as well as 45S5-BG related oxide layer.

A)

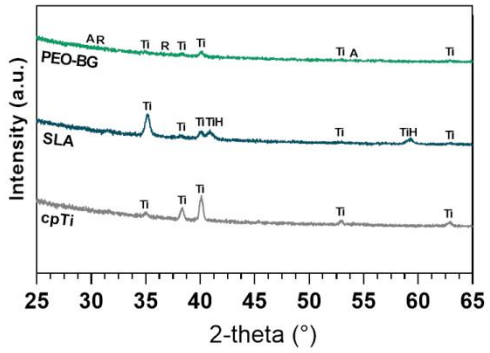

B)

Elemental spectral line	Groups		
	cpTi (at%)	SLA (at%)	PEO-BG (at%)
Ti 2p	33.7	38.2	23.2
O 1s	66.3	56.2	42.7
Al 2p	-	5.6	-
Si 2p	-	-	14.1
Ca 2p	-	-	9.2
Na 1s	-	-	8.7
P 2p	-	-	2.1

b')

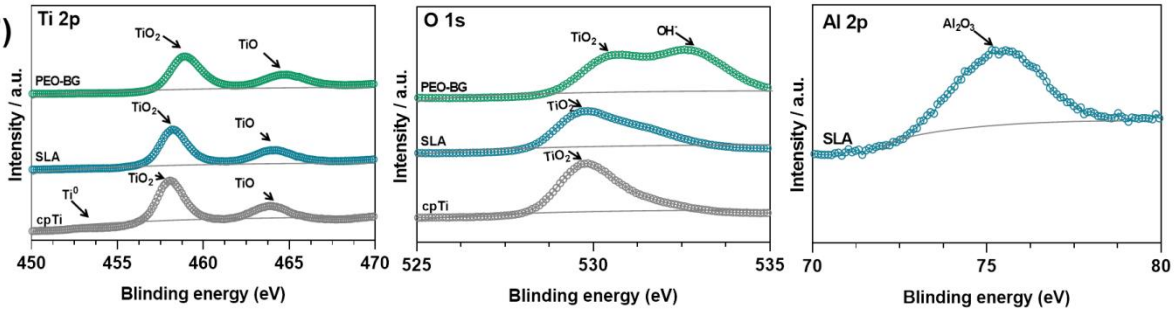

b'')

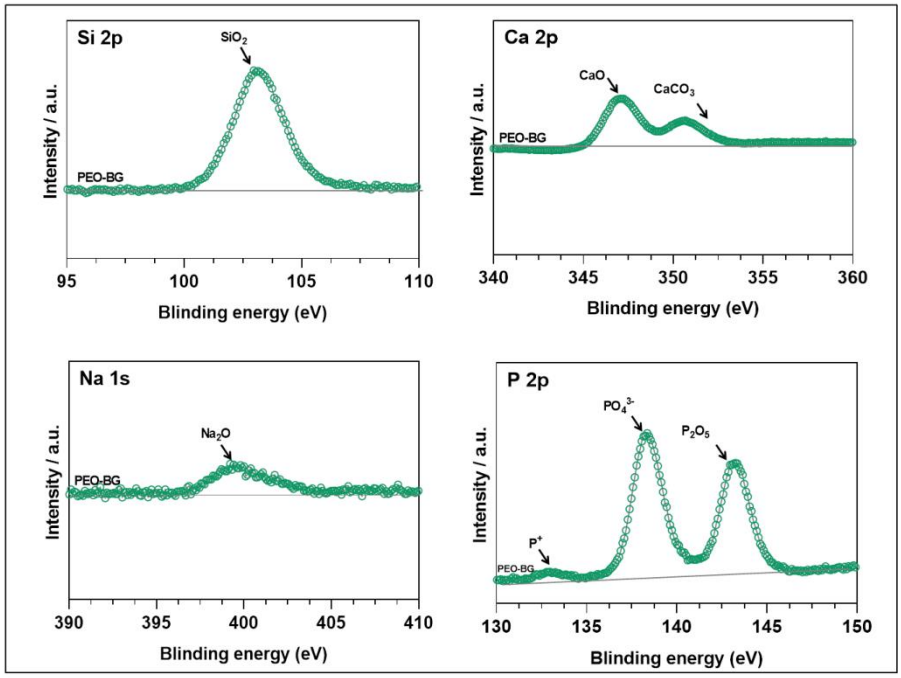

Figure 4. Crystalline phases and oxide layer composition. **(A)** X-ray diffraction pattern (Ti = titanium, TiH = titanium hydrate, A = anatase, and R = rutile). **(B)** Chemical composition details (atomic concentration %) and (b') oxide binding spectra obtained by XPS. (b'') For PEO-BG

coating, 45S5-bioglass oxides composition of bioactivity-related (SiO_2, CaO, Na_2O and P_4O_6) was observed.

3.3 PEO-BG coating enhances mechanical and tribological properties

The main problem with previously developed bioglass coatings is their poor mechanical properties[15,16,34,38,76]. Herein, the newly developed PEO-BG coating enhanced the mechanical properties compared to the well-established control surfaces for dental implants. Macroscopic analysis revealed wear of all coatings after tribological tests (Fig. 5A, on top). In agreement, SEM micrographs showed higher and wide wear scars for SLA surface, while for machined surface was observed deeper and more regular wear (Fig. 5A, on bottom). In contrast, PEO-BG demonstrated good substrate adherence with coating remnants after tribological phenomena with quantitatively lower surface wear area measured by optical microscopy analysis (Fig. 5A), suggesting an effect of the Ti crystalline structure (mainly rutile phase), which provided superior wear resistance due to the good coating adhesion with the substrate[46]. In addition, the presence of a highest coating thickness (Fig. 3B) and higher friction coefficient found in PEO-BG coating (Fig. 5B), can have led to lower mass loss (Fig. 5C) ($p<0.05$).

PEO-BG coating also showed higher microhardness when compared to controls surfaces (Fig. 5D) ($p<0.05$). This finding can be explained by the presence of Ca and Si, which has been previous associated with increased hardness and indirect with higher friction coefficient values[82]. The friction coefficient, with samples of the same tribological pair, was directly related to the resistance of the surface to mechanical wear[82]. In this way, the higher FC values are observed for PEO-BG ($\mu=0.6$) probably due to surface microhardness and coating influence[83], confirming the enhanced strength characteristic when compared to SLA ($\mu=0.3$) and cpTi ($\mu=0.5$) surfaces. During sliding, fluctuations were observed and associated with the build-up and entrapping of a large amount of particles (third bodies) in the contact area as a consequence of higher wear rates. It is

worthwhile to highlight that the higher FC has beneficial effect when considering dental implant due to greater stability and reduced possibility of micromotion that could be transferred to prosthetic components and bone tissue[59].

Although PEO-BG increased the flexural strength of Ti compared to non-treated surface ($p<0.05$) (Fig. 5E), the elastic modulus was not modified ($p>0.05$) (Fig. 5F). A previous review[56] reported that these mechanical properties are strongly related to Ti microstructure. Since PEO treatment changes only Ti surface without altering the bulk microstructure, which has been reported as the main factor that drives these mechanical properties[43]. It is noteworthy that despite not changing the microstructure, the presence of the experimental coating provided greater resistance when compared to machined surface, suggesting a protective effect of Ti surface treatment on structural mechanical damage.

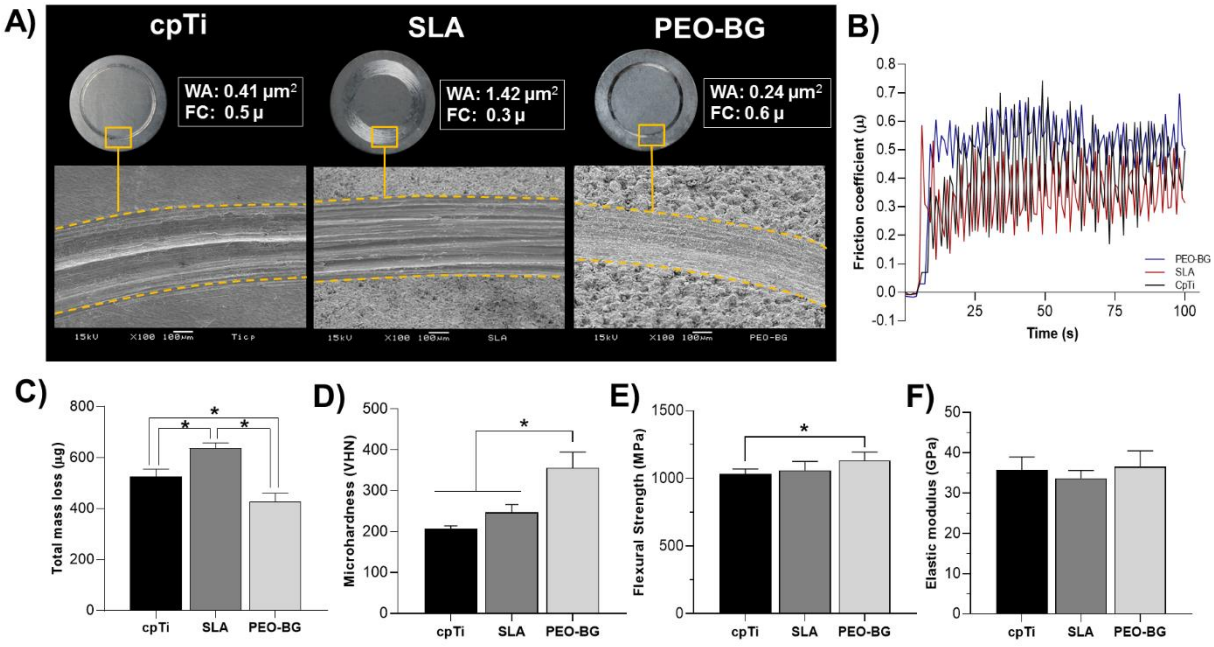

Figure 5. Mechanical properties of cpTi, SLA and PEO-BG coatings. **(A)** In top, visual characterizations of the wear surface and quantitative analyses (WA = wear area and FC = friction coefficient). In bottom, SEM micrographs (100× magnification, 15º inclination) showing surface

wear after tribological test. **(B)** Friction coefficient during sliding (μ). **(C)** Total mass loss of samples comparing before and after tribological wear (μg). **(D)** Microdureza vickers (VHN), **(E)** Flexural strength (MPa) and **(F)** elastic modulus (GPa) also are showed. *p<0.05, using the one-way ANOVA and Tukey (HSD). The error bars indicate standard deviations.

3.4 PEO-BG enhanced corrosion resistance of Ti after simulated degradation in SBF

To evaluate the effect of the oral environment on Ti susceptibility to corrosion, *in vitro* degradation model was performed. Samples were submitted to electrochemical tests (OCP, EIS and potentiodynamic) immediately after receiving the surface treatments (baseline) and after 14 and 28 days of immersion in SBF, following the above-mentioned HAp formation protocol[73]. For the baseline, all groups showed the formation of a stable oxide film after 1h of immersion in SBF with more electropositive OCP for SLA and PEO-BG surfaces, which can infer a less tendency to corrosion for these groups (Fig. S2).

The EIS assessment was carry out to verify the properties of the oxide layer formed in each surface. Initially, the cpTi surface presented greater impedance and phase angle at low frequencies, as well as higher magnitude of the Nyquist arch (wider diameter) compared to the other groups (Fig. S2). It is possible that the dissolution of the surface and consequent ion release of PEO-BG influenced its primary electrochemical stability[48]. In fact, the Na_2O that composes PEO-BG is poorly stable and highly reactive, which is suggestive of rapid dissociation into body fluids. These features also can be attributed to topography/morphology of the surface, where a higher surface roughness of PEO-BG coating may lead to the instability of the TiO_2 layer[56]. On the other hand, PEO-BG demonstrated an exponential improve of all variables (|Z|, θ and Nyquist arch) after 14 (Fig. S3) and 28 days (Fig. 7B-C) of immersion when compared to the other groups, indicating a greater corrosion resistance. In this line, the presence of two phases angle for the treated groups

after 28 days may be result of HAp layer formation on the surface that acts as an additional barrier to ions transport.

To obtain the electrical parameters of the surfaces after 28 days, data were modeled in equivalent electrical circuits (Fig. 7E). A simple circuit consisting of R_{sol} (resistance of the electrolyte), R_p (polarization resistance), and Q (constant phase element, CPE) was used for the machined group, while three electrochemical interfaces were considered for the SLA and PEO-BG surfaces since three layers that behave differently from each other were formed: HAp layer (Q_1 and R_1), oxide layer (Q_2 and R_2), and the substrate (Q_3 and R_3). The chi square (χ^2) values were in the order of 10^{-3}, which indicates an excellent agreement between the experimental and simulated EIS data. Q_{tot} and R_{ptot} were obtained by the sum of Q and R_p of each interface and used for statistical analysis. As expected, after 28 days of immersion PEO-BG showed higher polarization resistance than the others groups ($p<0.05$) and similar capacitance than cpTi surface ($p>0.05$) (Table 1). Probably, a later reactivity of PEO-BG surface with SBF stimulated the formation of an oxide layer more resistant to dissolution, improving its protection against ions exchanges with the electrolyte.

Potentiodynamic polarization curves for baseline (Fig. S2), 14 (Fig. S3) and 28 days (Fig. 7D) were obtained to understand the electrochemical behavior of each surface considering its response to a cyclic polarization. For all time points, PEO-BG displayed a greater passive behavior whit more stable plateau of passivation compared to controls, which can be confirmed by the shifting of its curve to lower current densities. However, cpTi presented the highest E_{corr} among the groups in the baseline and 14 days (Fig. S3). Concerning the electrochemical parameters obtained by the Tafel extrapolation method (Table 2) for 28 days of immersion, PEO-BG surface showed a significant improvement of its electrochemical properties with smaller values of i_{corr}, corrosion rate, and i_{pass} ($p<0.05$) than the other groups. PEO-BG presented a progressive improvement of Ti corrosion resistance after immersion tests, indicating a protective effect in the oral environment by hydroxyapatite-inducing ability (follow data showed). In addition, the presence of Si and Ca in the

PEO-BG surface may act as a ceramic barrier that reduces the diffusion of ions and accelerates HAp formation by decreasing coating instability time (prior to HAp formation).

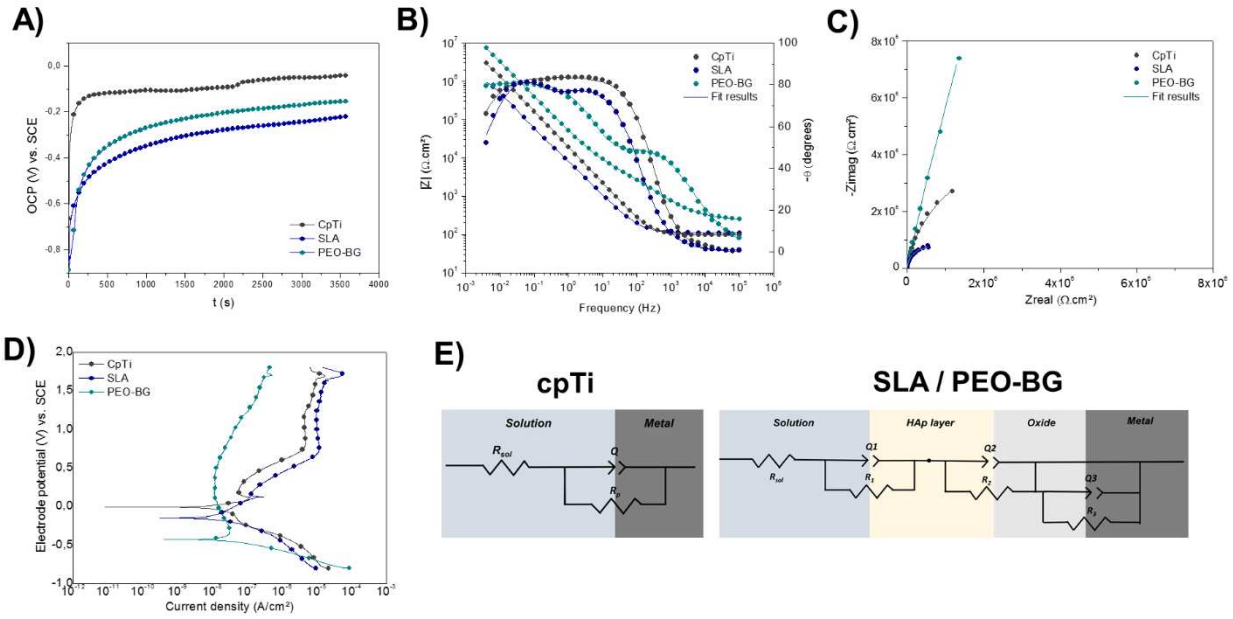

Figure 7. Electrochemical data after 28 days of HAp formation **A)** Evolution of open circuit potential of surfaces as a function of time in SBF. **(B)** Representative impedance ($|Z|$) and phase angle (Θ) plots. **(C)** Representative Nyquist diagrams. **(D)** Representative potentiodynamic polarization curves. **(E)** Equivalent electrical circuits used to fit EIS data.

Table 1. Means and (standard deviations) of electrical parameters (polarization resistance - R_p and capacitance - Q) obtained from the equivalent circuit models of each surfaces.

Groups	Rpx10^6 (MΩ·cm^2)	Qx10^{-5} (nΩ^{-1}s^n·cm^{-2})	η	X^{2}x10^{-3}
cpTi	2.63 (±1.6)^a	9.86 (±4.4)^a	0.93 (±0.11)	1.02 (±0.21)
SLA	3.03 (±2.7)^b	1.57 (±2.8)^b	0.89 (±0.07)	3.26 (±0.12)
PEO-BG	7.31 (±1.34)^c	9.06 (±8.6)^a	0.87 (±0.01)	4.34 (±0.43)

Different letters indicate statistically significant differences among the groups ($p < 0.05$, Tukey's HSD test). R_p = polarization resistance, Q = capacitance, n and X^2x10^{-3} obtained from EIS (goodness of fit on the order of 10^{-3}).

Table 2. Mean and (standard deviation) values of electrochemical parameters (E_{corr}, i_{corr}, β_a, $-\beta_c$, i_{pass} and corrosion rate) obtained from the potentiodynamic polarization curves of each surfaces.

Groups	E_{corr} (mV) vs. SCE	i_{corr} (nA cm^{-2})	βa (mV dec^{-1})	- β_c(mV dec^{-1})	i_{pass} (nA cm^{-2})	Corrosion rate (mpy) x10^{-4}
cpTi	-17.6(±5.8)^{a}	17.6 (±20.4)^{a}	0.90 (±0.3)	0.32(±0.03)	10.9(±2.1)^{a}	6.7(±0.01)^{a}
SLA	-201.3 (±85.05)^{b}	11.73(±11.88)^{a}	0.45(±0.1)	0.12(±0.03)	16.7(±3.6)^{a}	4.4(±0.02)^{b}
PEO-BG	-416.60 (±16.2)^{c}	5.67(±7.78)^{b}	0.70(±0.4)	0.07(±0.01)	5.2(±4.9)^{b}	2.1(±0.02)^{c}

Different letters indicate statistically significant differences among the groups ($p < 0.05$, Tukey's HSD test).

3.5 Developed coating modulates microbial adhesion and biofilm formation reducing pathogenic potential

Since 45S5-BG has antimicrobial effects related to biological mechanisms, we evaluated the possible effect of PEO-BG coating on biofilm formation. Considering the wide composition of oral microbiome, we first tested initial adhesion (2 h) using saliva as microbial inoculum. CSLM images (Fig. 8A) showed highest microbial adhesion on SLA surface with microbial clusters. In contrast, machined and PEO-BG groups demonstrated lower bacterial number that are sparsely distributed on the surface. In fact, PEO-BG coating showed a significant reduction (~1 log CFU) ($p<0.05$, Fig. 8B) on microbial adhesion with lower biovolume ($p<0.05$, Fig. 8C) compared to SLA surface, possibly related to its chemical composition. Afterwards, we evaluated whether this effect on microbial adhesion could affect the biofilm growth on experimental surface. Then, polymicrobial biofilms (saliva as inoculum) was cultivated for 24 h on samples. The SLA surface showed higher biofilm growth with thick bacterial clusters and microcolonies enmeshed in a 3D-extracellular matrix visualized by confocal images (Fig. 8D). Compared to SLA surface, PEO-BG revealed to be able to significantly reduce ($p<0.05$) polymicrobial biofilm formation on Ti as shown by total biovolume measure (Fig. 8E) and CFU counts (Fig. 8F). No significant difference ($p> 0.05$) was found for machined surfaces and PEO-BG in terms of CFU and total biovolume count in both microbial adhesion and biofilm formation. For analysis of bacterial morphology and interaction

with surfaces, the same pattern of biofilm formation was also visualized by SEM micrographs (Fig. S2).

It is well known that rough and hydrophilic dental implant surfaces improve bone responses as well as promote the accumulation of microorganisms[55]. However, PEO-BG coating (Ra = 2.8±0.5 μm) demonstrated similar adhesion and biofilm formation than machined surface (Ra = 0.2±0.1 μm) but reduced when compared to a well-established SLA implant surface (Ra = 0.7±0.2 μm). Although surface characteristics display an important role in biofilm growth, other factors such as chemical composition and related biological mechanisms should be considered. A previous study[20] revealed that particulate 45S5-bioglass reduces the viability of *S. sanguinis* biofilms, probably due to a diffuse antibacterial effect produced by increased pH levels. Similarly, it was also confirmed in *S. aureus* biofilms that increased pH is directly associated with ion release of the BG surface[21]. Hence, an alkaline environment generated by ion release induces a possible bactericidal effect through the osmotic difference and consequent disruption of the bacterial cell wall[15,38]. Additionally, the irregularities and crystalline structure can lead to bacterial death by surface interactions[22]. The biological mechanisms behind such antimicrobial effects were further evaluated (data showed follow).

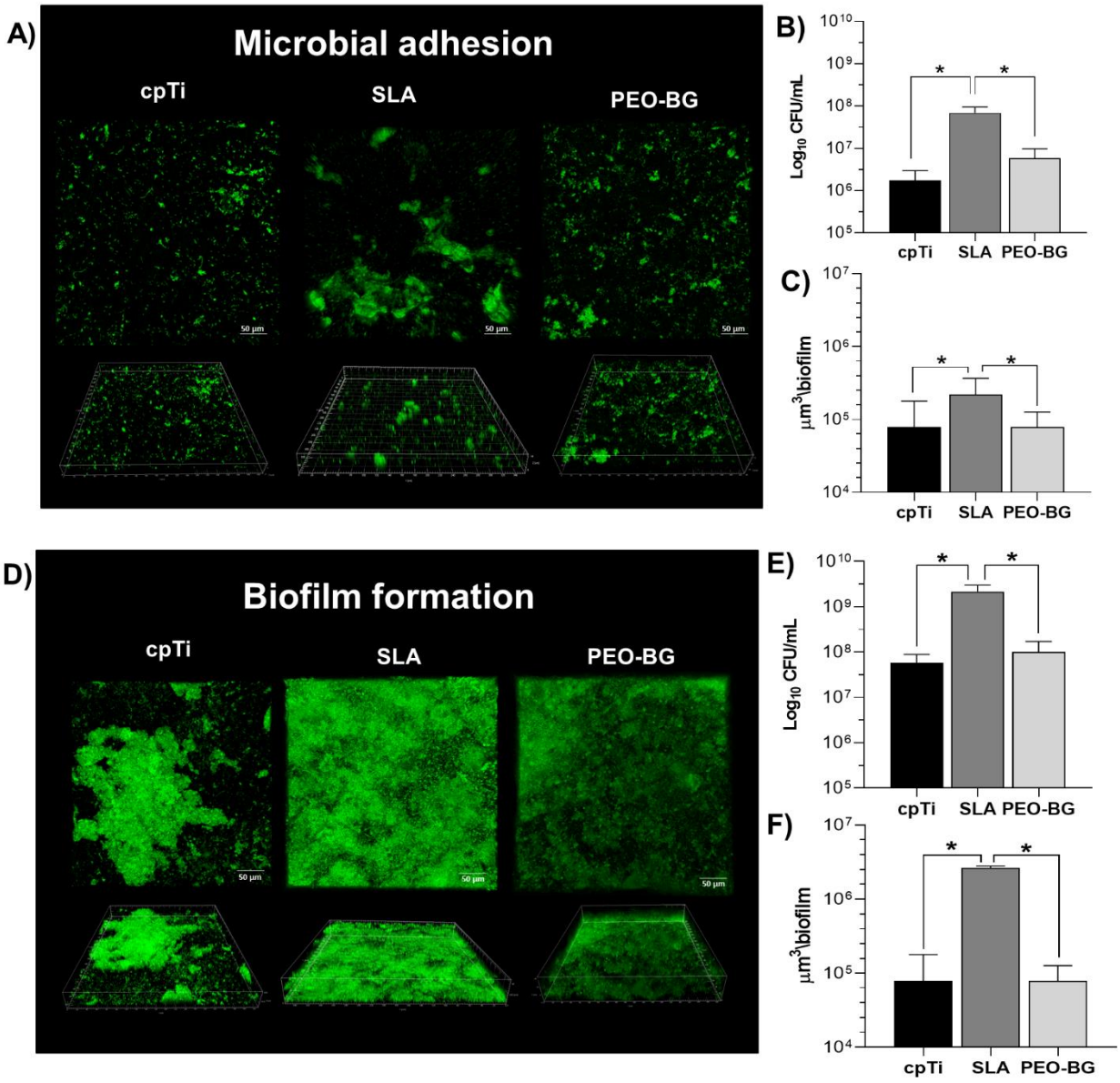

Figure 8. Microbiological assays on cpTi, SLA and PEO-BG surfaces. **(A)** X–Y isosurfaces (top panel) and three-dimensional reconstructions (bottom panel) of representative CLSM images, **(B)** total bacterial counts (CFU/mL) and **(C)** average total biovolumes (in μm^3) after microbial adhesion for 2 h using saliva as microbial inoculum. Similarly, **(D)** X–Y isosurfaces (top panel) and three-dimensional reconstructions (bottom panel) of representative CLSM images, **(E)** total bacterial counts (CFU/mL) and **(F)** average total biovolumes (in μm^3) were evaluated after biofilm formation for 24 h. Live cells were stained in green using SYTO-9 (480–500 nm). Scale bars, 50 µm (X–Y

isosurfaces) and 70 µm (three-dimensional reconstructions) for confocal images. *p<0.05, using the one-way ANOVA and Tukey (HSD). The error bars indicate standard deviations.

To better understand the surface effect and characterize these biofilms, we investigated the influence of PEO-BG on biofilm composition. For this, 40 bacterial species related to infections surrounding dental implants (described as peri-implant diseases)[84] were evaluated (Fig. 9A). For microbial adhesion, the total DNA count of 40 bacteria evaluated was higher for SLA surface (43.5 ±2.8) than cpTi (8.2 ±8.9) and PEO-BG (9.3 ± 4.4) groups, according to CFU counts. Although bacterial growth between cpTi and PEO-BG surfaces is similar, some periodontal pathogens such as *Actinomyces israelii*, *Actinomyces oris*, *Prevotella nigrescens* and *Treponema forsythia* showed significantly reduced adhesion on experimental surface ($p<0.05$). Importantly, PEO-BG modulated microbial adhesion and reduced the pathogenic potential of oral biofilm, decreasing significantly the colonization of red complex bacteria compared to machined and SLA surfaces ($p<0.05$).

Peri-implant biofilm control is an important characteristic to be considered in surface treatments proposed for dental implants[7]. However, previous studies with bioactive glasses coatings are focused on improving osseointegration and little is known about microbiological behavior[17,32]. Our findings showed that PEO-BG promoted the modulation of surface microbial adhesion and reduced the biofilm pathogenicity. Although PEO-BG has no antimicrobial activity, TiO_2 layer effect[85] and 45S5-BG-related oxides (Fig. 4b'') could trigger species-specific and bacteriostatic effect on oral microorganisms. Nowadays, clinical trends have led to the use of surface modified implants (i.e. SLA treatment) rather than machined surfaces[1], where PEO-BG coating may be a favorable approach for practical application. In addition, the biofilm structure formed on PEO-BG coating with lower density (Fig. 8D) and amount of periodontal pathogens (Fig. 9B) compared to SLA surface can even favor the effect of antimicrobials therapies and decrease of the peri-implantitis risk.

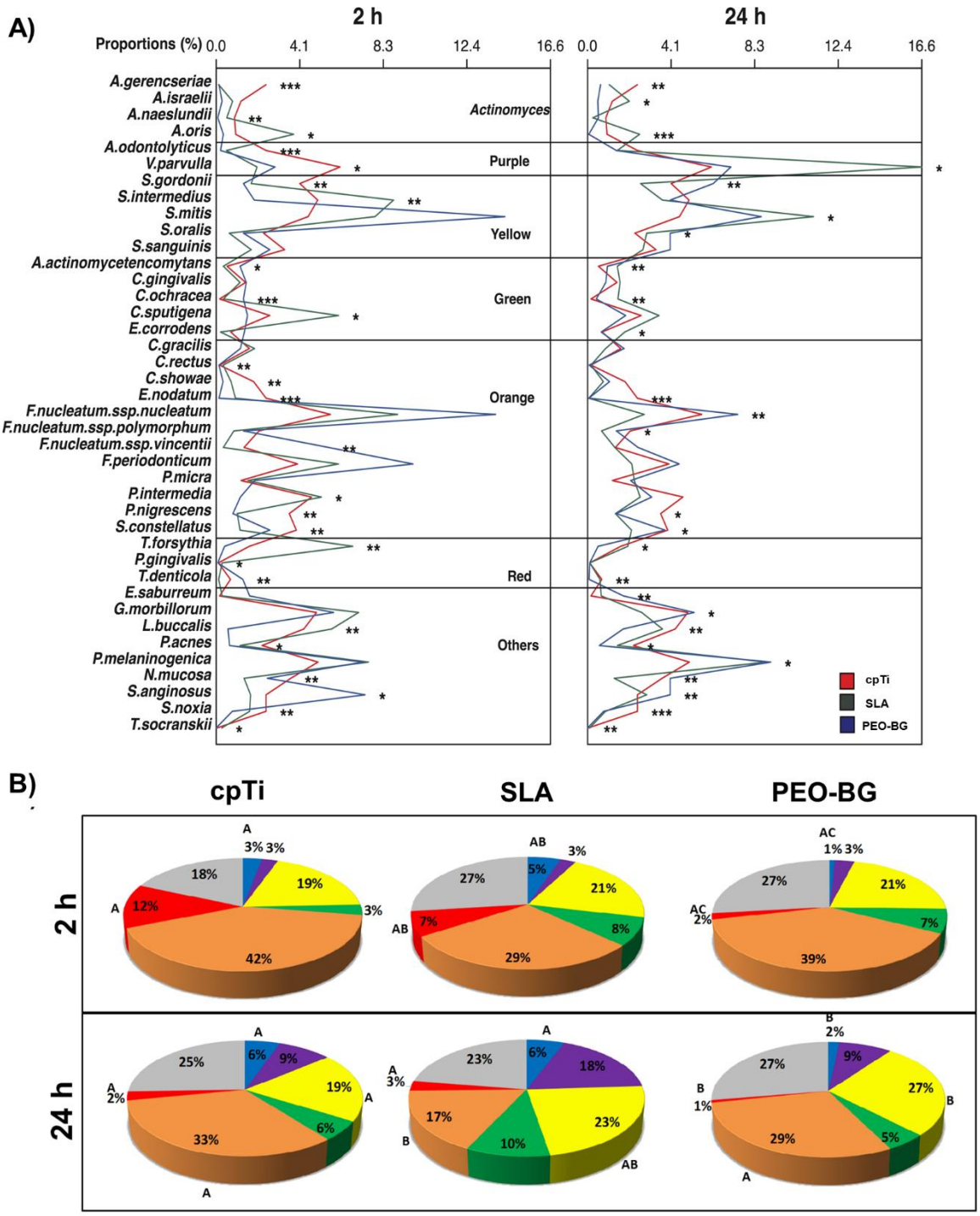

Figure 9. Checkerboard DNA-DNA hybridization analysis. **(A)** Profile of mean levels ($\times 10^5$) of 40 bacterial species in polymicrobial biofilms growth on cpTi, SLA and PEO-BG surfaces for microbial adhesion (2 h) and biofilm formation (24 h). Asterisks indicate difference between groups

indicate statistically significant difference among the groups (*p< 0.05**p < 0.01, ***p < 0.001, HSD Tukey test). Levels of individual species were computed in each sample and then averaged in each group. **(B)** Proportion of periodontal complexes. Different letters indicate statistically significant difference among the groups (p<0.05, HSD Tukey test).

3.6 PEO-BG is a bioactive coating by HAp-inducing ability with similar 45S5-BG biological mechanism

Bioactive glasses have gained attention in the biomedical area because their biological mechanisms such as release of bioactive ions and pH fluctuations, which create a suitable environment for rapid HAp-inducing[16]. Hence, the formation of HAp crystals in SBF was investigated to predict bioactivity *in vivo*[60,73]. After SBF immersion for 7 days, amorphous depositions were observed on all surfaces by SEM micrographs (Fig. 10A). However, XRD analysis did not confirm the presence of HAp peaks (Fig. 10B). These findings are suggestive only of calcium and phosphorus clusters that are strongly attracted to the surface by electrostatic difference[62]. In this study, the presence of a newly formed HAp phase was observed on the cpTi and PEO-BG coatings after 14 days the immersion. With the increase of immersion time to 28 days, the apatite layers were found for all surfaces. These results demonstrate that PEO-BG was able to induce HAp formation similar to CpTi and faster than SLA surface, suggesting that topography and chemical composition play an important role in HAp formation kinetics[44].

It is noteworthy that morphology of newly formed HAp was different between surfaces. Notably, machined surface presented HAp with classical morphology of the nanosize granular particles. In contrast, SLA and PEO-BG surfaces presented the nanosize Ca-P particles that together form a micro ball-like structure.. Similar HAp morphology has already been described as nano flake-like structure formation on PEO surface[63]. Since PEO-BG is a rough coating with several surface craters (Fig. 2A), these regions may lead to accumulation of Ca-P, forming clusters rather

than a layer as on machined surface. However, increased roughness as a consequence of irregular HAp deposition may favor osteogenic responses. Thus, our findings suggest that PEO-BG may be considered a bioactive coating in biological systems.

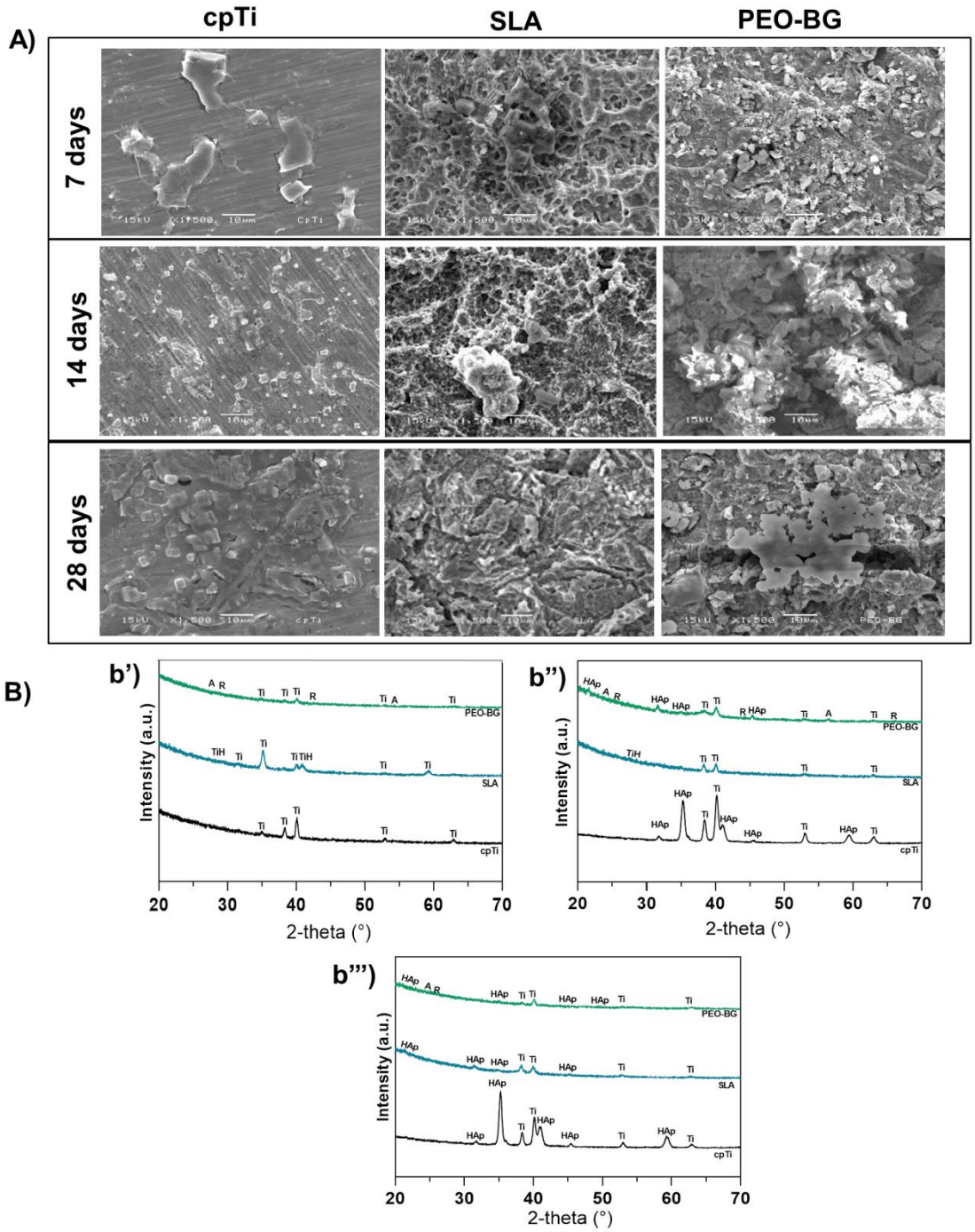

Figure 10. *In vitro* bioactivity assay. PEO-BG, SLA and cpTi samples were immersed in SBF solution to induce hydroxyapatite formation on surfaces. **(A)** SEM micrographs were performed after 7, 14 and 28 days of immersion to evaluate the hydroxyapatite morphology. **(B)** XRD analysis was conducted to confirm the hydroxyapatite formation after 7 (b'), 14 (b'') and 28 (b''') days (Ti = titanium, TiH = titanium hydrate, A = anatase, R = rutile and Hap = hydroxyapatite).

The biological effects of bioactive glasses have been associated also with ion release and pH fluctuation of environment [15,16,22,38]. Based on this, these properties were evaluated on all surfaces tested herein. cpTi and SLA surfaces showed progressive release of Ti^{4+} (Fig. 11A) and Ti^{4+} and Al^{3+}(Fig. 11B) ion, respectively. PEO-BG coating also demonstrated progressive release of all bioactive elements (Fig. 11C). Remarkably, highest Na+ release followed by Ca2+, Si4+ and P+ was observed (first 8 h) and maintaining the proportion of the released elements up to 72 h (Fig. 11c"). These bioactive ion release triggers biological mechanisms[38], while may reduce Ti^{4+} release that has been associated to osteoblast cell damage[86] and peri implant biofilm dysbiosis[87]. Regarding pH (Fig. 11D), PEO-BG coating presented higher values (~5.5) up to 12 h compared to control surface ($p < 0.05$), confirming the effect of ion release on pH increase[16].

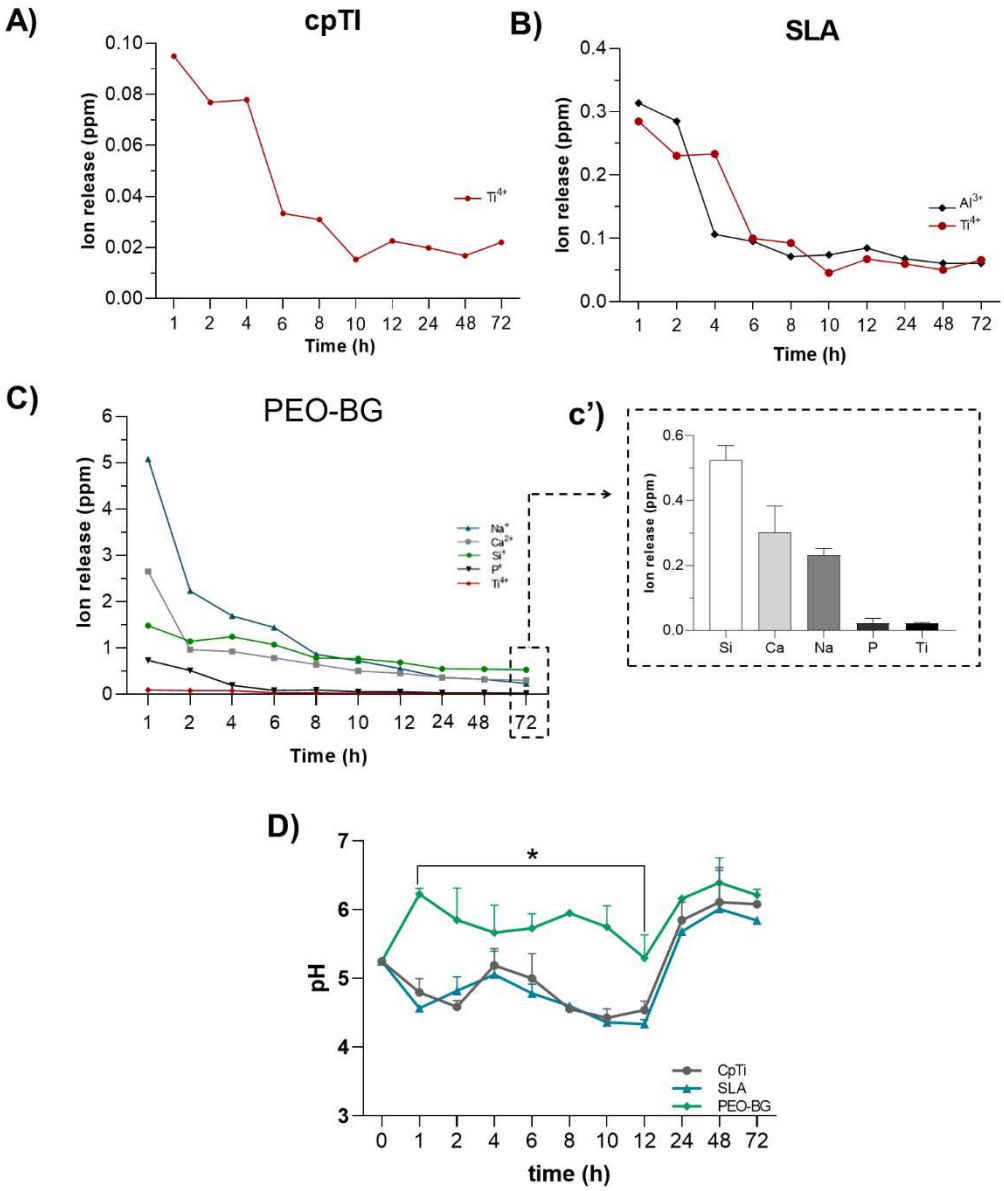

Figure 11. Biological mechanisms of PEO-BG. Ion release on **(A)** cpTi, **(B)** SLA and **(C)** PEO-BG surfaces with progressive release of bioactive elements up to 72 h **(c')** evaluated by ICP-OES analysis. **(D)** pH measurement.

3.7 PEO-BG coating is biocompatible to human cells and improved blood protein adsorption

From the materials perspective, cytotoxicity tests of newly surfaces are considered a prerequisite to enable their future biomedical application[50]. In order to evaluate the biocompatibility

of this newly developed surface, we then tested whether the PEO-BG coating would affect human fibroblast cell colonization and proliferation. During the natural process of cellular metabolism, the resazurin dye, from alamarBlue fluorometric assay, is reduced to resorufin and generates a highly fluorescent pink signal. Conversely, nonviable cells lose the ability to convert the dye into the fluorescent product and thus do not generate the fluorescent signal. Our data clearly revealed no statistically significant difference in cell proliferation among cpTi and PEO-BG, and positive control (Fig. 12A-a'), 24 h after seeding. Consistent with the above-determined quantitative outcomes, fluorescent live/dead staining also revealed viable fibroblast cells growing on cpTi and PEO-BG samples. The green fluorescence from CFSE evidenced an obvious similarity in the overall live cells between PEO-BG and control samples (C+ and cpTi) (Fig. 12B). The surface properties of materials have a strong impact on cell behavior[47]. In fact, a notable alteration in cell alignment can be observed after our treatments change the Ti surface roughness from smooth (untreated surface) to rough (treated surface). In the case of cpTi samples, fibroblast cells appear to favor the orientation in the direction of the longitudinal grooves as compared to the random organization observed on flat polystyrene plate substrates used as controls. Interestingly, the rough surface topography of the PEO-BG samples induced fibroblast cell organization in a particular spatial pattern. Taken together the present findings, we clearly demonstrate that PEO-BG surfaces did not interfere on fibroblast cell viability may be considered biocompatibility coating.

One of the ways to predict the osseointegration responses of biomedical materials is to investigate protein adsorption on their surfaces[74]. In this way, PEO-BG provided a noticeable increase in protein adsorption (~2-fold increase) ($p<0.05$) compared to control surfaces, making it a suitable coating for providing a response to the early stages of osseointegration. Beline et al.[48] demonstrated that PEO coatings provided more binding sites for fibrinogen and fibronectin (important blood plasma proteins) than sandblasted surfaces due to non-specific attractions between functional groups of the protein (negatively charged) or OH^- groups with Ca^{2+} ions present on PEO

surface. Similar results were also found for albumin adsorption on PEO surface related to the hydrophilicity compared to machined surface[49,50].

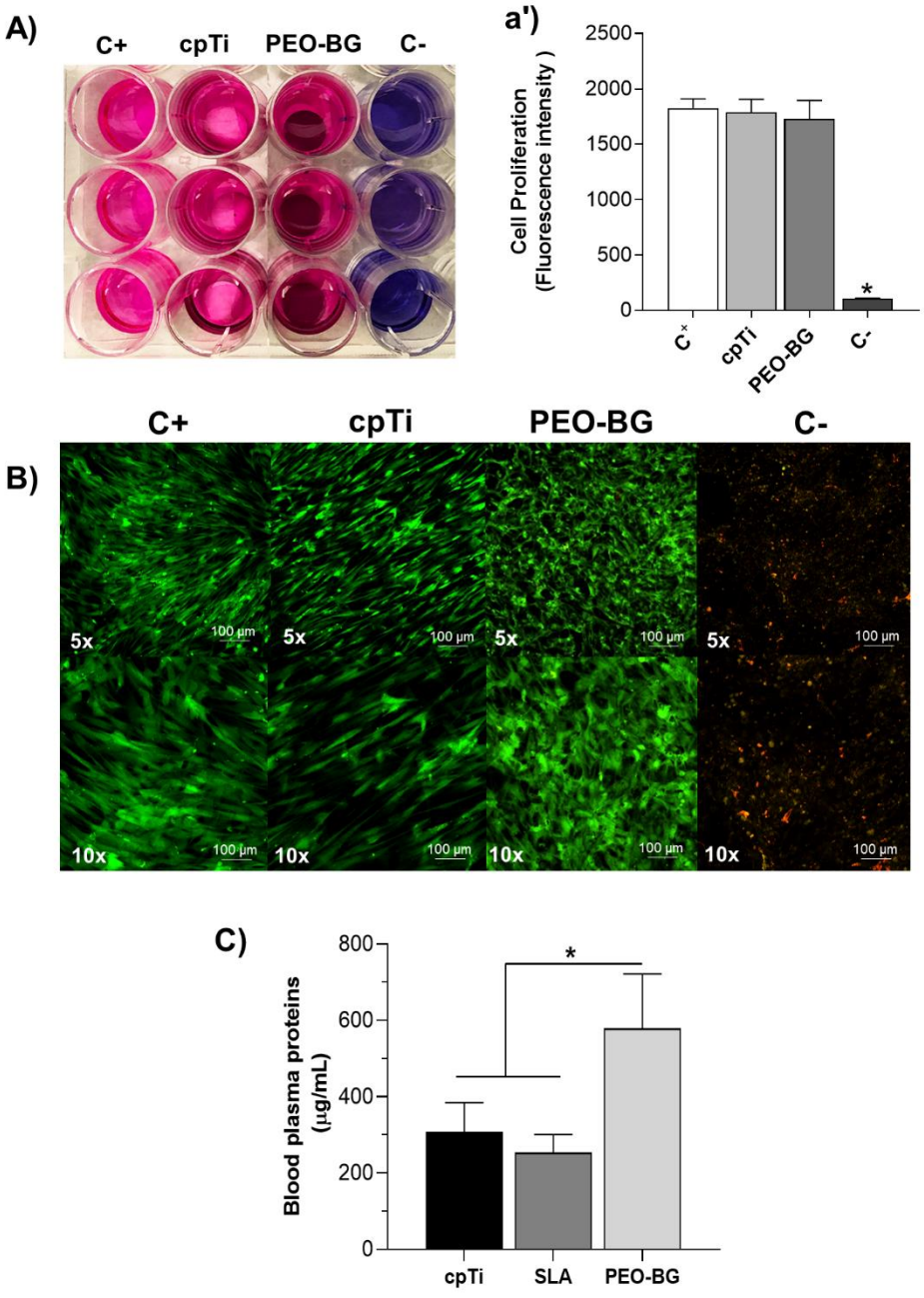

Figure 12. (A) Effect of PEO-BG and cpTi surfaces on HGF cell proliferation and **(B)** cell viability at 24 h. Representative images of fluorescence staining through 20× objectives illustrated live/dead cell distribution on each control (C^+, C^-, and cpTi) and PEO-BG samples (green for live cells, red

for dead cells). The scale bar corresponds to 50 μm. **(C)** Blood plasma proteins adsorption (μg/mL).* indicates a statistically significant difference between groups ($p<0.05$; Tukey HSD test).

3.8 Practical Implications and Future Aim

From the viewpoint of oral rehabilitation, our results support the possibility of using the PEO-BG coating on Ti for dental implant application. The two main challenges in the implantology field are related to inferior osseointegration[88] and peri-implant infections[89], which could be minimized by PEO-BG coatings. It is important to emphasize that for the first time a bioactive glass-based coating exhibited improved mechanical properties on Ti surface. Additionally, biological properties related to chemical composition of 45S5-BG may promote oral biofilm modulation, induce HAp formation and increase protein adsorption, which may trigger better response to the early stages of osseointegration. Hence, PEO-BG may be indicated for dental implant coating due to its ability to modulate and reduce the pathogenic potential of peri-implant biofilm, feature that is not presented in recent surface treatments (i.e. SLA coating).

Furthermore, it is important to highlight that although PEO-BG has showed interesting biomechanical responses, it is still need to understand better the role of this new coating in the mechanisms involved in biological systems. In parallel, future steps can be focused to understand the behavior of PEO-BG coating against simultaneous wear, chemical and microbiological degradation processes by tribocorrosion tests and their osseointegration behaviour in animal models. Finally, our findings here also encourage further studies to continue the investigation of the bioactive glass-based coating deposited by PEO on Ti alloys, Zr substrate and biomedical devices.

4. CONCLUSIONS

PEO-BG coating was successfully synthesized via plasma electrolytic oxidation bio-inspired on 45S5-BG. The newly developed coating showed complex surface topography, that enhances mechanical properties and corrosion resistance. PEO-BG was also able to modulate

surface microbial adhesion and reduce the pathogenicity of oral biofilm. Additionally, PEO-BG coating displays prolonged ion release and pH variation, which leads to HAp inducing ability and excellent blood plasma proteins adsorption. Thus, PEO-BG coating with improved biomechanical properties can be considered a new approach for dental implants due to its probable better response to osseointegration and reduction of the peri-implant biofilm pathogenicity.

AUTHOR INFORMATION

Corresponding Author

*E-mail: vbarao@unicamp.br

Author Contributions

The manuscript was written through contributions of all authors. All authors have given approval to the final version of the manuscript.

Notes

The authors declare no competing financial interests.

ACKNOWLEDGMENTS

This study was financed by the State of Sao Paulo Research Foundation (FAPESP) (grant number 2018/04630-2) and by FAEPEX UNICAMP through a research grant (3164/18). The authors also thank the Oral Biochemistry Laboratory at Piracicaba Dental School at the University of Campinas (UNICAMP) for the microbiology facility, the Laboratory of Technological Plasmas at the São Paulo State University (UNESP) for the PEO facility, and the Brazilian Nanotechnology National Laboratory (LNNano) at the Brazilian Center of Research in Energy and Materials (CNPEM) for the CSLM facilities.

REFERENCES

(1) Spriano, S.; Yamaguchi, S.; Baino, F.; Ferraris, S. A Critical Review of Multifunctional Titanium Surfaces: New Frontiers for Improving Osseointegration and Host Response, Avoiding Bacteria Contamination. *Acta Biomaterialia* **2018**, *79*, 1–22. https://doi.org/10.1016/j.actbio.2018.08.013.

(2) Zembic, A.; Kim, S.; Zwahlen, M.; Kelly, J. R. Systematic Review of the Survival Rate and Incidence of Biologic, Technical, and Esthetic Complications of Single Implant Abutments Supporting Fixed Prostheses. *Int J Oral Maxillofac Implants* **2014**, *29 Suppl*, 99–116. https://doi.org/10.11607/jomi.2014suppl.g2.2.

(3) Srinivasan, M.; Meyer, S.; Mombelli, A.; Müller, F. Dental Implants in the Elderly Population: A Systematic Review and Meta-Analysis. *Clin Oral Implants Res* **2017**, *28* (8), 920–930. https://doi.org/10.1111/clr.12898.

(4) Mathew, M. T.; Kerwell, S.; Lundberg, H. J.; Sukotjo, C.; Mercuri, L. G. Tribocorrosion and Oral and Maxillofacial Surgical Devices. *Br J Oral Maxillofac Surg* **2014**, *52* (5), 396–400. https://doi.org/10.1016/j.bjoms.2014.02.010.

(5) Arciola, C. R.; Campoccia, D.; Montanaro, L. Implant Infections: Adhesion, Biofilm Formation and Immune Evasion. *Nat Rev Microbiol* **2018**, *16* (7), 397–409. https://doi.org/10.1038/s41579-018-0019-y.

(6) Beline, T.; da Silva, J. H. D.; Matos, A. O.; Azevedo Neto, N. F.; de Almeida, A. B.; Nociti Júnior, F. H.; Leite, D. M. G.; Rangel, E. C.; Barão, V. A. R. Tailoring the Synthesis of Tantalum-Based Thin Films for Biomedical Application: Characterization and Biological Response. *Mater Sci Eng C Mater Biol Appl* **2019**, *101*, 111–119. https://doi.org/10.1016/j.msec.2019.03.072.

(7) Chrcanovic, B. R.; Kisch, J.; Albrektsson, T.; Wennerberg, A. Factors Influencing Early Dental Implant Failures. *J. Dent. Res.* **2016**, *95* (9), 995–1002. https://doi.org/10.1177/0022034516646098.

(8) Suárez-López Del Amo, F.; Garaicoa-Pazmiño, C.; Fretwurst, T.; Castilho, R. M.; Squarize, C. H. Dental Implants-Associated Release of Titanium Particles: A Systematic Review. *Clin Oral Implants Res* **2018**. https://doi.org/10.1111/clr.13372.

(9) Gao, A.; Hang, R.; Bai, L.; Tang, B.; Chu, P. K. Electrochemical Surface Engineering of Titanium-Based Alloys for Biomedical Application. *Electrochimica Acta* **2018**, *271*, 699–718. https://doi.org/10.1016/j.electacta.2018.03.180.

(10) Shibata, Y.; Tanimoto, Y. A Review of Improved Fixation Methods for Dental Implants. Part I: Surface Optimization for Rapid Osseointegration. *J Prosthodont Res* **2015**, *59* (1), 20–33. https://doi.org/10.1016/j.jpor.2014.11.007.

(11) Hotchkiss, K. M.; Ayad, N. B.; Hyzy, S. L.; Boyan, B. D.; Olivares-Navarrete, R. Dental Implant Surface Chemistry and Energy Alter Macrophage Activation in Vitro. *Clin Oral Implants Res* **2017**, *28* (4), 414–423. https://doi.org/10.1111/clr.12814.

(12) Santos-Coquillat, A.; Mohedano, M.; Martinez-Campos, E.; Arrabal, R.; Pardo, A.; Matykina, E. Bioactive Multi-Elemental PEO-Coatings on Titanium for Dental Implant Applications. *Materials Science and Engineering: C* **2019**, *97*, 738–752. https://doi.org/10.1016/j.msec.2018.12.097.

(13) Hench, L. L.; Splinter, R. J.; Allen, W. C.; Greenlee, T. K. Bonding Mechanisms at the Interface of Ceramic Prosthetic Materials. *Journal of Biomedical Materials Research* **1971**, *5* (6), 117–141. https://doi.org/10.1002/jbm.820050611.

(14) Moura, J.; Teixeira, L. N.; Ravagnani, C.; Peitl, O.; Zanotto, E. D.; Beloti, M. M.; Panzeri, H.; Rosa, A. L.; Oliveira, P. T. de. In Vitro Osteogenesis on a Highly Bioactive Glass-Ceramic (Biosilicate®). *Journal of Biomedical Materials Research Part A* **2007**, *82A* (3), 545–557. https://doi.org/10.1002/jbm.a.31165.

(15) Jones, J. R. Reprint of: Review of Bioactive Glass: From Hench to Hybrids. *Acta Biomater* **2015**, *23 Suppl*, S53-82. https://doi.org/10.1016/j.actbio.2015.07.019.

(16) Hench, L. L. The Story of Bioglass. *J Mater Sci Mater Med* **2006**, *17* (11), 967–978. https://doi.org/10.1007/s10856-006-0432-z.

(17) Rohr, N.; Nebe, J. B.; Schmidli, F.; Müller, P.; Weber, M.; Fischer, H.; Fischer, J. Influence of Bioactive Glass-Coating of Zirconia Implant Surfaces on Human Osteoblast Behavior in Vitro. *Dent Mater* **2019**, *35* (6), 862–870. https://doi.org/10.1016/j.dental.2019.02.029.

(18) Montazerian, M.; Zanotto, E. D. Bioactive and Inert Dental Glass-Ceramics. *J Biomed Mater Res A* **2017**, *105* (2), 619–639. https://doi.org/10.1002/jbm.a.35923.

(19) Rizwan, M.; Alias, R.; Zaidi, U. Z.; Mahmoodian, R.; Hamdi, M. Surface Modification of Valve Metals Using Plasma Electrolytic Oxidation for Antibacterial Applications: A Review. *J Biomed Mater Res A* **2018**, *106* (2), 590–605. https://doi.org/10.1002/jbm.a.36259.

(20) Allan, I.; Newman, H.; Wilson, M. Particulate Bioglass Reduces the Viability of Bacterial Biofilms Formed on Its Surface in an in Vitro Model. *Clin Oral Implants Res* **2002**, *13* (1), 53–58. https://doi.org/10.1034/j.1600-0501.2002.130106.x.

(21) Coraça-Huber, D. C.; Fille, M.; Hausdorfer, J.; Putzer, D.; Nogler, M. Efficacy of Antibacterial Bioactive Glass S53P4 against S. Aureus Biofilms Grown on Titanium Discs in Vitro. *J. Orthop. Res.* **2014**, *32* (1), 175–177. https://doi.org/10.1002/jor.22463.

(22) Drago, L.; Toscano, M.; Bottagisio, M. Recent Evidence on Bioactive Glass Antimicrobial and Antibiofilm Activity: A Mini-Review. *Materials (Basel)* **2018**, *11* (2). https://doi.org/10.3390/ma11020326.

(23) Asif, I. M.; Shelton, R. M.; Cooper, P. R.; Addison, O.; Martin, R. A. In Vitro Bioactivity of Titanium-Doped Bioglass. *J Mater Sci Mater Med* **2014**, *25* (8), 1865–1873. https://doi.org/10.1007/s10856-014-5230-4.

(24) Verné, E.; Fernández Vallés, C.; Vitale Brovarone, C.; Spriano, S.; Moisescu, C. Double-Layer Glass-Ceramic Coatings on Ti6Al4V for Dental Implants. *Journal of the European Ceramic Society* **2004**, *24* (9), 2699–2705. https://doi.org/10.1016/j.jeurceramsoc.2003.09.004.

(25) Esteban-Tejeda, L.; Díaz, L. A.; Cabal, B.; Prado, C.; López-Piriz, R.; Torrecillas, R.; Moya, J. S. Biocide Glass–Ceramic Coating on Titanium Alloy and Zirconium Oxide for Dental Applications. *Materials Letters* **2013**, *111*, 59–62. https://doi.org/10.1016/j.matlet.2013.08.049.

(26) Nelson, G. M.; Nychka, J. A.; McDonald, A. G. Structure, Phases, and Mechanical Response of Ti-Alloy Bioactive Glass Composite Coatings. *Materials Science and Engineering: C* **2014**, *36*, 261–276. https://doi.org/10.1016/j.msec.2013.12.017.

(27) Popa, A. C.; Stan, G. E.; Enculescu, M.; Tanase, C.; Tulyaganov, D. U.; Ferreira, J. M. F. Superior Biofunctionality of Dental Implant Fixtures Uniformly Coated with Durable Bioglass Films by Magnetron Sputtering. *Journal of the Mechanical Behavior of Biomedical Materials* **2015**, *51*, 313–327. https://doi.org/10.1016/j.jmbbm.2015.07.028.

(28) Díaz, L. A.; Cabal, B.; Prado, C.; Moya, J. S.; Torrecillas, R.; Fernández, A.; Arhire, I.; Krieg, P.; Killinger, A.; Gadow, R. High-Velocity Suspension Flame Sprayed (HVSFS) Soda-Lime Glass Coating on Titanium Substrate: Its Bactericidal Behaviour. *Journal of the European Ceramic Society* **2016**, *36* (10), 2653–2658. https://doi.org/10.1016/j.jeurceramsoc.2016.02.046.

(29) Xue, B.; Guo, L.; Chen, X.; Fan, Y.; Ren, X.; Li, B.; Ling, Y.; Qiang, Y. Electrophoretic Deposition and Laser Cladding of Bioglass Coating on Ti. *Journal of Alloys and Compounds* **2017**, *710*, 663–669. https://doi.org/10.1016/j.jallcom.2017.03.209.

(30) Mehana Usmaniya, U.; Anusha Thampi, V. V.; Subramanian, B. Electrophoretic Deposition of Bioactive Glass-Nanoclay Nanocomposites on Titanium. *Applied Clay Science* **2019**, *167*, 1–8. https://doi.org/10.1016/j.clay.2018.10.002.

(31) Kirsten, A.; Hausmann, A.; Weber, M.; Fischer, J.; Fischer, H. Bioactive and Thermally Compatible Glass Coating on Zirconia Dental Implants. *J Dent Res* **2015**, *94* (2), 297–303. https://doi.org/10.1177/0022034514559250.

(32) Barros, S. A. de L.; Soares, D. G.; Leite, M. L.; Basso, F. G.; Costa, C. A. de S.; Adabo, G. L.; Barros, S. A. de L.; Soares, D. G.; Leite, M. L.; Basso, F. G.; et al. Influence of Zirconia-Coated Bioactive Glass on Gingival Fibroblast Behavior. *Brazilian Dental Journal* **2019**, *30* (4), 333–341. https://doi.org/10.1590/0103-6440201902417.

(33) Koller, G.; Cook, R. J.; Thompson, I. D.; Watson, T. F.; Di Silvio, L. Surface Modification of Titanium Implants Using Bioactive Glasses with Air Abrasion

Technologies. *J Mater Sci Mater Med* **2007**, *18* (12), 2291–2296. https://doi.org/10.1007/s10856-007-3137-z.

(34) Matinmanesh, A.; Rodriguez, O.; Towler, M. R.; Zalzal, P.; Schemitsch, E. H.; Papini, M. Quantitative Evaluation of the Adhesion of Bioactive Glasses onto Ti6Al4V Substrates. *Materials & Design* **2016**, *97*, 213–221. https://doi.org/10.1016/j.matdes.2016.02.086.

(35) Xiao, Y.; Song, L.; Liu, X.; Huang, Y.; Huang, T.; Wu, Y.; Chen, J.; Wu, F. Nanostructured Bioactive Glass–Ceramic Coatings Deposited by the Liquid Precursor Plasma Spraying Process. *Applied Surface Science* **2011**, *257* (6), 1898–1905. https://doi.org/10.1016/j.apsusc.2010.09.023.

(36) Pérez-Tanoira, R.; Kinnari, T. J.; Hyyrynen, T.; Soininen, A.; Pietola, L.; Tiainen, V.-M.; Konttinen, Y. T.; Aarnisalo, A. A. Effects of S53P4 Bioactive Glass on Osteoblastic Cell and Biomaterial Surface Interaction. *J Mater Sci Mater Med* **2015**, *26* (10), 246. https://doi.org/10.1007/s10856-015-5568-2.

(37) Chellappa, M.; Vijayalakshmi, U. Electrophoretic Deposition of Silica and Its Composite Coatings on Ti-6Al-4V, and Its in Vitro Corrosion Behaviour for Biomedical Applications. *Materials Science and Engineering: C* **2017**, *71*, 879–890. https://doi.org/10.1016/j.msec.2016.10.075.

(38) Baino, F.; Hamzehlou, S.; Kargozar, S. Bioactive Glasses: Where Are We and Where Are We Going? *J Funct Biomater* **2018**, *9* (1). https://doi.org/10.3390/jfb9010025.

(39) Cordeiro, J. M.; Pantaroto, H. N.; Paschoaleto, E. M.; Rangel, E. C.; Cruz, N. C. da; Sukotjo, C.; Barão, V. A. R. Synthesis of Biofunctional Coating for a TiZr Alloy: Surface, Electrochemical, and Biological Characterizations. *Applied Surface Science* **2018**, *452*, 268–278. https://doi.org/10.1016/j.apsusc.2018.05.044.

(40) Krupa, D.; Baszkiewicz, J.; Zdunek, J.; Sobczak, J. W.; Lisowski, W.; Smolik, J.; Słomka, Z. Effect of Plasma Electrolytic Oxidation in the Solutions Containing Ca, P, Si, Na on the Properties of Titanium. *Journal of Biomedical Materials Research Part B: Applied Biomaterials* **2012**, *100B* (8), 2156–2166. https://doi.org/10.1002/jbm.b.32781.

(41) Lin, D.-J.; Tsai, M.-T.; Shieh, T.-M.; Huang, H.-L.; Hsu, J.-T.; Ko, Y.-C.; Fuh, L.-J. In Vitro Antibacterial Activity and Cytocompatibility of Bismuth Doped Micro-Arc Oxidized Titanium. *J Biomater Appl* **2013**, *27* (5), 553–563. https://doi.org/10.1177/0885328211414942.

(42) Wojcieszak, D.; Mazur, M.; Kalisz, M.; Grobelny, M. Influence of Cu, Au and Ag on Structural and Surface Properties of Bioactive Coatings Based on Titanium. *Materials Science and Engineering: C* **2017**, *71*, 1115–1121. https://doi.org/10.1016/j.msec.2016.11.091.

(43) Santos-Coquillat, A.; Gonzalez Tenorio, R.; Mohedano, M.; Martinez-Campos, E.; Arrabal, R.; Matykina, E. Tailoring of Antibacterial and Osteogenic Properties of Ti6Al4V

by Plasma Electrolytic Oxidation. *Applied Surface Science* **2018**, *454*, 157–172. https://doi.org/10.1016/j.apsusc.2018.04.267.

(44) Sobolev, A.; Valkov, A.; Kossenko, A.; Wolicki, I.; Zinigrad, M.; Borodianskiy, K. Bioactive Coating on Ti Alloy with High Osseointegration and Antibacterial Ag Nanoparticles. *ACS Appl. Mater. Interfaces* **2019**, *11* (43), 39534–39544. https://doi.org/10.1021/acsami.9b13849.

(45) Marques, I. da S. V.; da Cruz, N. C.; Landers, R.; Yuan, J. C.-C.; Mesquita, M. F.; Sukotjo, C.; Mathew, M. T.; Barão, V. A. R. Incorporation of Ca, P, and Si on Bioactive Coatings Produced by Plasma Electrolytic Oxidation: The Role of Electrolyte Concentration and Treatment Duration. *Biointerphases* **2015**, *10* (4), 041002. https://doi.org/10.1116/1.4932579.

(46) Marques, I. da S. V.; Barão, V. A. R.; da Cruz, N. C.; Yuan, J. C.-C.; Mesquita, M. F.; Ricomini-Filho, A. P.; Sukotjo, C.; Mathew, M. T. Electrochemical Behavior of Bioactive Coatings on Cp-Ti Surface for Dental Application. *Corros Sci* **2015**, *100*, 133–146. https://doi.org/10.1016/j.corsci.2015.07.019.

(47) Marques, I. da S. V.; Alfaro, M. F.; Saito, M. T.; da Cruz, N. C.; Takoudis, C.; Landers, R.; Mesquita, M. F.; Nociti Junior, F. H.; Mathew, M. T.; Sukotjo, C.; et al. Biomimetic Coatings Enhance Tribocorrosion Behavior and Cell Responses of Commercially Pure Titanium Surfaces. *Biointerphases* **2016**, *11* (3), 031008. https://doi.org/10.1116/1.4960654.

(48) Beline, T.; Marques, I. da S. V.; Matos, A. O.; Ogawa, E. S.; Ricomini-Filho, A. P.; Rangel, E. C.; da Cruz, N. C.; Sukotjo, C.; Mathew, M. T.; Landers, R.; et al. Production of a Biofunctional Titanium Surface Using Plasma Electrolytic Oxidation and Glow-Discharge Plasma for Biomedical Applications. *Biointerphases* **2016**, *11* (1), 011013. https://doi.org/10.1116/1.4944061.

(49) Cordeiro, J. M.; Pantaroto, H. N.; Paschoaleto, E. M.; Rangel, E. C.; Cruz, N. C. da; Sukotjo, C.; Barão, V. A. R. Synthesis of Biofunctional Coating for a TiZr Alloy: Surface, Electrochemical, and Biological Characterizations. *Applied Surface Science* **2018**, *452*, 268–278. https://doi.org/10.1016/j.apsusc.2018.05.044.

(50) Nagay, B. E.; Dini, C.; Cordeiro, J. M.; Ricomini-Filho, A. P.; de Avila, E. D.; Rangel, E. C.; da Cruz, N. C.; Barão, V. A. R. Visible-Light-Induced Photocatalytic and Antibacterial Activity of TiO2 Codoped with Nitrogen and Bismuth: New Perspectives to Control Implant-Biofilm-Related Diseases. *ACS Appl Mater Interfaces* **2019**, *11* (20), 18186–18202. https://doi.org/10.1021/acsami.9b03311.

(51) Barão, V. A. R.; Mathew, M. T.; Assunção, W. G.; Yuan, J. C.-C.; Wimmer, M. A.; Sukotjo, C. Stability of Cp-Ti and Ti-6Al-4V Alloy for Dental Implants as a Function of Saliva PH – an Electrochemical Study. *Clinical Oral Implants Research* **2012**, *23* (9), 1055–1062. https://doi.org/10.1111/j.1600-0501.2011.02265.x.

(52) Li, S.; Ni, J.; Liu, X.; Zhang, X.; Yin, S.; Rong, M.; Guo, Z.; Zhou, L. Surface Characteristics and Biocompatibility of Sandblasted and Acid-Etched Titanium Surface Modified by Ultraviolet Irradiation: An in Vitro Study. *J. Biomed. Mater. Res. Part B Appl. Biomater.* **2012**, *100* (6), 1587–1598. https://doi.org/10.1002/jbm.b.32727.

(53) Ogawa, E. S.; Matos, A. O.; Beline, T.; Marques, I. S. V.; Sukotjo, C.; Mathew, M. T.; Rangel, E. C.; Cruz, N. C.; Mesquita, M. F.; Consani, R. X.; et al. Surface-Treated Commercially Pure Titanium for Biomedical Applications: Electrochemical, Structural, Mechanical and Chemical Characterizations. *Materials Science and Engineering: C* **2016**, *65*, 251–261. https://doi.org/10.1016/j.msec.2016.04.036.

(54) ISO 21968. 2007.

(55) Elias, C. N.; Oshida, Y.; Lima, J. H. C.; Muller, C. A. Relationship between Surface Properties (Roughness, Wettability and Morphology) of Titanium and Dental Implant Removal Torque. *J Mech Behav Biomed Mater* **2008**, *1* (3), 234–242. https://doi.org/10.1016/j.jmbbm.2007.12.002.

(56) Cordeiro, J. M.; Beline, T.; Ribeiro, A. L. R.; Rangel, E. C.; da Cruz, N. C.; Landers, R.; Faverani, L. P.; Vaz, L. G.; Fais, L. M. G.; Vicente, F. B.; et al. Development of Binary and Ternary Titanium Alloys for Dental Implants. *Dent Mater* **2017**, *33* (11), 1244–1257. https://doi.org/10.1016/j.dental.2017.07.013.

(57) ISO 4049.

(58) Fugolin, A. P.; Dobson, A.; Huynh, V.; Mbiya, W.; Navarro, O.; Franca, C. M.; Logan, M.; Merritt, J. L.; Ferracane, J. L.; Pfeifer, C. S. Antibacterial, Ester-Free Monomers: Polymerization Kinetics, Mechanical Properties, Biocompatibility and Anti-Biofilm Activity. *Acta Biomater* **2019**. https://doi.org/10.1016/j.actbio.2019.09.039.

(59) Bordin, D.; Cavalcanti, I. M. G.; Jardim Pimentel, M.; Fortulan, C. A.; Sotto-Maior, B. S.; Del Bel Cury, A. A.; da Silva, W. J. Biofilm and Saliva Affect the Biomechanical Behavior of Dental Implants. *J Biomech* **2015**, *48* (6), 997–1002. https://doi.org/10.1016/j.jbiomech.2015.02.004.

(60) Bohner, M.; Lemaitre, J. Can Bioactivity Be Tested in Vitro with SBF Solution? *Biomaterials* **2009**, *30* (12), 2175–2179. https://doi.org/10.1016/j.biomaterials.2009.01.008.

(61) Beline, T.; Garcia, C. S.; Ogawa, E. S.; Marques, I. S. V.; Matos, A. O.; Sukotjo, C.; Mathew, M. T.; Mesquita, M. F.; Consani, R. X.; Barão, V. A. R. Surface Treatment Influences Electrochemical Stability of CpTi Exposed to Mouthwashes. *Materials Science and Engineering: C* **2016**, *59*, 1079–1088. https://doi.org/10.1016/j.msec.2015.11.045.

(62) Rao, X.; Chu, C. L.; Sun, Q.; Zheng, Y. Y. Fabrication and Apatite Inducing Ability of Different Porous Titania Structures by PEO Treatment. *Mater Sci Eng C Mater Biol Appl* **2016**, *66*, 297–305. https://doi.org/10.1016/j.msec.2016.04.038.

(63) Du, Q.; Wei, D.; Wang, Y.; Cheng, S.; Liu, S.; Zhou, Y.; Jia, D. The Effect of Applied Voltages on the Structure, Apatite-Inducing Ability and Antibacterial Ability of Micro Arc Oxidation Coating Formed on Titanium Surface. *Bioactive Materials* **2018**, *3* (4), 426–433. https://doi.org/10.1016/j.bioactmat.2018.06.001.

(64) Barão, V. A. R.; Ricomini-Filho, A. P.; Faverani, L. P.; Del Bel Cury, A. A.; Sukotjo, C.; Monteiro, D. R.; Yuan, J. C.-C.; Mathew, M. T.; do Amaral, R. C.; Mesquita, M. F.; et al. The Role of Nicotine, Cotinine and Caffeine on the Electrochemical Behavior and Bacterial Colonization to Cp-Ti. *Mater Sci Eng C Mater Biol Appl* **2015**, *56*, 114–124. https://doi.org/10.1016/j.msec.2015.06.026.

(65) Souza, J. G. S.; Lima, C. V.; Costa Oliveira, B. E.; Ricomini-Filho, A. P.; Faveri, M.; Sukotjo, C.; Feres, M.; Del Bel Cury, A. A.; Barão, V. A. R. Dose-Response Effect of Chlorhexidine on a Multispecies Oral Biofilm Formed on Pure Titanium and on a Titanium-Zirconium Alloy. *Biofouling* **2018**, *34* (10), 1175–1184. https://doi.org/10.1080/08927014.2018.1557151.

(66) Ccahuana-Vásquez, R. A.; Cury, J. A. S. Mutans Biofilm Model to Evaluate Antimicrobial Substances and Enamel Demineralization. *Braz Oral Res* **2010**, *24* (2), 135–141. https://doi.org/10.1590/s1806-83242010000200002.

(67) Souza, J. G. S.; Cury, J. A.; Ricomini Filho, A. P.; Feres, M.; Faveri, M. de; Barão, V. A. R. Effect of Sucrose on Biofilm Formed in Situ on Titanium Material. *J. Periodontol.* **2019**, *90* (2), 141–148. https://doi.org/10.1002/JPER.18-0219.

(68) Aires, C. P.; Del Bel Cury, A. A.; Tenuta, L. M. A.; Klein, M. I.; Koo, H.; Duarte, S.; Cury, J. A. Effect of Starch and Sucrose on Dental Biofilm Formation and on Root Dentine Demineralization. *Caries Res.* **2008**, *42* (5), 380–386. https://doi.org/10.1159/000154783.

(69) Costa Oliveira, B. E.; Cury, J. A.; Ricomini Filho, A. P. Biofilm Extracellular Polysaccharides Degradation during Starvation and Enamel Demineralization. *PLoS ONE* **2017**, *12* (7), e0181168. https://doi.org/10.1371/journal.pone.0181168.

(70) Socransky, S. S.; Smith, C.; Martin, L.; Paster, B. J.; Dewhirst, F. E.; Levin, A. E. "Checkerboard" DNA-DNA Hybridization. *BioTechniques* **1994**, *17* (4), 788–792.

(71) Miranda, S. L. F.; Damasceno, J. T.; Faveri, M.; Figueiredo, L.; da Silva, H. D.; Alencar, S. M. de A.; Rosalen, P. L.; Feres, M.; Bueno-Silva, B. Brazilian Red Propolis Reduces Orange-Complex Periodontopathogens Growing in Multispecies Biofilms. *Biofouling* **2019**, *35* (3), 308–319. https://doi.org/10.1080/08927014.2019.1598976.

(72) Mestnik, M. J.; Feres, M.; Figueiredo, L. C.; Duarte, P. M.; Lira, E. A. G.; Faveri, M. Short-Term Benefits of the Adjunctive Use of Metronidazole plus Amoxicillin in the Microbial Profile and in the Clinical Parameters of Subjects with Generalized Aggressive Periodontitis. *J. Clin. Periodontol.* **2010**, *37* (4), 353–365. https://doi.org/10.1111/j.1600-051X.2010.01538.x.

(73) Kokubo, T.; Takadama, H. How Useful Is SBF in Predicting in Vivo Bone Bioactivity? *Biomaterials* **2006**, *27* (15), 2907–2915. https://doi.org/10.1016/j.biomaterials.2006.01.017.

(74) Dini, C.; Nagay, B. E.; Cordeiro, J. M.; da Cruz, N. C.; Rangel, E. C.; Ricomini-Filho, A. P.; de Avila, E. D.; Barão, V. A. R. UV-Photofunctionalization of a Biomimetic Coating for Dental Implants Application. *Materials Science and Engineering: C* **2020**, *110*, 110657. https://doi.org/10.1016/j.msec.2020.110657.

(75) Kazek-Kęsik, A.; Dercz, G.; Kalemba, I.; Suchanek, K.; Kukharenko, A. I.; Korotin, D. M.; Michalska, J.; Krząkała, A.; Piotrowski, J.; Kurmaev, E. Z.; et al. Surface Characterisation of Ti-15Mo Alloy Modified by a PEO Process in Various Suspensions. *Mater Sci Eng C Mater Biol Appl* **2014**, *39*, 259–272. https://doi.org/10.1016/j.msec.2014.03.008.

(76) Rizwan, M.; Hamdi, M.; Basirun, W. J. Bioglass® 45S5-Based Composites for Bone Tissue Engineering and Functional Applications. *J Biomed Mater Res A* **2017**, *105* (11), 3197–3223. https://doi.org/10.1002/jbm.a.36156.

(77) Gnedenkov, S. V.; Sinebryukhov, S. L.; Puz, A. V.; Egorkin, V. S.; Kostiv, R. E. In Vivo Study of Osteogenerating Properties of Calcium-Phosphate Coating on Titanium Alloy Ti-6Al-4V. *Biomed Mater Eng* **2016**, *27* (6), 551–560. https://doi.org/10.3233/BME-161608.

(78) He, J.; Feng, W.; Zhao, B.-H.; Zhang, W.; Lin, Z. In Vivo Effect of Titanium Implants with Porous Zinc-Containing Coatings Prepared by Plasma Electrolytic Oxidation Method on Osseointegration in Rabbits. *Int J Oral Maxillofac Implants* **2018**, *33* (2), 298–310. https://doi.org/10.11607/jomi.5764.

(79) Park, J.-M.; Koak, J.-Y.; Jang, J.-H.; Han, C.-H.; Kim, S.-K.; Heo, S.-J. Osseointegration of Anodized Titanium Implants Coated with Fibroblast Growth Factor-Fibronectin (FGF-FN) Fusion Protein. *Int J Oral Maxillofac Implants* **2006**, *21* (6), 859–866.

(80) Sun, Y.-S.; Liu, J.-F.; Wu, C.-P.; Huang, H.-H. Nanoporous Surface Topography Enhances Bone Cell Differentiation on Ti–6Al–7Nb Alloy in Bone Implant Applications. *Journal of Alloys and Compounds* **2015**, *643*, S124–S132. https://doi.org/10.1016/j.jallcom.2015.01.019.

(81) Durdu, S.; Usta, M.; Berkem, A. S. Bioactive Coatings on Ti6Al4V Alloy Formed by Plasma Electrolytic Oxidation. *Surface and Coatings Technology* **2016**, *301*, 85–93. https://doi.org/10.1016/j.surfcoat.2015.07.053.

(82) Marques, I. da S. V.; Alfaro, M. F.; Cruz, N. C. da; Mesquita, M. F.; Takoudis, C.; Sukotjo, C.; Mathew, M. T.; Barão, V. A. R. Tribocorrosion Behavior of Biofunctional Titanium Oxide Films Produced by Micro-Arc Oxidation: Synergism and Mechanisms. *Journal of the Mechanical Behavior of Biomedical Materials* **2016**, *60*, 8–21. https://doi.org/10.1016/j.jmbbm.2015.12.030.

(83) Vieira, A. C.; Ribeiro, A. R.; Rocha, L. A.; Celis, J. P. Influence of PH and Corrosion Inhibitors on the Tribocorrosion of Titanium in Artificial Saliva. *Wear* **2006**, *261* (9), 994–1001. https://doi.org/10.1016/j.wear.2006.03.031.

(84) Lee, C.-T.; Huang, Y.-W.; Zhu, L.; Weltman, R. Prevalences of Peri-Implantitis and Peri-Implant Mucositis: Systematic Review and Meta-Analysis. *J Dent* **2017**, *62*, 1–12. https://doi.org/10.1016/j.jdent.2017.04.011.

(85) Pantaroto, H. N.; Ricomini-Filho, A. P.; Bertolini, M. M.; Dias da Silva, J. H.; Azevedo Neto, N. F.; Sukotjo, C.; Rangel, E. C.; Barão, V. A. R. Antibacterial Photocatalytic Activity of Different Crystalline TiO2 Phases in Oral Multispecies Biofilm. *Dent Mater* **2018**, *34* (7), e182–e195. https://doi.org/10.1016/j.dental.2018.03.011.

(86) Mine, Y.; Makihira, S.; Nikawa, H.; Murata, H.; Hosokawa, R.; Hiyama, A.; Mimura, S. Impact of Titanium Ions on Osteoblast-, Osteoclast- and Gingival Epithelial-like Cells. *J Prosthodont Res* **2010**, *54* (1), 1–6. https://doi.org/10.1016/j.jpor.2009.07.003.

(87) Souza, J. G. S.; Costa Oliveira, B. E.; Bertolini, M.; Lima, C. V.; Retamal-Valdes, B.; de Faveri, M.; Feres, M.; Barão, V. A. R. Titanium Particles and Ions Favor Dysbiosis in Oral Biofilms. *J. Periodont. Res.* **2019**. https://doi.org/10.1111/jre.12711.

(88) Soares, P. B. F.; Moura, C. C. G.; Chinaglia, C. R.; Zanotto, E. D.; Zanetta-Barbosa, D.; Stavropoulos, A. Effect of Titanium Surface Functionalization with Bioactive Glass on Osseointegration: An Experimental Study in Dogs. *Clin Oral Implants Res* **2018**. https://doi.org/10.1111/clr.13375.

(89) Mombelli, A.; Décaillet, F. The Characteristics of Biofilms in Peri-Implant Disease. *J. Clin. Periodontol.* **2011**, *38 Suppl 11*, 203–213. https://doi.org/10.1111/j.1600-051X.2010.01666.x.

SUPPLEMENTARY MATERIAL

Synthesis of bioactive glass-based coating by plasma electrolytic oxidation: untangling a new deposition pathway toward for titanium implant surface

Running title: Bioactive glass-based coating for implant application

Raphael Cavalcante Costa[1], João Gabriel Silva Souza[1], Jairo Matozinho Cordeiro[1], Martinna Bertolini[2], Érica D.de Avila[3], Richard Landersf[4], Elidiane C. Rangel[5], Nilson C da Cruz[5], Carlos A. Fortulan[6], Belén Retamal-Valdes[7], Magda Feres[7], Valentim A. R. Barão[1*]

1. Department of Prosthodontics and Periodontology, Piracicaba Dental School, University of Campinas (UNICAMP), Av. Limeira, 901, Piracicaba, São Paulo 13414-903, Brazil.

2. Oral Health and Diagnostic Sciences Department, Division of Periodontology, University of Connecticut, School of Dental Medicine, 263 Farmington Avenue, Farmington, CT 06030, USA.

3. Department of Dental Materials and Prosthodontics, School of Dentistry at Araraquara, São Paulo State University (UNESP), R. Humaitá, 1680, Araraquara, São Paulo 14801-903, Brazil.

4. Institute of Physics Gleb Wataghin, University of Campinas (UNICAMP), Cidade Universitária Zeferino Vaz, Barão Geraldo, Campinas, São Paulo 13083-859, Brazil

5. Laboratory of Technological Plasmas, Institute of Science and Technology, São Paulo State University (UNESP), Av. Três de Março, 511, Sorocaba, São Paulo 18087-180, Brazil.

6. Department of Mechanical Engineering, University of São Paulo (USP), Trabalhador São Carlense, 400, São Carlos, São Paulo, 13566-590, Brazil.

7. Department of Periodontology, Dental Research Division, Guarulhos University, Eng Prestes Maia, 88,Guarulhos, São Paulo, 07023-070 Brazil.

***Corresponding author**

Valentim A.R. Barão, Department of Prosthodontics and Periodontology, Piracicaba Dental School, University of Campinas (UNICAMP), Av. Limeira, 901, Piracicaba, São Paulo 13414-903, Brazil.

E-mail: vbarao@unicamp.br

A)

Electrolyte solution			PEO characteristics	
	M	gL^{-1}	Working parameters	
Na_2SiO_3-$5H_2O$	0.014	1.51	Voltage (V)	Anodic, 500
$C_4H_6O_4Ca$	0.20	17.61	Frequency (Hz)	Unipolar, 1000
$NaNO_3$	0.50	21.24	Duty cycle (%)	Alternate, 10 (+) and 70(-)
$C_3H_7Na_2O_6P$	0.0010	0.11	Time (s)	420
$Na_2EDTA{\cdot}_2H_2O$	0.025	10.25	Temperature	23°C (±1.5)
pH	4.38		Microdischarge	~178
σ, $mS{\cdot}cm^{-1}$	137.5		-	-

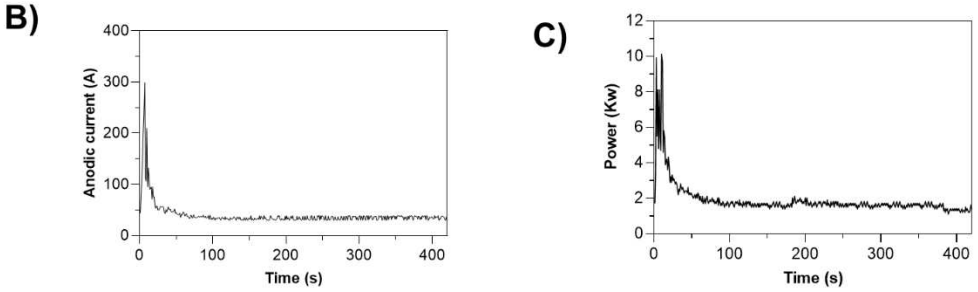

Figure S1. (A) PEO-BG coating were obtained from electrolyte solution (Si, Ca, Na and P in the composition) and PEO parameters previously tested. During the treatment, density current **(C)** and power **(D)** of the equipment were measured.

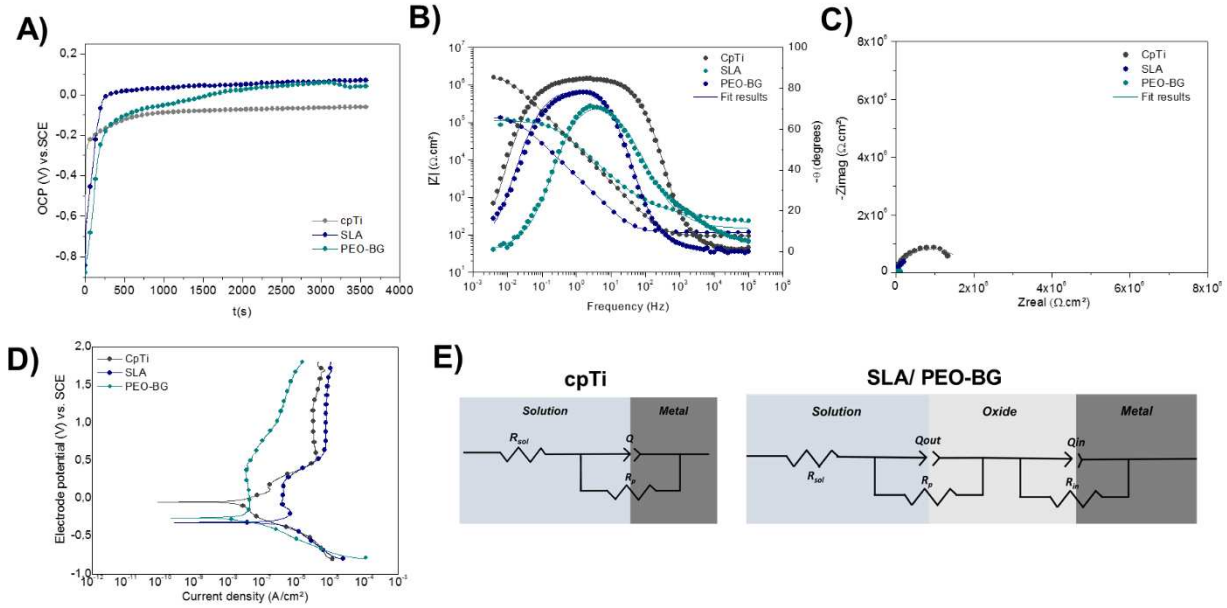

Figure S2. Electrochemical data at baseline. **(A)** Evolution of open circuit potential of surfaces as a function of time in SBF. **(B)** Representative impedance (|Z|) and phase angle (Θ) plots. **(C)** Representative Nyquist diagrams. **(D)** Representative potentiodynamic polarization curves. **(E)** Equivalent electrical circuits used to fit EIS data.

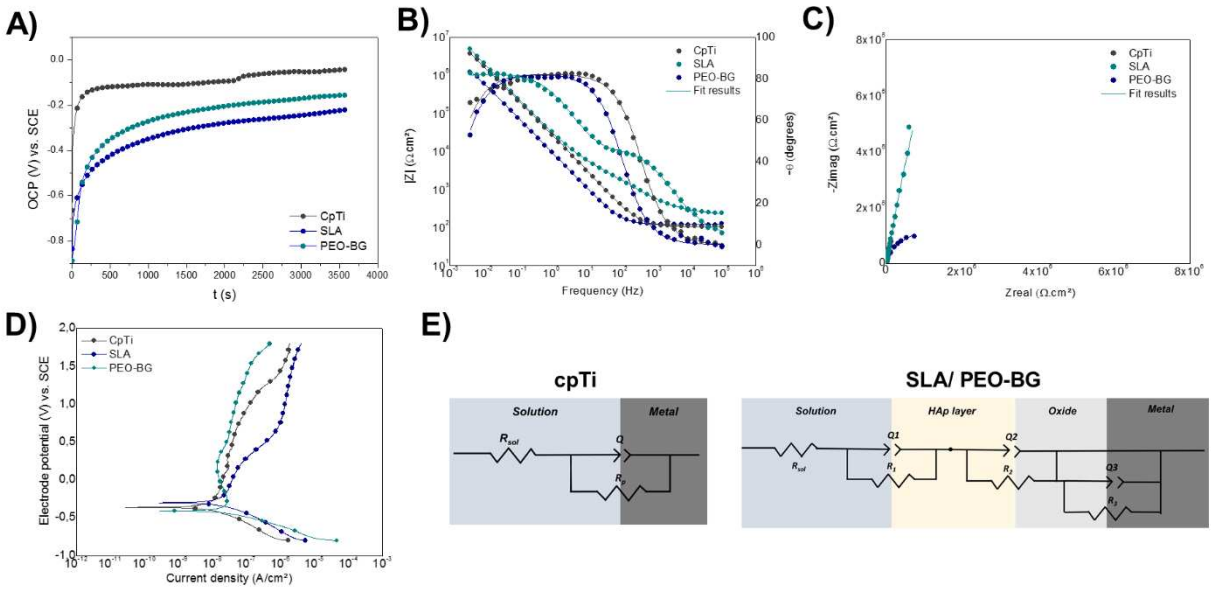

Figure S3. Electrochemical data at 14 days. **(A)** Evolution of open circuit potential of surfaces as a function of time in SBF. **(B)** Representative impedance (|Z|) and phase angle (Θ) plots. **(C)** Representative Nyquist diagrams. **(D)** Representative potentiodynamic polarization curves. **(E)** Equivalent electrical circuits used to fit EIS data.

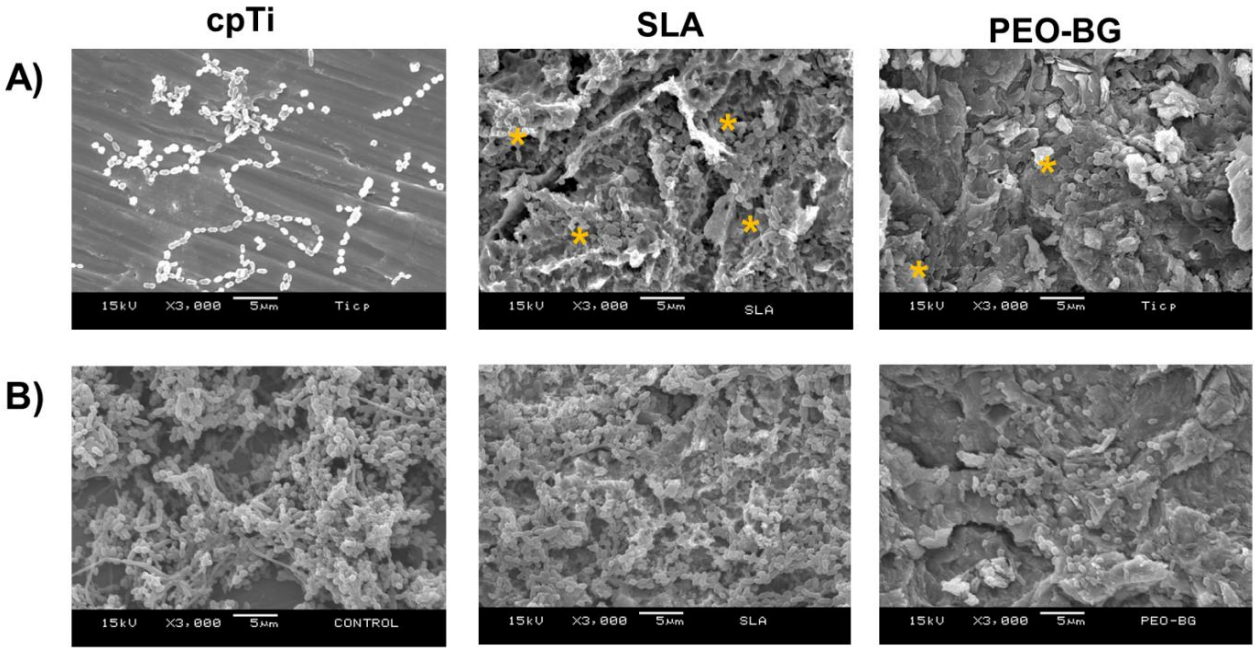

Figure S4. Microbiological assay on cpTi, SLA and PEO-BG surfaces. **(A)** Microbial adhesion for 2 h using saliva as microbial inoculum. **(B)** Polymicrobial biofilm formed for 24 h using saliva as microbial inoculum. The asterisks indicate bacterial clusters.

2.2 ARTIGO[#]: Extracellular biofilm matrix leads to a microbiological dysbiosis and reduces biofilm susceptibility to antimicrobials on titanium biomaterial

Running title: Biofilm matrix favors dysbiosis and microbial resistance

Raphael Cavalcante Costa[1], João Gabriel Silva Souza[1], Martinna Bertolini[2], Belén Retamal-Valdes[3], Magda Feres[3], Valentim A. R. Barão[1,*]

1. Department of Prosthodontics and Periodontology, Piracicaba Dental School, University of Campinas (UNICAMP), Av. Limeira, 901, Piracicaba, São Paulo 13414-903, Brazil.

2. University of Connecticut (UCONN), School of Dental Medicine, 263 Farmington Avenue, Farmington, CT 06030, USA.

3. Department of Periodontology, Dental Research Division, Guarulhos University (UnG), Eng. Prestes Maia, 88,Guarulhos, São Paulo, 07023-070, Brazil.

***Corresponding authors**

Valentim A.R. Barão, Department of Prosthodontics and Periodontology, Piracicaba Dental School, University of Campinas (UNICAMP), Av. Limeira, 901, Piracicaba, São Paulo 13414-903, Brazil. E-mail: vbarao@unicamp.br

#Artigo foi submetido ao periódico **Molecular Oral Microbiology** (IF = 2.925).

SUMMARY

Biofilms are highly structured microbial communities embedded in a three-dimensional extracellular matrix (ECM) which allow adhesion and accumulation on biotic and abiotic surfaces in human body, such as soft tissues and implanted biomaterials, respectively. In the oral cavity ECM creates a more favorable environment for microorganism colonization and metabolim. Therefore, we hypothesized that this suitable ECM-rich environment may drive deleterious shifts in the microbial composition on titanium biomaterial. Our data shows that ECM-rich environment, driven by sucrose exposure, promoted increased bacterial accumulation and led to a microbiological dysbiosis on biofilm, favoring *Streptococcus, Fusobacterium* and *Campylobacter* species growth. ECM-rich biofilm also transitioned from a commensal aerobic to a pathogenic anaerobic profile. Even restrict anaerobic species related to peri-implant infections, such as *Porphyromonas gingivalis* and *Tannerella forsythia,* were increased ~3-fold in ECM-rich biofilms. ECM increased biofilm virulence promoting host cell damage and also reduced antimicrobial susceptibility of biofilms, but the use of a dual-targeting approach to first disrupt ECM assembly (povidone-iodine) increased antibiotic effect on *in situ* biofilms. Altogether, our data provide new insights of how ECM creates an environment that favors putative pathogens growth and highlights a promising approach with matrix disruption to improve treatments on implant related infections.

Keywords: Biofilms, extracellular polymeric substance matrix, anti-infective agents, titanium, dental implants

Introduction

Biofilms are highly structured microbial communities enmeshed in a three-dimensional extracellular matrix (ECM) (Costerton *et al.*, 1995; Bowen *et al.*, 2018a). Microorganism growing in biofilms have enhanced metabolism, high co-aggregation and interaction with other microbes as well as reduced antimicrobial susceptibility (Costerton *et al.*, 1995; Flemming and Wingender, 2010), being a critical virulence factor in the pathogenesis of microbial infections (Bowen *et al.*, 2018a). In the oral environment, indigenous microorganisms from oral microbiome live in symbiotic state with the host by adhering on biotic (Xu *et al.*, 2017) and abiotic surfaces (Matos *et al.*, 2017) leading to biofilm accumulation. On abiotic surfaces, such as implanted materials made of titanium (Ti), polymicrobial biofilm formation starts on surfaces exposed to saliva and microorganisms, usually supra-gingivally where the majority of colonizers are aerobic species (Zheng *et al.*, 2015). Due to the non-desquamative property of abiotic surfaces, as biofilms grow it act as a "stress factor" to the host triggering an inflammatory response (Lang *et al.*, 1993). This condition often changes the local environmental factors, such as nutrient content, and promote a transition from a commensal to a more invasive and pathogenic biofilm, further increasing the load of anaerobic pathogens in subgingival sites (de Freitas *et al.*, 2011; Marsh *et al.*, 2011).

Furthermore, different factors can contribute modelling the biofilm structure and to a shift towards a more pathogenic biofilm community (Rickard *et al.*, 2003; Jenkinson, 2011; Bowen *et al.*, 2018b), such as changes in the environment due to inflammatory process and even carbohydrate consumption, which favors the overgrowth of endogenous aciduric bacteria. (Marsh *et al.*, 2011; Rosier *et al.*, 2018; Souza *et al.*, 2019). Importantly, sucrose is the most-consumed dietary carbohydrate and it has been reported to lead to a microbiological dysbiosis in oral biofilms formed *in situ* on Ti surface (Souza *et al.*, 2019). Similarly, other different fermentable carbohydrates (e.g. glucose) are also used for microorganism metabolism, increasing bacterial counts (Vale *et al.*, 2007) and biofilm biomass (Duarte *et al.*, 2008). However, sucrose has unique characteristics regarding

biofilm formation, being the only substrate for synthesis of extracellular glucan polymers on biofilms, via bacterial exoenzymes (glucosyltransferase –gtf) that break sucrose into soluble and insoluble polymers, which contribute to the ECM on the three-dimensional architecture of biofilms (Costerton *et al.*, 1995; Vacca-Smith *et al.*, 1996; Kopec *et al.*, 1997; Bowen and Koo, 2011a; Costa Oliveira *et al.*, 2017). Although ECM has other components, such as proteins and eDNA, which are also present under glucose exposure, the insoluble extracellular polymers are synthesized only by sucrose cleavage, and they represent the main portion of ECM (Flemming and Wingender, 2010). These matrix-rich biofilms generated in the presence of sucrose have high nutrient availability and reduced O_2 level (Xiao *et al.*, 2012), which may create a suitable microenvironment for anaerobic pathogens growth. Although previous studies have shown the effect of local nutrient content and sucrose exposure on oral biofilm dysbiosis (Naginyte *et al.*, 2019; Souza *et al.*, 2019), it has been conducted using a protein-rich medium, which favor proteolytic species (Naginyte *et al.*, 2019); or *in situ* under the effect of host characteristics, such as others nutrient source and salivary content (Souza *et al.*, 2019). Thus, the isolated and specific effect of ECM to favor anaerobic putative pathogens growth on abiotic surfaces and the transition process from a commensal to a pathogenic anaerobic biofilm have not been tested experimentally.

In the oral cavity, most specifically around dental implants, the chronic accumulation of biofilms can lead to polymicrobial infections know as peri-implant mucositis and peri-implantitis (Derks and Tomasi, 2015). Non-surgical therapy in these cases can be extremely difficult because of the difficult access of disease sites and due harbor biofilms strongly adhered to Ti surfaces embedded on ECM, acting as a protection barrier (Mombelli and Décaillet, 2011; Derks and Tomasi, 2015). This may explain the ineffectiveness of non-surgical treatment for peri-implant diseases, as highlighted by several systematic reviews (Ntrouka *et al.*, 2011; Esposito *et al.*, 2012; Suárez-López Del Amo *et al.*, 2016). In this sense, ECM may be a key factor to be considered when aiming to eradicate polymicrobial biofilms on implant surfaces (Hwang *et al.*, 2017; Matos *et al.*,

2017). Previous studies have proposed different therapies to degrade biofilms by targetting ECM in order to enhance antimicrobial agents effectiveness (Hwang *et al.*, 2017; Kim *et al.*, 2018; Ren *et al.*, 2019). For this, povidone-iodine (PI) [$(C_6H_9NO)_nI$], a low cost agent has been used as a matrix-targeting disruption strategy as it has shown ability to degrade the ECM of duo-species biofilms and to reduce extracellular polymers synthesis, thus increasing their susceptibility to antimicrobial agents (Kim *et al.*, 2018). Although matrix-targeting therapy strategy is a promising approach to enhance the effect of antimicrobial agents, this has not been tested experimentally for polymicrobial biofilms formed on Ti surfaces. *In vivo*, the currently existing non-surgical treatments for peri implant infections combine mechanical debridement for biofilm disruption and adjunct antibiotics, such as a combination of amoxicillin and metronidazole (Mestnik *et al.*, 2010; Stein *et al.*, 2018), this therapy has been very effective for teeth associated inflammation with satisfactory clinical results for oral infections (Shibli *et al.*, 2019), but has shown no effect to reduce putative pathogens related to infections surrounding implanted materials (Suárez-López Del Amo *et al.*, 2016).

Therefore, we investigate whether the biofilm ECM can lead to a microbiological dysbiosis in oral biofilms leading to the increased load of pathogenic species within the biofilm; and if the ECM-rich biofilm structure generated by high sucrose availability is also responsible to enhance the antimicrobial resistance of biofilms formed on Ti surfaces. We also hypothesized that ECM-targeting therapy with PI can disrupt biofilm matrix and improve the antimicrobial agent of amoxicillin and metronidazole effect against polymicrobial *in situ* biofilms on Ti material.

Results

ECM-rich biofilm promotes specific bacterial species growth and leads to a microbiological dysbiosis on Ti surface

To test the role of biofilm ECM to favor microbial accumulation on Ti surface and biofilm dysbiosis we used sucrose (only substrate for insoluble extracellular polymers synthesis) to form ECM-rich biofilms and glucose (as carbohydrate source but a negative control for insoluble ECM

formation) as matrix control biofilm. For this, microcosm biofilms using human saliva were formed in two phases, initially (72 h) under aerobic condition and carbohydrate exposure and then transferred to an anaerobic condition (72 h). Although both carbohydrate exposures shows a trend to promote increased bacterial growth on Ti, ECM-rich biofilms exposed to sucrose showed higher *Streptococcus* counts in the aerobic condition (phase I of the experiment – 0 to 72 hours) ($p<0.05$) (Fig. 1A), genus recognized to have exoenzymes responsible for synthesizing extracellular polymers to form a biofilm with ECM-rich characteristics (Flemming and Wingender, 2010; Koo *et al.*, 2010). Interestingly, ECM-rich biofilm under an anerobic condition (phase II of the experiment – 72 to 144 hours) also promoted bacterial accumulation, statistically increasing total bacteria, as well as further elevating *Streptococcus* counts ($p<0.05$) (Fig. 1A). In fact, *Streptococcus* counts enlarged drastically on ECM-rich biofilms, mainly in an anaerobic environment (~120 fold compared to glucose) ($p<0.05$) (Fig. 1B), condition that favor facultative and anaerobic species (Ahn *et al.*, 2009).

Biofilms growing in sucrose showed dense bacterial clusters enmeshed by ECM in aerobic and anaerobic condition (Fig. 1C), exhibiting a total biovolume ~1.5 times higher ($p<0.05$) (Fig. 1D) than biofilms growing in glucose supplemented media. Under the same growth conditions biofilms growing in glucose were able to form mostly a monolayer of cells with a thin biofilm configuration (Fig. 1C), probably due to the absence of insoluble ECM. This effect in total biovolume cannot be explained solely by the effect in bacterial biomass, but also due to the matrix volume presence in biofilms exposed to sucrose (Fig. 1E). As expected, extracellular matrix synthesis favors bacteria growth, mainly for facultative *Streptococcus* species, even in an anaerobic condition.

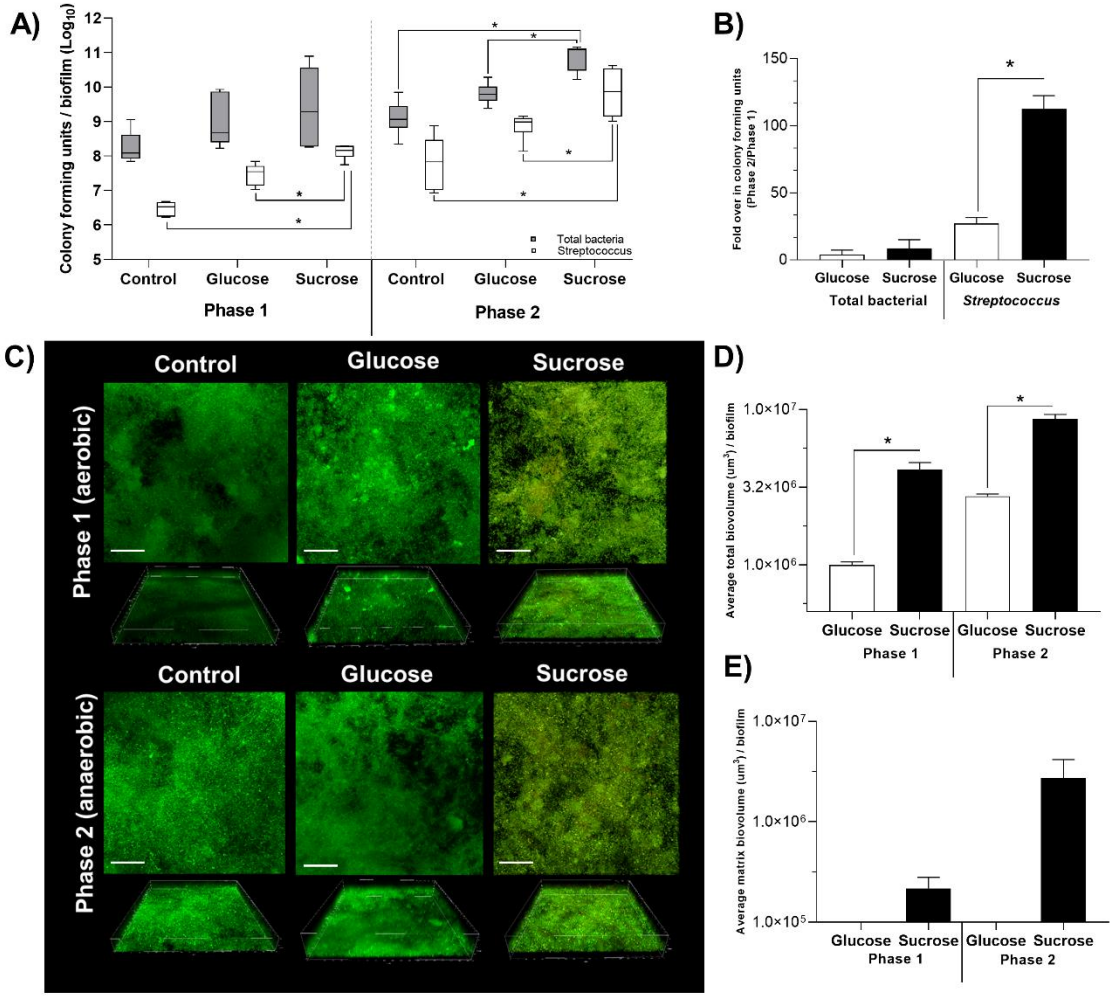

Figure 1. Oral *in vitro* biofilms growing on titanium in a aerobic condition (Phase 1 – 72 h) followed by an anaerobic condition (Phase 2 – 72 h) to mimic a transition process from supragingival to subgingival biofilm. Biofilms were exposed to 10% sucrose during phase 1 as substrate for insoluble extracellular matrix synthesis. Glucose exposure was used as matrix control. NaCl exposure was used as non-carbohydrate control. **(A)** *Streptococcus* and total bacterial counts by CFU in the aerobic and anaerobic phases. **(B)** *Streptococcus* and total bacterial counts (CFU) expressed as fold of phase 2 (aerobic) over phase 1 (anaerobic). **(C)** X–Y surfaces (top panel) and three-dimensional reconstructions (bottom panel) of representative confocal laser scanning microscopy images of biofilms. Live cells (green) was visualized after stained with Syto-9. Alexa Fluor 647-labeled dextran conjugate probe (red) was used to stain biofilm matrix. Scale bars, 50 µm

(X–Y surfaces) and 70 µm (three-dimensional reconstructions). **(D)** Average total biovolumes (in μm^3) for phase 1 and 2 biofilms exposed to glucose (white bars) or sucrose (black bars). **(E)** Biofilm matrix biovolumes (in μm^3). *$p<0.05$, using the one-way ANOVA and Tukey (HSD) or student's t-test. The error bars indicate standard deviations.

To better understand and characterize these biofilms, we next investigated the influence of ECM on microbiological composition of biofilms. To explore differences in bacterial community composition within each condition (sucrose, EMC-rich biofilm and glucose, matrix control biofilm) we quantified the levels of 40 different bacteria and grouped them at genus level for final analysis. An increase in the level (load) of genus *Fusobacterium* and, mainly, *Streptococcus, Eikenella, Campylobacter, Parvimonas* and *Prevotella* was found for ECM-rich biofilms on both phases (aerobic and anaerobic) (Fig. 2); with the most dramatic increase for *Streptococcus*. This suggest that ECM-rich environment favors specific microbial communities. In fact, ECM-rich biofilm enhanced the transition from a commensal to a pathogenic biofilm (Fig. 3). Some bacterial species, such as *Campylobacter gracilis*, *Actinomyces israelii* and *Parvimonas micra,* increased more than 10-fold in sucrose group over glucose group. Even strict anaerobic species which are recognized to be highly associated to peri-implant disease, such as *Porphyromonas gingivalis* and *Tannerella forsythia* (Retamal-Valdes *et al.*, 2019), were increased ~3-fold in ECM-rich biofilms. Collectively these results show that biofilm ECM plays an important role in the transition process from a commensal to a more pathogenic biofilm, promoting a dysbiotic shift on biofilms growing on Ti surface.

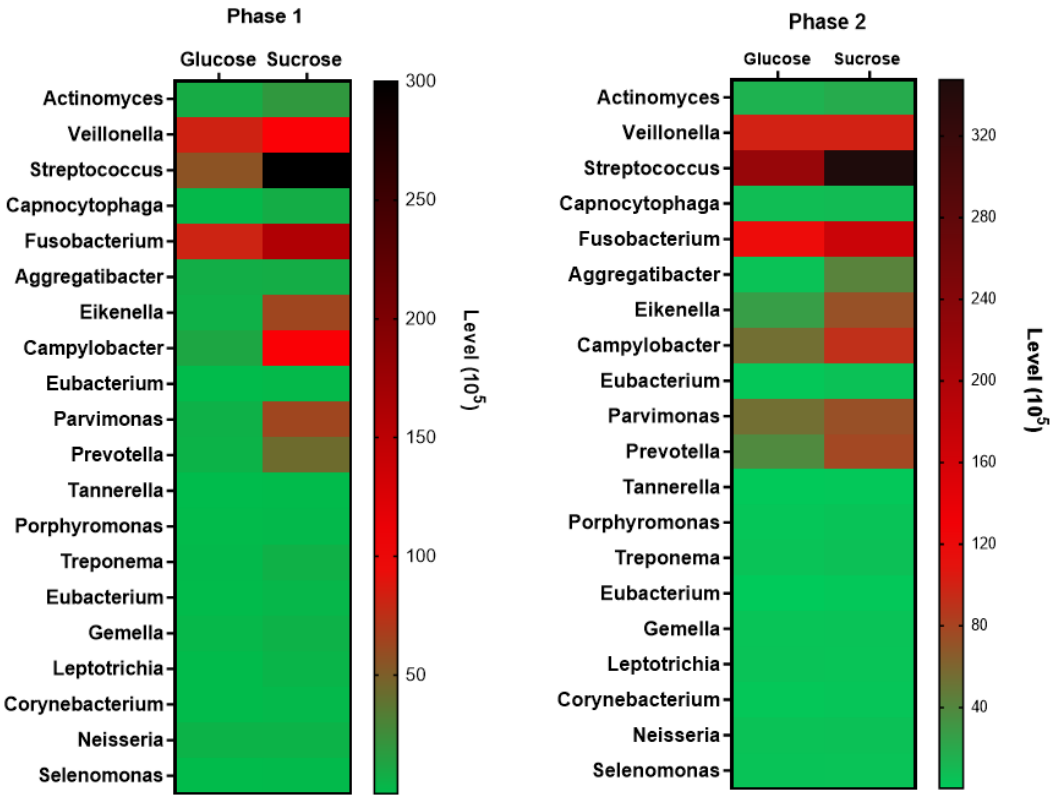

Figure 2. Microbiological composition by Checkerboard DNA-DNA hybridization of oral *in vitro* biofilms growing on titanium in an aerobic condition (Phase 1 – 0 to 72 h) followed by an anaerobic condition (Phase 2 – 72 to 144 h). Biofilms were exposed to 10% sucrose during aerobic phase as substrate for extracellular matrix synthesis. Glucose exposure was used as matrix control. Bacteria species were grouped into its bacterial genus to express the level of each community according with treatment groups.

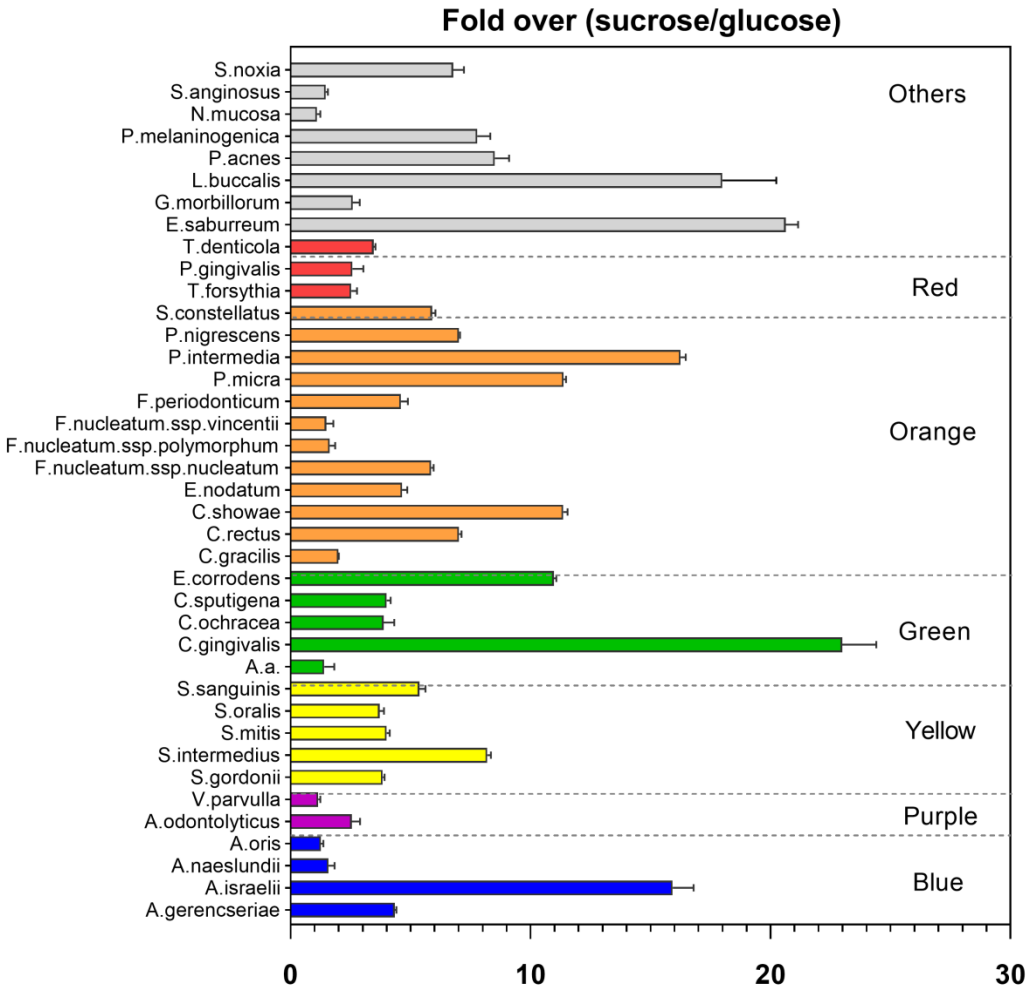

Figure 3. Profile of levels of 39 bacterial species by Checkerboard DNA-DNA hybridization of oral *in vitro* biofilms growing on titanium in an aerobic condition (Phase 1 – 0 to72 h) followed by an anaerobic condition (Phase 2 – 72 to 144 h). Biofilms were exposed to 10% sucrose during aerobic phase as substrate for extracellular matrix synthesis. Glucose exposure was used as matrix control. Results were expressed as fold change in bacteria count (bacteria level - 10^5) of sucrose group over glucose in the anaerobic (phase 2) condition. The error bars indicate standard deviations.

ECM favors biofilm virulence and cell damage

Prompted by the effect of ECM-rich biofilm to increase bacteria accumulation and biovolume, as well as playing an important role in the transition process from a commensal to a

more pathogenic biofilm, we further explored the pathogenic potential of these biofilms to induce cell damage. For this, 72 hours biofilms preformed on Ti surface were placed in contact with a fibroblast monolayer. ECM-rich biofilms showed higher cell damage measured by LDH assay, compared to non-ECM-rich biofilms control ($p<0.05$) (Fig. 4). Moreover, the more pathogenic biofilm also increased inflammatory cytokine IL-8 release by almost 2 fold on fibroblast cells ($p<0.05$) (Fig. 4). These results show that biofilm matrix plays an important role to enhance biofilm virulence leading to cell death and increased chemokine IL-8 levels, which is a neutrophil-activating and chemotactic factor responsible for modulating the host immune response under a more pathogenic biofilm accumulation on host tissues.

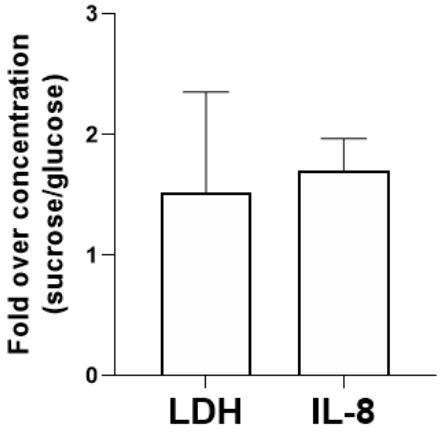

Figure 4. 72 h preformed biofilms on titanium surface exposed to fibroblast monolayer for additional 16 h. Biofilms were supplemented with 1% sucrose as substrate for ECM synthesis. Glucose supplementation was used as matrix control. Preformed biofilms were immersed in medium over an insert membrane on the top compartment with the presence of a fibroblast monolayer on the bottom compartment. Lactate dehydrogenase released by fibroblasts and interleukin-8 (IL-8) concentration for 16 h in the presence of preformed biofilms on titanium were expressed as fold of sucrose (ECM-rich biofilm) over glucose (non-ECM-rich biofilm). The error bars indicate standard deviations.

ECM enhances antimicrobial resistance of biofilms on Ti surface

Besides microbial dysbiosis, ECM-rich biofilms were associated with a higher microbial accumulation, as well as higher total biovolume due to the matrix volume presence in biofilms exposed to sucrose. Hence, we asked whether ECM-rich dysbiotic biofilm would present similar antimicrobial susceptibility as glucose exposed biofilms. For 24 h mature ECM-rich biofilm (sucrose) (Fig. 5A) showed higher viable cells (CFU) counts after chlorhexidine antimicrobial treatment, when compared to non-ECM-rich biofilms ($p<0.05$) (Fig. 5B), due to ECM presence (Fig. 5C). This result shows that ECM-rich biofilm presented reduced the antimicrobial susceptibility of biofilms growing on Ti.

To further dissect this observation, we next explored whether a pre-treatment for biofilm matrix degradation could then enhance the effect of antimicrobials on EMC-rich biofilms. For this, we used Povidone iodine (PI) (2%) as local agent to disrupt extracellular biofilm matrix before antimicrobial treatments (Kim *et al.*, 2018). As expected, our 72 h *in vitro* ECM-rich biofilms treated with a dual-targeting approach, to first disrupt the matrix and then to kill microorganisms, showed higher bacterial cell death, compared to untreated control group and biofilms treated with only antimicrobial or antibiotics agents (Fig. 5D). In fact, PI pre-treatment followed by chlorhexidine or antibiotic therapy increased death cell volume by 3x in biofilms growing on Ti ($p<0.05$) (Fig. 5E). A synergistic effect was found for dual-targeting therapy, since the total death cell volume for PI + antibiotic (amoxicilin and metronidazole) group was ≈1.5 higher than the sum of PI and AMX + MTZ effect separately. In summary, these data suggest that ECM degradation can improve antimicrobial effect of different drugs, achieving better results to eradicate biofilms growing on Ti surface.

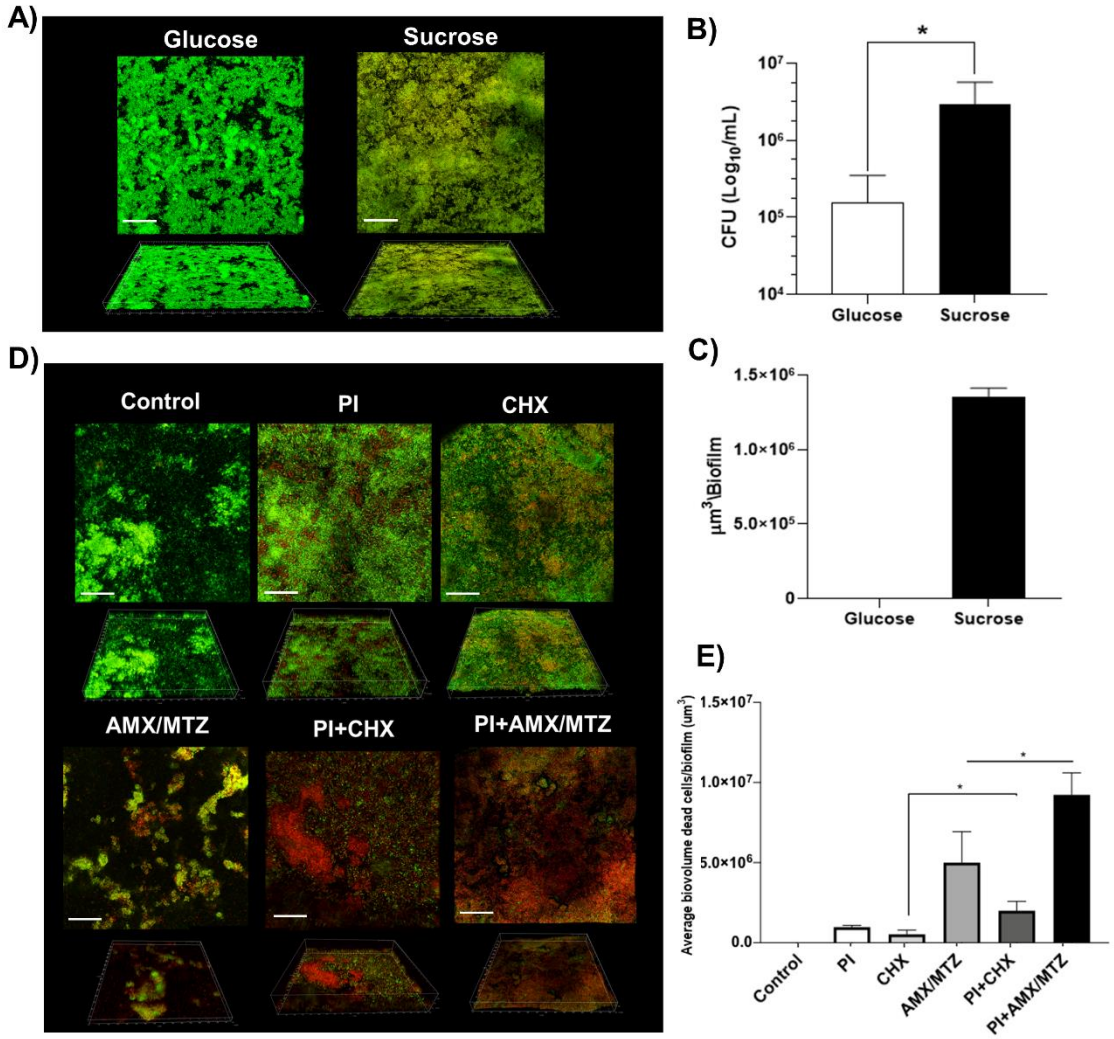

Figure 5. Biofilms (24-72 h) growing on titanium surface to test the effect of ECM on antimicrobial susceptibility of biofilms. Biofilms were supplemented with 1% sucrose as substrate for ECM synthesis. Glucose supplementation was used as matrix control. **(A)** X–Y surfaces (top panel) and three-dimensional reconstructions (bottom panel) of representative confocal laser scanning microscopy images of 24 h biofilms. Live cells (green) was visualized after stained with Syto-9. Alexa Fluor 647-labeled dextran conjugate probe (red) was used to stain biofilm matrix. Scale bars, 50 µm (X–Y surfaces) and 70 µm (three-dimensional reconstructions). **(B)** Average colony-forming units (CFU) of biofilms exposed to glucose (white bars) or sucrose (black bars) after CHX treatment. **(C)** Biofilm matrix biovolumes (in μm^3). **(D)** Representative confocal laser scanning microscopy images after treatment of 72 h biofilms growing under sucrose supplementation. Live cells were stained as mentioned above, dead cells (red) were stained by propidium iodide solution. **(E)** Dead cells biovolume (in μm^3) after treatments. Control – 0.9%

NaCl; PI – povidone iodine (2%); AMX – amoxicillin (4 μg/mL); MTZ – metronidazole (4 μg/mL). *$p<0.05$, using the one-way ANOVA and Tukey (HSD) or student's t-test. The error bars indicate standard deviations.

Dual-targeting approach to reduce *in situ* biofilm formation on oral environment

Since different environmental factors can affect oral biofilm formation (Marsh *et al.*, 2011; Xu *et al.*, 2015), and considering the impressive results obtained in the *in vitro* study, mainly for the use of PI associated with antibiotics, we further evaluate the dual-targeting approach to reduce biofilm formation on Ti using an oral *in situ* model. *In situ* biofilms formed for 5 days in the oral cavity of volunteers and then treated with antimicrobial agents (PI and/or antibiotics) showed higher bacterial cell death, compared to control groups untreated or each therapy alone (Fig. 6A). Although the use of only PI or antibiotics (amoxicillin and metronidazole) alone led to significant bacterial cell death (Fig. 6B), the dual-targeting approach increased death cell proportion eradicating biofilms growing on Ti ($p<0.05$) (Fig. 6B). Therefore, the ECM degradation strategy was effective to enhance antimicrobial effect of antibiotics in biofilms growing on Ti surface in the oral environment.

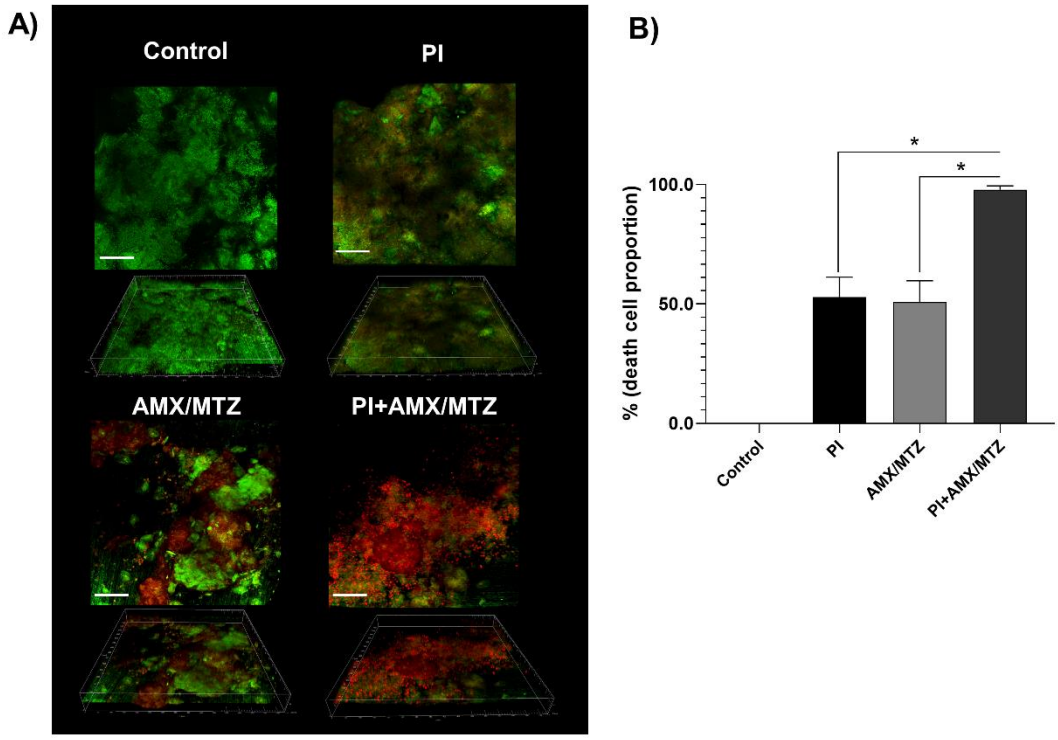

Figure 6. Oral *in situ* biofilms formed for 5 days on titanium discs placed in a palatal appliance and treated by matrix-targeting and antimicrobial agents. Biofilms were exposed extra-orally to 20% sucrose solution as substrate for extracellular matrix synthesis. **(A)** X–Y isosurfaces (top panel) and three-dimensional reconstructions (bottom panel) of representative confocal laser scanning microscopy images of *in situ* biofilms. Live cells (green) was visualized after stained with Syto-9 and dead cells (red) were stained by propidium iodide solution. Scale bars, 50 µm (X–Y surfaces) and 70 µm (three-dimensional reconstructions). **(B)** Proportion (%) of dead cells in relation total biovolume (live + dead cells) after treatments. Control – 0.9% NaCl; PI – povidone iodine (2%); AMX – amoxicillin (4 µg/mL); MET – metronidazole (4 µg/mL). *$p<0.05$, using Bonferroni t-test. The error bars indicate standard deviations.

Discussion

Extracellular polymeric matrix has a critical role in the pathogenicity of microorganisms growing in biofilm state, and confers an ecological advantage for growth and virulence factors of

oral biofilms (Flemming and Wingender, 2010). Our study is the first one to provide experimental evidence of the specific effect of biofilm ECM favoring a transition process from a commensal to a pathogenic biofilm Ti material, creating a suitable environment to anaerobic pathogens growth. Importantly, we also showed that ECM reduced antimicrobial susceptibility of biofilms on Ti surface and that a dual-targeting therapy approach, which disrupted biofilm ECM prior to antibiotic treatment, was able to reduce live organisms.

Our results also suggested that the significant higher bacterial counts on ECM-rich biofilm may be related to biofilm ECM properties, such as increased bacterial adhesion, nutrient source, enhanced interaction among microorganisms and to the 3D matrix organization (Flemming and Wingender, 2010; Klein *et al.*, 2015; Bowen *et al.*, 2018a), as observed by bacterial clusters embedded in a ECM on biofilms growing in culture media supplemented with sucrose. Although same bacterial counts for single-specie biofilms growing under glucose or sucrose exposure has been reported (Costa Oliveira *et al.*, 2017), these carbohydrates differ drastically in terms of effect on biofilm structure and biovolume. Our results, however, showed that for a polymicrobial biofilm, sucrose exposure increased total bacterial loads, mainly for *Streptococcus* counts. A possible explanation for this finding is the high diversity of bacterial species which have gtfs genes (Xiao *et al.*, 2012), and the ability of some gtfs to bind avidly to other microorganisms and allow them to become glucan producers (Ricker *et al.*, 2014). Moreover, considering the co-adhesion and interaction properties of polymicrobial biofilms, some bacteria may positively affect streptococci growth. Additionally, some extracellular polymers synthesized by gtfs may be used by *Streptoccocus* as nutrient source during starvation periods (Bowen and Koo, 2011a), keeping the bacteria metabolism active.

Here, we also observed that biofilm ECM is a key factor to create an advantageous ecological environment which allow facultative and anaerobic pathogens growth on Ti. Previous results from our group have showed that sucrose exposure can favor microbiological dysbiosis in

biofilms formed *in situ* on Ti material increasing anaerobic species growth (Souza *et al.*, 2019), and it has been associated with elevated biofilm biomass, when compared to no sucrose exposed group. However, in this previous study the continuous biofilm growth *in situ* and increased biofilm biomass may also affected microbiological composition, and host properties may affected microbiological composition, such as other nutrient source from diet and salivar content. Therefore, in the present study we showed the isolated and specific role of ECM to promote a transition from a commensal to a pathogenic microbial profile by allowing biofilm growth in phase I (aerobic) and phase II (anaerobic) and showing that only EMC-rich biofilm significantly shifted towards a more pathogenic composition when compared to non EMC-rich biofilm. The microbiological shift in oral biofilms has been attributed mainly to local environmental changes due inflammatory process (Marsh *et al.*, 2011), such as nutrient content which favor proteolytic species (Naginyte *et al.*, 2019). However, we have showed that sucrose exposure (Souza *et al.*, 2019) and in the present study the biofilm structure, specifically ECM-rich environment also drives toward a more putative anaerobic biofilm, suggesting a paradigms shift considering others factors, such as biofilm-related properties, which promote microbiological dysbiosis.

ECM increase the biofilm volume and changes the physical-biologic properties of biofilms creating a variety of microenvironments with localized gradients of oxygen levels and nutrients source (Koo *et al.*, 2013), which may favor even strict anaerobic pathogens, such as *T. forsythia,* which is in accordance with findings of the present study. This microbiological shift on ECM-rich biofilms suggests a more pathogenic biofilm that clinically acts as a physical-chemical stress factor to trigger inflammatory process on surrounding implant tissues. In fact, putative pathogens from red microbial complex represented by *T. forsythia, P. gingivalis* and *T. denticola* which are strongly associated to the etiology of peri-implant infections (Pérez-Chaparro *et al.*, 2016) and oral tissues destruction (Arciola *et al.*, 2018) were found ≈3-fold higher in matrix-rich biofilms. The virulence of these biofilms was confirmed by fibroblast assay, in which matrix-rich biofilms led to higher cell

death even without direct contact of biofilms with fibroblast cells. This result suggests that the complex structure of biofilm matrix and bacterial products released into the culture media can trigger or further amplify cell damage in peri-implant tissues.

The ability of extracellular matrix to enhance antimicrobial resistance of biofilms has been recognized by *in vitro* and animal models, but has been mostly described for dental surfaces (Xiao *et al.*, 2012; Thurnheer *et al.*, 2014; Klein *et al.*, 2015; Kim *et al.*, 2018; Ren *et al.*, 2019) or other dental materials, such as acrylic resin(Hwang *et al.*, 2017; Lobo *et al.*, 2019; Weldrick *et al.*, 2019). Notably, ECM-rich biofilms growing on Ti surface presented reduced susceptibility against antimicrobials, which is in agreement with results demonstrated on hydroxyapatite surfaces (Kim *et al.*, 2018; Ren *et al.*, 2019). This effect has been attributed to the ability of ECM to create microenvironments which restrict the access of antimicrobial agents into bacterial cells and due to the negative charge of extracellular polymers reducing the diffusion of positively charged antimicrobials, such as CHX (Xiao *et al.*, 2012). Furthermore, the adhesive interaction of extracellular polymers and the binding ability of bacterial cells (Falsetta *et al.*, 2014) may create a protective layer restricting the direct access for antimicrobial agents diffusion. Thus, antimicrobial agents alone have trouble spreading in matrix-rich biofilms, which reduces their efficacy.

Trying to overcome this limitation, we used a dual-targeting approach to disrupt the assembly of protective ECM followed by different antimicrobial agents to reduce bacterial viability. Although PI (matrix-targeting agent) has a moderate bactericidal effect against bacteria, due to irreversible binding to the bacterial cell wall (lower than CHX), its use in combination with all tested antimicrobials showed a synergistic effect and almost completely eliminated *in vitro* and *in situ* polymicrobial biofilms viability on Ti. This effect has been attributed to the ability of iodine to change biofilm structure reducing bacterial microcolonies and disrupting ECM, which change the density of biofilms and promote the access of antimicrobials (Ren *et al.*, 2019). Moreover, PI can inhibit the activity of gtfs to synthetize glucan polymers in mixed biofilms (Kim *et al.*, 2018),

suggesting a suitable preventive approach to reduce the pathogenicity of oral biofilms. PI is a low-cost agent and has some bactericidal effect (Oduwole *et al.*, 2010), favoring its use for peri-implant disease therapy. Although the use of AMX + MTZ has shown no effect to reduce putative pathogens during peri-implant disease (Suárez-López Del Amo *et al.*, 2016), the effect of dual-targeting strategy with PI seems promising and needs to be elucidated by *in vivo* models.

Considering the process of oral biofilm formation *in vitro* (dynamic model) and *in situ*, our observations confirm that dual-targeting approach was able to reduce oral bacteria viability on Ti surface due to ECM degradation (Fig. 7). The findings developed here encourage future studies to evaluate *in vivo* this dual-targeting approach and the effect on clinical outcomes. Summarizing the above-mentioned findings, we showed that ECM-rich biofilms presented higher bacterial accumulation on Ti surface, and once mature these biofilms shifted towards a more pathogenic state, leading to dysbiosis and anaerobic pathogens overgrowth. This microbiological shift increases biofilm virulence and host immune response. The dual-targeting approach was able to disrupt the ECM and allow higher bactericidal effect of tested drugs. These results contribute to a better understanding of the role of biofilm ECM as an etiologic factor for peri-implant disease and shed light on the development of therapeutic strategies aiming to reduce ECM prior antibacterial therapies for the treatment of inflammatory response on tissues surrounding implanted materials.

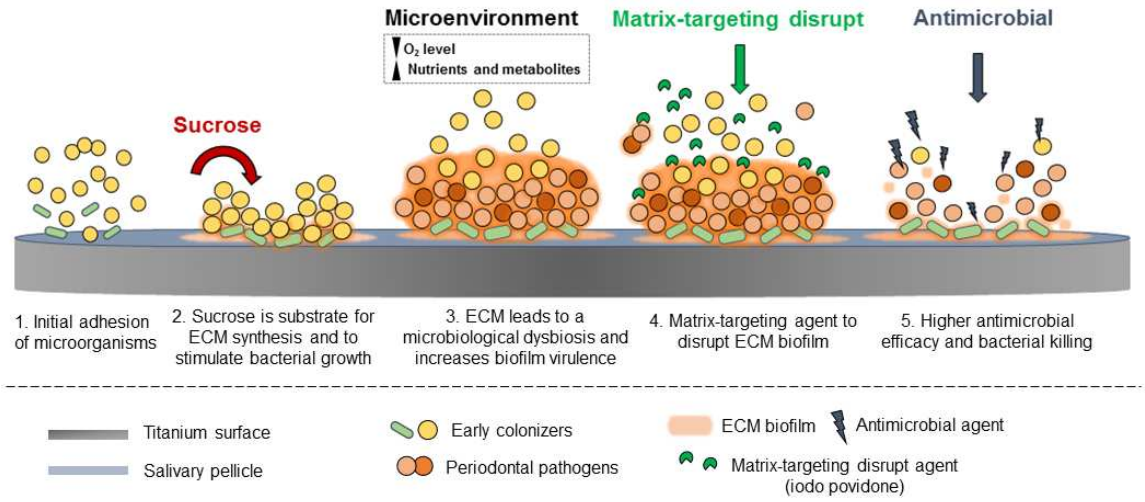

Figure 7. Schematic representation of the possible (1) effect of ECM in the microbiological dysbiosis of biofilms growing on titanium surface; (2) and mechanism of bacterial susceptibility related to ECM and their disruption as an approach to enhance antimicrobials efficacy on biofilms growing on titanium surface.

Experimental Procedures

Sample preparation

Commercially pure Ti (cpTi) discs grade II (ø = 8 mm x 2 mm) (Conexão Ltd., São Paulo, Brazil) were polished (roughness average, Ra 0.20 ±0.06µm) and used as substratum for biofilm growth (Nagay *et al.*, 2019). All samples were ultrasonically cleaned with deionized water (10 min), degreased with 70% propanol (10 min) and hot-air dried (250 °C) (Barão *et al.*, 2012). Then, cpTi discs were autoclaved (121 °C, 30 min).

In vitro biofilm model and growth conditions to test biofilm matrix effect

Biofilm microcosm model used was based on previous studies which considered the oral microbiome composition (Souza *et al.*, 2018) and microbiological shift from an aerobic (supragingival) to an anaerobic profile (subgingival) (Thurnheer *et al.*, 2016; Souza *et al.*, 2018). For this, fresh stimulated human saliva was collected from 5 healthy volunteers and used as

microbial inoculum (approved by local Research and Ethics Committee, number: 86638918.0.0000.5418). Volunteers inclusion and exclusion criteria have been previously described (Souza *et al.*, 2019).

First, samples were coated with filtered saliva (0.22 μm membrane filter) for 30 min at 37 °C to simulate acquired salivary pellicle, stimulating bacterial adhesion and to mimic an *in vivo* condition (Ccahuana-Vásquez and Cury, 2010). Microcosm biofilm was then allowed to develop in mFUM-modified fluid universal medium (Gmür and Guggenheim, 1983) and 10% (v/v) BHI medium (Becton-Dickinson, Sparks, MD, USA). For biofilm growth, stimulated human saliva (unfiltered) was used as bacterial inoculum (1:10 v/v) to mimic oral microbiological composition (Souza *et al.*, 2018) with final concentration of ~10^8 cell/mL. Biofilm growth conditions, such as medium and bacteria inoculum source, were previously standardized (See Supplemental Material, Fig. S1). Initially, oral biofilms were grown in microaerophilia (10% CO_2, 37 °C) simulating a supragingival/aerobic condition (Phase 1). After initial biofilm formation (24 h), biofilms were exposed/immersed to 10% (w/v) sucrose treatments 4×/day (3 min each) for 2 days (48 h) as substrate to insoluble ECM synthesis to form matrix-rich biofilms (Aires *et al.*, 2008; Xiao *et al.*, 2012). As a negative control for insoluble ECM production 10% (w/v) glucose was used. A non-carbohydrate control was 0.9% NaCl exposure. After each treatment, discs were washed in 0.9% NaCl solution and then returned to the culture media for incubation.

To test whether the ECM synthesized can favor biofilm dysbiosis and increase peri-implant pathogens which growth mainly under anaerobic conditions, after 72 h of biofilm formation, the growing conditions were changed for an anaerobic condition (Phase 2 - 10% H_2, 5% CO_2, 85% N_2, 37 ºC). Biofilms were exposed to a new human saliva inoculum (1:10 v/v, same volunteers of phase 1) - as bacteria source of anaerobic pathogens - in mFUM media. Fresh medium was supplied each 24 h. Experiments were conducted in triplicate. An overview of this *in vitro* biofilm model is illustrated in Figure 8.

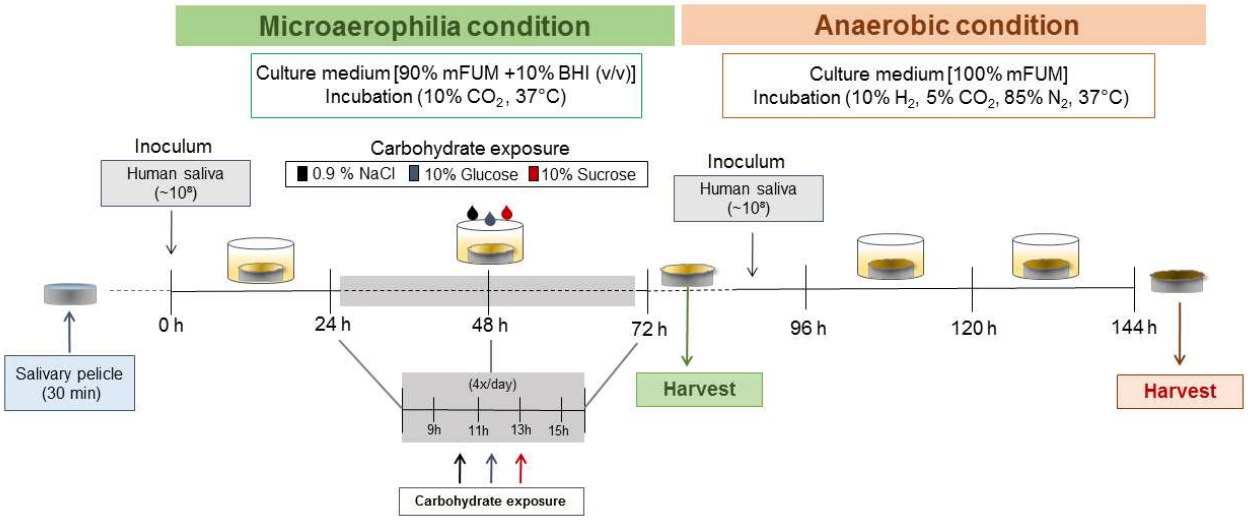

Figure 8. Experimental design of oral *in vitro* biofilm model. Biofilm was developed to mimic a transition process from a microaerophilia/supragingival (phase 1) to an anaerobic/subgingival (phase 2) condition. After salivary pellicle (stimulated filtered human saliva) formation to promote microbial adhesion, titanium discs were exposed to initial biofilm growth in mFum medium (1:80 v/v) + 10% BHI (1:10 v/v) + unfiltered human saliva as microbial inoculum for 24 h in a microaerophilia condition (10% CO_2, 37 °C). Then, biofilms were exposed to 10% sucrose treatments 4×/day for 2 days (48 h) as substrate to biofilm matrix synthesis. Glucose and NaCl exposure were used as controls. After 72 h, biofilms were transferred to an anaerobic condition (10% H_2, 5% CO_2, 85% N_2, 37 ºC), exposed to a new microbial inoculum (unfiltered human saliva) and allowed to develop for additional 72 h. Harvest of the biofilms were performed at the end of each phase and taken to analysis.

Biofilm virulence

The virulence and pathogenicity of matrix-rich biofilms were tested using a fibroblast cellular monolayer. Phase 1 biofilm conditions (microaerophilia/supragingival) mentioned above was used for biofilm growth, since after 48 h of biofilm growth high levels of ECM synthesized and putative pathogens is expected (Xiao *et al.*, 2012). Biofilms were supplemented with 1% sucrose (matrix-rich biofilm) or 1% glucose (control). Fibroblasts monolayer (3T3) (10^7 cells) was cultivated in Dulbecco's Modified Eagle's Medium with 10% bovine calf serum on 12-well plate bottom under a cell culture insert to create a 2-chamber compartment in each well. Next, Ti discs

with preformed biofilm (72 h) were inverted over the insert (on the top compartment, without direct contact with fibroblast cells) and immersed in medium to be incubated for 16 h. In this way, we tested whether products released by each biofilm in the culture medium could affect fibroblast viability. Lactate dehydrogenase (LDH) release into the basal culture media was used as an indicator of cell damage (CytoTox-ONE Homogeneous Membrane Integrity Assay kit - Promega, Madison, WI, USA) and the optical density units (490 nm) was checked, results were expressed as fold over (sucrose/glucose). Since chemokine IL-8, plays multiple roles as a proinflammatory cytokine by mediating the activation and chemotaxis of various immune cell types, IL-8 concentration in the media was used as an indicator of immune response from fibroblasts to the biofilm products and was measured by ELISA (R&D Systems, Minneapolis, MN, USA). Results expressed as pg of protein per mL was showed as fold over (sucrose/glucose).

Biofilm susceptibility to antimicrobials

Next, we examined the role of ECM to reduce antimicrobial susceptibility of biofilms growing on Ti. For this, *Streptococcus mutans*, which is recognized to have three glucosyltransferases exoenzymes able to use sucrose as substrate to synthesize insoluble ECM (Bowen and Koo, 2011b), was added into the microcosm biofilm model to favor matrix-rich biofilms (sucrose supplementation). For this, *S. mutans* UA159 strain overnight culture in tryptone-yeast extract broth (UTYEB) was adjusted to obtain 10^7 cells/mL (17). Samples were incubated in mFUM media + microbial inoculum (stimulated human saliva ~10^8 cells/mL and *S. mutans* ~10^7 cells/mL) + 1% sucrose at 37 °C with 10% CO_2 for 24 h. ECM negative control was 1% glucose supplementation. After 24 h biofilms were exposed to 0.2% (v/v) chlorhexidine antimicrobial, a common topical antimicrobial using for oral biofilms including on Ti surface (Heitz-Mayfield *et al.*, 2011; Souza *et al.*, 2018) for 10 min. Then, discs were washed twice in 0.9% NaCl and taken for microbial analysis consisting of bacteria count.

To test a matrix-targeting approach to disrupt biofilm ECM and to enhance antimicrobial effect in biofilms growing *in vitro* on Ti surface we used the 72 h microcosm oral biofilm as mentioned above. Supplementing the human saliva inoculum (~10^8 cells/mL), *S. mutans* (10^7 cells/mL) was added to increase ECM synthesis. Biofilms were allowed to develop for 72 h in mFUM media + 1% sucrose. PI (2%) immersion was used as agent to disrupt biofilm matrix (Kim *et al.*, 2018). After 48 and 72 h, the biofilms were treated for 10 min by immersion with one of the following treatments: 0.2% (v/v) chlorhexidine (CHX) (Souza *et al.*, 2018)(32); 2% (v/v) povidone iodine (PI) (Kim *et al.*, 2018); 4 µg (w/v) amoxicillin/4 µg (w/v) metronidazole (AMX/MTZ) (Shibli *et al.*, 2019); or by the combination of treatments: 2% (v/v) povidone iodine + 0.2% (v/v) chlorhexidine (PI+CHX); and 2% (v/v) povidone iodine + 4 µg (w/v) amoxicillin/4 µg (w/v) metronidazole (PI+AMX/MET). 0.9% NaCl solution was used as a control and for washing and removing the treatment residues. Biofilms were then analyzed for live/dead cells by confocal laser scanning microscopic.

***In situ* model**

Based on the results obtained on the *in vitro* microcosm biofilm assay, an *in situ* oral biofilm model was used to test the dual-targeting approach (matrix disruption and antimicrobial drugs) to reduce biofilm growing on Ti surface exposed to oral environment (approved by local Research and Ethics Committee, number: 5366416.0.0000.5418). For this, 5 volunteers were selected based on their good general and oral health, as previously described (Vale *et al.*, 2007). Volunteers wore a palatal appliance containing Ti discs (8×2 mm) protected by a plastic mesh to allow biofilm accumulation for 5 days. Samples were exposed extra-orally to 20% sucrose solution 4×/day (11) to provide substrate for ECM synthesis. In the morning of the 6th day, the discs with biofilms were removed, randomized and treated by immersion for 30 min with one of the following treatments: (1) 2% PI; (2) 4 µg amoxicillin + 4 µg metronidazole; (3) 2% PI + 4µg amoxicillin +

4µg metronidazole. Biofilms not treated were used as controls. Biofilms were then analyzed for live/dead cells by confocal laser scanning microscopic.

Microorganism count

Microorganisms count in biofilms growing on Ti was determined by colony-forming units (CFUs). After sonication (Aires *et al.*, 2008) biofilm suspensions was serially diluted and plated on the following culture media: Columbia blood agar (CBA) medium supplemented with 5% (v/v) defibrinated sheep blood for total bacteria count (Nagay *et al.*, 2019) and Mitis Salivarius agar (MSA) medium for total *Streptococcus* count (Cavalcanti *et al.*, 2014). Plates were incubated at 37 °C in 10% CO_2 atmosphere for 48 h. Colony-forming units (CFUs) were counted by stereomicroscopy, and the results were expressed as CFUs per biofilm.

Confocal laser scanning microscopy (CLSM)

Confocal laser scanning microscopy (CLSM) was used for biovolume and 3D structure analyses of biofilms. Live and dead cells were stained with 1 µM SYTO-9 green fluorescent nucleic acid (485-498 nm; Thermo Scientific, USA) and propidium iodide solution (490−635 nm; Thermo Scientific, USA) under protection from light for 20 min (Costa Oliveira *et al.*, 2017). The insoluble ECM was stained during the biofilm formation with 1 µM Alexa Fluor 647-labeled dextran conjugate (650-668 nm; Thermo Scientific, USA). This probe is incorporated into glucans polymers produced during ECM formation (Klein *et al.*, 2009). Images were obtained in a DMI 6000 CS inverted microscope coupled to a TCS SP5 computer-operated confocal laser scanning system (Leica Microsystems CMS, Mannheim, Baden-Württemberg, Germany). The IMARIS software (Bitplane, Inc., Saint Paul, MN, USA) was used for reconstructed into 3-D images. Surface reconstructions using the surpass mode and total fluorescent staining of the confocal micrographs were used to calculate the biovolumes (in μm^3) of biofilms.

Microbiological composition

Microbiological composition in the microcosm oral biofilm model was evaluated by checkerboard DNA–DNA hybridization technique (Socransky *et al.*, 1994; Miranda *et al.*, 2019). Biofilms on Ti surface were collected by means of a modified cell scraper (length, 240mm) (TPP, Trasadingen, Switzerland) in one movement from a central area of each disc. Then, samples collected were analyzed for levels of 39 bacterial species related to peri-implant disease (Mestnik *et al.*, 2010; Souza *et al.*, 2018). Data were expressed by bacterial genus (grouping bacterial species) and as fold change in each bacteria count of sucrose over glucose exposure biofilms in anaerobic condition (phase 2) grouped by periodontal microbial complexes (Socransky *et al.*, 1994).

Statistics

The normality of errors and homoscedasticity of data were checked for each response variable. One-way ANOVA followed by Tukey HSD test, and student's t-test were used for statistical analysis. SPSS software (IBM SPSS Statistics for Windows, v.21.0., IBM Corp., Armonk, NY, USA) was used and a significance level of 5% was adopted.

REFERENCES

Ahn, Sug-Joon, Ahn, Sang-Joon, Browngardt, C.M., and Burne, R.A. (2009) Changes in Biochemical and Phenotypic Properties of Streptococcus mutans during Growth with Aeration. *Appl Environ Microbiol* **75**: 2517–2527.

Aires, C.P., Del Bel Cury, A.A., Tenuta, L.M.A., Klein, M.I., Koo, H., Duarte, S., and Cury, J.A. (2008) Effect of starch and sucrose on dental biofilm formation and on root dentine demineralization. *Caries Res* **42**: 380–386.

Arciola, C.R., Campoccia, D., and Montanaro, L. (2018) Implant infections: adhesion, biofilm formation and immune evasion. *Nat Rev Microbiol* **16**: 397–409.

Barão, V.A.R., Mathew, M.T., Assunção, W.G., Yuan, J.C.-C., Wimmer, M.A., and Sukotjo, C. (2012) Stability of cp-Ti and Ti-6Al-4V alloy for dental implants as a function of saliva pH – an electrochemical study. *Clinical Oral Implants Research* **23**: 1055–1062.

Bowen, W.H., Burne, R.A., Wu, H., and Koo, H. (2018a) Oral Biofilms: Pathogens, Matrix and Polymicrobial Interactions in Microenvironments. *Trends Microbiol* **26**: 229–242.

Bowen, W.H., Burne, R.A., Wu, H., and Koo, H. (2018b) Oral Biofilms: Pathogens, Matrix, and Polymicrobial Interactions in Microenvironments. *Trends Microbiol* **26**: 229–242.

Bowen, W.H. and Koo, H. (2011a) Biology of Streptococcus mutans-derived glucosyltransferases: role in extracellular matrix formation of cariogenic biofilms. *Caries Res* **45**: 69–86.

Bowen, W.H. and Koo, H. (2011b) Biology of Streptococcus mutans-derived glucosyltransferases: role in extracellular matrix formation of cariogenic biofilms. *Caries Res* **45**: 69–86.

Cavalcanti, Y.W., Bertolini, M.M., da Silva, W.J., Del-Bel-Cury, A.A., Tenuta, L.M.A., and Cury, J.A. (2014) A three-species biofilm model for the evaluation of enamel and dentin demineralization. *Biofouling* **30**: 579–588.

Ccahuana-Vásquez, R.A. and Cury, J.A. (2010) S. mutans biofilm model to evaluate antimicrobial substances and enamel demineralization. *Braz Oral Res* **24**: 135–141.

Costa Oliveira, B.E., Cury, J.A., and Ricomini Filho, A.P. (2017) Biofilm extracellular polysaccharides degradation during starvation and enamel demineralization. *PLoS ONE* **12**: e0181168.

Costerton, J.W., Lewandowski, Z., Caldwell, D.E., Korber, D.R., and Lappin-Scott, H.M. (1995) Microbial biofilms. *Annu Rev Microbiol* **49**: 711–745.

Derks, J. and Tomasi, C. (2015) Peri-implant health and disease. A systematic review of current epidemiology. *J Clin Periodontol* **42 Suppl 16**: S158-171.

Duarte, S., Klein, M.I., Aires, C.P., Cury, J.A., Bowen, W.H., and Koo, H. (2008) Influences of starch and sucrose on Streptococcus mutans biofilms. *Oral Microbiol Immunol* **23**: 206–212.

Esposito, M., Grusovin, M.G., and Worthington, H.V. (2012) Interventions for replacing missing teeth: treatment of peri-implantitis. *Cochrane Database Syst Rev* **1**: CD004970.

Falsetta, M.L., Klein, M.I., Colonne, P.M., Scott-Anne, K., Gregoire, S., Pai, C.-H., et al. (2014) Symbiotic Relationship between Streptococcus mutans and Candida albicans Synergizes Virulence of Plaque Biofilms In Vivo. *Infect Immun* **82**: 1968–1981.

Flemming, H.-C. and Wingender, J. (2010) The biofilm matrix. *Nat Rev Microbiol* **8**: 623–633.

de Freitas, M.M., da Silva, C.H.P., Groisman, M., and Vidigal, G.M. (2011) Comparative analysis of microorganism species succession on three implant surfaces with different roughness: an in vivo study. *Implant Dent* **20**: e14-23.

Gmür, R. and Guggenheim, B. (1983) Antigenic heterogeneity of Bacteroides intermedius as recognized by monoclonal antibodies. *Infect Immun* **42**: 459–470.

Heitz-Mayfield, L.J.A., Salvi, G.E., Botticelli, D., Mombelli, A., Faddy, M., Lang, N.P., and Implant Complication Research Group (2011) Anti-infective treatment of peri-implant mucositis: a randomised controlled clinical trial. *Clin Oral Implants Res* **22**: 237–241.

Hwang, G., Koltisko, B., Jin, X., and Koo, H. (2017) Nonleachable Imidazolium-Incorporated Composite for Disruption of Bacterial Clustering, Exopolysaccharide-Matrix Assembly, and Enhanced Biofilm Removal. *ACS Appl Mater Interfaces* **9**: 38270–38280.

Jenkinson, H.F. (2011) Beyond the oral microbiome. *Environ Microbiol* **13**: 3077–3087.

Kim, D., Liu, Y., Benhamou, R.I., Sanchez, H., Simón-Soro, Á., Li, Y., et al. (2018) Bacterial-derived exopolysaccharides enhance antifungal drug tolerance in a cross-kingdom oral biofilm. *ISME J* **12**: 1427–1442.

Klein, M.I., Duarte, S., Xiao, J., Mitra, S., Foster, T.H., and Koo, H. (2009) Structural and Molecular Basis of the Role of Starch and Sucrose in Streptococcus mutans Biofilm Development. *Appl Environ Microbiol* **75**: 837–841.

Klein, M.I., Hwang, G., Santos, P.H.S., Campanella, O.H., and Koo, H. (2015) Streptococcus mutans-derived extracellular matrix in cariogenic oral biofilms. *Front Cell Infect Microbiol* **5**: 10.

Koo, H., Falsetta, M.L., and Klein, M.I. (2013) The exopolysaccharide matrix: a virulence determinant of cariogenic biofilm. *J Dent Res* **92**: 1065–1073.

Koo, H., Xiao, J., Klein, M.I., and Jeon, J.G. (2010) Exopolysaccharides Produced by Streptococcus mutans Glucosyltransferases Modulate the Establishment of Microcolonies within Multispecies Biofilms. *J Bacteriol* **192**: 3024–3032.

Kopec, L.K., Vacca-Smith, A.M., and Bowen, W.H. (1997) Structural aspects of glucans formed in solution and on the surface of hydroxyapatite. *Glycobiology* **7**: 929–934.

Lang, N.P., Brägger, U., Walther, D., Beamer, B., and Kornman, K.S. (1993) Ligature-induced peri-implant infection in cynomolgus monkeys. I. Clinical and radiographic findings. *Clin Oral Implants Res* **4**: 2–11.

Lobo, C.I.V., Rinaldi, T.B., Christiano, C.M.S., De Sales Leite, L., Barbugli, P.A., and Klein, M.I. (2019) Dual-species biofilms of Streptococcus mutans and Candida albicans exhibit more biomass and are mutually beneficial compared with single-species biofilms. *J Oral Microbiol* **11**: 1581520.

Marsh, P.D., Moter, A., and Devine, D.A. (2011) Dental plaque biofilms: communities, conflict and control. *Periodontol 2000* **55**: 16–35.

Matos, A.O., Ricomini-Filho, A.P., Beline, T., Ogawa, E.S., Costa-Oliveira, B.E., de Almeida, A.B., et al. (2017) Three-species biofilm model onto plasma-treated titanium implant surface. *Colloids Surf B Biointerfaces* **152**: 354–366.

Mestnik, M.J., Feres, M., Figueiredo, L.C., Duarte, P.M., Lira, E.A.G., and Faveri, M. (2010) Short-term benefits of the adjunctive use of metronidazole plus amoxicillin in the microbial profile and in the clinical parameters of subjects with generalized aggressive periodontitis. *J Clin Periodontol* **37**: 353–365.

Miranda, S.L.F., Damasceno, J.T., Faveri, M., Figueiredo, L., da Silva, H.D., Alencar, S.M. de A., et al. (2019) Brazilian red propolis reduces orange-complex periodontopathogens growing in multispecies biofilms. *Biofouling* **35**: 308–319.

Mombelli, A. and Décaillet, F. (2011) The characteristics of biofilms in peri-implant disease. *J Clin Periodontol* **38 Suppl 11**: 203–213.

Nagay, B.E., Dini, C., Cordeiro, J.M., Ricomini-Filho, A.P., de Avila, E.D., Rangel, E.C., et al. (2019) Visible-Light-Induced Photocatalytic and Antibacterial Activity of TiO2 Codoped with Nitrogen and Bismuth: New Perspectives to Control Implant-Biofilm-Related Diseases. *ACS Appl Mater Interfaces* **11**: 18186–18202.

Naginyte, M., Do, T., Meade, J., Devine, D.A., and Marsh, P.D. (2019) Enrichment of periodontal pathogens from the biofilms of healthy adults. *Scientific Reports* **9**: 1–9.

Ntrouka, V.I., Slot, D.E., Louropoulou, A., and Van der Weijden, F. (2011) The effect of chemotherapeutic agents on contaminated titanium surfaces: a systematic review. *Clin Oral Implants Res* **22**: 681–690.

Oduwole, K.O., Glynn, A.A., Molony, D.C., Murray, D., Rowe, S., Holland, L.M., et al. (2010) Anti-biofilm activity of sub-inhibitory povidone-iodine concentrations against Staphylococcus epidermidis and Staphylococcus aureus. *J Orthop Res* **28**: 1252–1256.

Pérez-Chaparro, P.J., Duarte, P.M., Shibli, J.A., Montenegro, S., Lacerda Heluy, S., Figueiredo, L.C., et al. (2016) The Current Weight of Evidence of the Microbiologic Profile Associated With Peri-Implantitis: A Systematic Review. *J Periodontol* **87**: 1295–1304.

Ren, Z., Kim, D., Paula, A.J., Hwang, G., Liu, Y., Li, J., et al. (2019) Dual-Targeting Approach Degrades Biofilm Matrix and Enhances Bacterial Killing. *J Dent Res* **98**: 322–330.

Retamal-Valdes, B., Formiga, M. de C., Almeida, M.L., Fritoli, A., Figueiredo, K.A., Westphal, M., et al. (2019) Does subgingival bacterial colonization differ between implants and teeth? A systematic review. *Brazilian Oral Research* **33**:.

Rickard, A.H., Gilbert, P., High, N.J., Kolenbrander, P.E., and Handley, P.S. (2003) Bacterial coaggregation: an integral process in the development of multi-species biofilms. *Trends Microbiol* **11**: 94–100.

Ricker, A., Vickerman, M., and Dongari-Bagtzoglou, A. (2014) Streptococcus gordonii glucosyltransferase promotes biofilm interactions with Candida albicans. *J Oral Microbiol* **6**:.

Rosier, B.T., Marsh, P.D., and Mira, A. (2018) Resilience of the Oral Microbiota in Health: Mechanisms That Prevent Dysbiosis. *J Dent Res* **97**: 371–380.

Shibli, J.A., Ferrari, D.S., Siroma, R.S., Figueiredo, L.C. de, Faveri, M. de, and Feres, M. (2019) Microbiological and clinical effects of adjunctive systemic metronidazole and amoxicillin in the non-surgical treatment of peri-implantitis: 1 year follow-up. *Braz Oral Res* **33**: e080.

Socransky, S.S., Smith, C., Martin, L., Paster, B.J., Dewhirst, F.E., and Levin, A.E. (1994) "Checkerboard" DNA-DNA hybridization. *BioTechniques* **17**: 788–792.

Souza, J.G.S., Cury, J.A., Ricomini Filho, A.P., Feres, M., Faveri, M. de, and Barão, V.A.R. (2019) Effect of sucrose on biofilm formed in situ on titanium material. *J Periodontol* **90**: 141–148.

Souza, J.G.S., Lima, C.V., Costa Oliveira, B.E., Ricomini-Filho, A.P., Faveri, M., Sukotjo, C., et al. (2018) Dose-response effect of chlorhexidine on a multispecies oral biofilm formed on pure titanium and on a titanium-zirconium alloy. *Biofouling* **34**: 1175–1184.

Stein, J.M., Hammächer, C., and Michael, S.S.-Y. (2018) Combination of ultrasonic decontamination, soft tissue curettage, and submucosal air polishing with povidone-iodine application for non-surgical therapy of peri-implantitis: 12-month clinical outcomes. *Journal of Periodontology* **89**: 139–147.

Suárez-López Del Amo, F., Yu, S.-H., and Wang, H.-L. (2016) Non-Surgical Therapy for Peri-Implant Diseases: a Systematic Review. *J Oral Maxillofac Res* **7**: e13.

Thurnheer, T., Belibasakis, G.N., and Bostanci, N. (2014) Colonisation of gingival epithelia by subgingival biofilms in vitro: Role of "red complex" bacteria. *Archives of Oral Biology* **59**: 977–986.

Thurnheer, T., Bostanci, N., and Belibasakis, G.N. (2016) Microbial dynamics during conversion from supragingival to subgingival biofilms in an in vitro model. *Mol Oral Microbiol* **31**: 125–135.

Vacca-Smith, A.M., Venkitaraman, A.R., Quivey, R.G., and Bowen, W.H. (1996) Interactions of streptococcal glucosyltransferases with alpha-amylase and starch on the surface of saliva-coated hydroxyapatite. *Arch Oral Biol* **41**: 291–298.

Vale, G.C., Tabchoury, C.P.M., Arthur, R.A., Del Bel Cury, A.A., Paes Leme, A.F., and Cury, J.A. (2007) Temporal relationship between sucrose-associated changes in dental biofilm composition and enamel demineralization. *Caries Res* **41**: 406–412.

Weldrick, P.J., Hardman, M.J., and Paunov, V.N. (2019) Enhanced Clearing of Wound-Related Pathogenic Bacterial Biofilms Using Protease-Functionalized Antibiotic Nanocarriers. *ACS Appl Mater Interfaces*.

Xiao, J., Klein, M.I., Falsetta, M.L., Lu, B., Delahunty, C.M., Yates, J.R., et al. (2012) The Exopolysaccharide Matrix Modulates the Interaction between 3D Architecture and Virulence of a Mixed-Species Oral Biofilm. *PLoS Pathog* **8**:.

Xu, H., Sobue, T., Bertolini, M., Thompson, A., Vickerman, M., Nobile, C.J., and Dongari-Bagtzoglou, A. (2017) S. oralis activates the Efg1 filamentation pathway in C. albicans to promote cross-kingdom interactions and mucosal biofilms. *Virulence* **8**: 1602–1617.

Xu, X., He, J., Xue, J., Wang, Y., Li, K., Zhang, K., et al. (2015) Oral cavity contains distinct niches with dynamic microbial communities. *Environ Microbiol* **17**: 699–710.

Zheng, H., Xu, L., Wang, Z., Li, L., Zhang, J., Zhang, Q., et al. (2015) Subgingival microbiome in patients with healthy and ailing dental implants. *Sci Rep* **5**:.

Supplementary material

Part I. Supplementary Materials and Methods

In vitro biofilm model adapted

In this study, the biofilm model proposed by Thurnheer et al. 2016 was adapted for titanium surfaces. For this, we analyzed the influence of different sources of bacterial inoculum (supra-gingival oral biofilm x stimulated saliva) and culture media (BHI, mFum and TSB medium) on bacterial count (CFU). The hypothesis tested was that these factors could favor or inhibit the bacterial growth in a aerobic and anaerobic conditions.

To obtain the microbiological inoculum, volunteers (n = 6) older than 18 years old, good systemic and oral health and normal stimulated salivary flow rate (> 0.7 mL/min) (approved by local Research and Ethics Committee, number: 86638918.0.0000.5418) were selected. For all volunteers (baseline), dental prophylaxis and supra-gingival scraping procedures for standardization of biofilm formation were conducted. After this procedure, participants were instructed to not brush molars (mesial and distal faces), and to not use oral antiseptics and dental floss in these teeth for 3 days (72 h).

On the day of collection, after at least 2 h of last food intake and tooth brushing the supra-gingival biofilms were collected with sterile metal curettes (Mc Call 17-18, Golgran-Instrumentos Odontológicos, São Caetano do Sul, São Paulo, Brazil) and immersed in culture medium (1 mL) corresponding to the group tested (BHI, mFUM or TSB medium). After this procedure, the same volunteers provided saliva obtained by stimulation with plastic film. The microbiological inoculum (oral biofilm and human saliva) were stored in ice (-4 ºC) and used immediately after collection. Bacterial inoculum and culture media was tested growing biofilms considering a aerobic and

anaerobic conditions, as mentioned on our microcosm biofilm model. Tests were performed in triplicate and the results obtained can be visualized in Fig. S1.

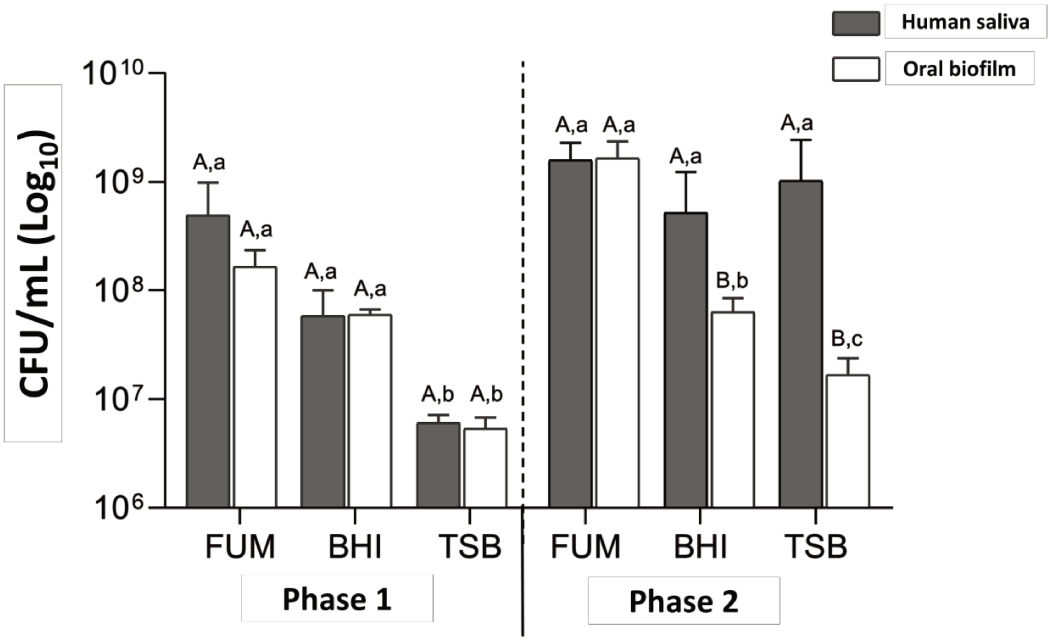

Figure S1. CFU/mL (Log10) of microscom biofilms formed using human saliva and human supragingival biofilm formed on the Ti surface. Incubation conditions (microaerophilia and anaerobiosis), culture media (mFUM, BHI and TSB), inoculum (saliva or biofilm) were evaluated. Different capital letters indicate statistical difference between bacterial inoculum with each culture medium ($p<0.05$, Tukey HSD test). Different lower-case letters indicate statistical difference between culture media with each type of bacterial inoculum ($p<0.05$, Tukey HSD test). The error bars indicate standard deviations.

REFERENCES

LIMA, Carolina V.; TENUTA, Livia M. A.; CURY, Jaime A. Fluoride Increase in Saliva and Dental Biofilm due to a Meal Prepared with Fluoridated Water or Salt: A Crossover Clinical Study. **Caries Research**, [s. l.], v. 53, n. 1, p. 41–48, 2019.

SOUZA, J. G. S. et al. Dose-Response Effect of Chlorhexidine on a Multispecies Oral Biofilm Formed on Pure Titanium and on a Titanium-Zirconium Alloy. **Biofouling**, v. 34, n. 10, p. 1175–1184, 2018.

THURNHEER, T.; BOSTANCI, N.; BELIBASAKIS, G. N. Microbial dynamics during conversion from supragingival to subgingival biofilms in an in vitro model. **Molecular Oral Microbiology**, [s. l.], v. 31, n. 2, p. 125–135, 2016.

3. DISCUSSÃO

Embora as reabilitações com implantes dentários apresentem altas taxas de sucesso (~80%), tanto em maxila como em mandíbula em pacientes saudáveis (Kern et al., 2018), a prevalência de mucosite peri-implantar e peri-implantite é de aproximadamente 47 e 20%, respectivamente (Derks; Tomasi, 2015; Lee et al., 2017). Em adição, problemas relacionados com falhas no processo de osseointegração podem contribuir para aumentar essas incidências nos primeiros meses após a instalação (CHRCANOVIC et al., 2016)(CHRCANOVIC *et al.*, 2016) ou potencializar os efeitos a longo prazo devido ao maior acúmulo de microrganismos e aumento da patogenicidade e virulência do biofilme peri-implantar (DERKS; TOMASI, 2015; LEE et al., 2017) Para tanto, neste estudo propusermos de forma inédita duas novas abordagens visando o aprimoramento da bioatividade do Ti e o controle do biofilme peri-implantar.

Evidências experimentais do primeiro estudo mostraram que o PEO pode ser indicado como uma nova via para síntese de revestimento a base de vidros bioativos para superfície do Ti, superando as limitações dos métodos até então utilizados com esta finalidade, tais como: baixa adesão ao revestimento, perdas das propriedades biológica pela cristalização do vidro e a ausência de efeito anti-microbiano. O recém-desenvolvido revestimento PEO-BG foi caracterizado como de complexa estrutura topográfica, super-hidrofílico, cristalino (fases anatase e rutilo) e com composição química e da camada de óxido semelhante ao 45S5-bioglass. Estas propriedades mostraram melhorar, principalmente, o comportamento mecânico, tribológico e as respostas biológicas do Ti quando comparado com superfícies usinadas e SLA. Adicionalmente, PEO-BG demonstrou também ser capaz de modular a formação do biofilme peri-implantar, reduzindo o

crescimento de patógenos periodontais e, consequentemente, a patogenicidade do biofilme. Portanto, considerado também o potencial osteogênico do 45S5-bioglass ainda não testado neste trabalho, novos estudos devem ser conduzidos para avaliar o efeito deste novo revestimentos nos processos relacionados com a cinética de neoformação e biomineração do tecido ósseo.

Considerando também o impacto de infecções peri-implantares no sucesso e sobrevida de reabilitações com implantes dentários, o segundo estudo foi conduzido visando entender o papel da ME do biofilme e os efeitos da sua degradação na manutenção dos implantes dentários. Pela primeira vez, foi comprovado que a ME do biofilme pode favorecer uma disbiose microbiológica de biofilmes orais formados em material de Ti, criando um ambiente adequado para o crescimento de patógenos anaeróbicos relacionados com a peri-implantite. Além disso, também foi evidenciado que ME reduz a susceptibilidade antimicrobiana de biofilmes na superfície do Ti quando tratada com clorexidina ou uma combinação antibiótica de amoxicilina e metronidazol.

Diante destes resultados, uma nova abordagem terapêutica combinada, que interrompeu a ME do biofilme anteriormente ao tratamento antimicrobiano, conseguiu reduzir os microrganismos vivos. Para extrapolar estes dados para uma condição clínica, um biofilme formados em modelo de transição microbiológica neste estudo foi exposto a associação antimicrobianos sistêmicos com concentrações basais simulando a liberação do fluido crevicular e um possível tratamento tópico diário com agente desregulador da matriz, como o iodopovidona foi testado. Interessantemente, essa nova abordagem terapêutica demonstrou potencializar a eficácia antimicrobiana em biofilmes orais.

Mesmo diante de algumas limitações por se tratar de um estudo inicial *in vitro,* este trabalho lança um novo caminho possível a ser investigado para o manejo da peri-implantite. Portanto, novos estudos utilizando modelos animais devem ser conduzidos para confirmar os efeitos em condições orais, avaliando a citotoxicidade, biodisponibilidade e estabelecendo protocolos de tratamento. Além disso, implantes com tratamentos de superfície devem ser utilizados em estudos futuros para comprovar o efeito desta terapia, uma vez que sabe-se do papel das propriedades de superfície também na adesão e formação dos biofilmes orais (Bowen et al., 2018; Soares et al., 2018; Song; Koo; Ren, 2015), como confirmados também no primeiro estudo desta dissertação.

Em suma, as novas abordagens terapêuticas investigadas neste trabalho de dissertação, apesar de avaliadas independentes, foram idealizadas visando superar as limitações de problemas corriqueiramente relatados na prática clínica da área da implantodontia, que impactam diretamente na qualidade dos tratamentos e na sobrevida dos implantes dentários.

4. CONCLUSÃO

Considerando as características necessárias para o sucesso de um revestimento experimental para implantes dentários, o tratamento de superfície PEO-BG pode ser considerado uma nova alternativa promissora no campo da implantodontia. Propriedades de superfície anteriormente limitadas em revestimentos baseados em vidros bioativos no Ti foram aprimoradas pelo tratamento com PEO, como a adesão e resistência ao desgaste dos revestimentos, bem como, proporcionou o controle do biofilme oral sem apresentar efeito citotóxico em células humanas como um importante fator inerente a este revestimento.

Além disso, identificou-se que similarmente a outras superfícies abiótica, a matriz extracelular do biofilme favorece a disbiose e aumenta a virulência do biofilme desenvolvido na superfície do Ti. Além disso, com base na natureza polimicrobina e na complexa estrutura dos biofilmes peri-implantares, a recente estratégia terapêutica testada para desestruturar a matriz demonstrou resultados satisfatórios no controle de biofilmes proporcionando aumento da eficácia de antimicrobianos de uso tópico (clorexidina) e sistêmicos (amoxicilina e metronidazol).

REFERÊNCIAS*

ABUSHAHBA, F. et al. Air-Abrasion with Bioactive Glass Eradicates S. Mutans Biofilm from Sandblasted and Acid Etched Titanium Surface. The Journal of Oral Implantology, 19 set. 2019.

AL-HASHEDI, A. A. et al. Clinical Oral Implants Research, v. 28, n. 8, p. 1013–1021, ago. 2017.

ARCIOLA, C. R.; CAMPOCCIA, D.; MONTANARO, L. Implant Infections: Adhesion, Biofilm Formation and Immune Evasion. Nature Reviews Microbiology, v. 16, n. 7, p. 397–409, jul. 2018.

ASIF, I. M. et al. In Vitro Bioactivity of Titanium-Doped Bioglass. Journal of Materials Science. Materials in Medicine, v. 25, n. 8, p. 1865–1873, ago. 2014.

BAINO, F.; HAMZEHLOU, S.; KARGOZAR, S. Bioactive Glasses: Where Are We and Where Are We Going? Journal of Functional Biomaterials, v. 9, n. 1, 19 mar. 2018.

BAKKER, M. H. et al. Mandibular Implant-Supported Overdentures in (Frail) Elderly: A Prospective Study with 20-Year Follow-Up. Clinical Implant Dentistry and Related Research, v. 21, n. 4, p. 586–592, ago. 2019.

BARÃO, V. A. R. et al. Stability of Cp-Ti and Ti-6Al-4V Alloy for Dental Implants as a Function of Saliva PH – an Electrochemical Study. Clinical Oral Implants Research, v. 23, n. 9, p. 1055–1062, 2012.

BARROS, S. A. de L. et al. Influence of Zirconia-Coated Bioactive Glass on Gingival Fibroblast Behavior. Brazilian Dental Journal, v. 30, n. 4, p. 333–341, jul. 2019.

BELINE, T. et al. Production of a Biofunctional Titanium Surface Using Plasma Electrolytic Oxidation and Glow-Discharge Plasma for Biomedical Applications. Biointerphases, v. 11, n. 1, p. 011013, 16 mar. 2016.

BELINE, T. et al. Tailoring the Synthesis of Tantalum-Based Thin Films for Biomedical Application: Characterization and Biological Response. Materials Science & Engineering. C, Materials for Biological Applications, v. 101, p. 111–119, ago. 2019.

BOWEN, W. H. et al. Oral Biofilms: Pathogens, Matrix, and Polymicrobial Interactions in Microenvironments. Trends in Microbiology, v. 26, n. 3, p. 229–242, 2018.

BOWEN, W. H.; KOO, H. Biology of Streptococcus Mutans-Derived Glucosyltransferases: Role in Extracellular Matrix Formation of Cariogenic Biofilms. Caries Research, v. 45, n. 1, p. 69–86, 2011.

* De acordo com as normas da UNICAMP/FOP, baseadas na padronização do International Committee of Medical Journal Editors - Vancouver Group. Abreviatura dos periódicos em conformidade com o PubMed.

BRÅNEMARK, P. I. et al. Osseointegrated Titanium Fixtures in the Treatment of Edentulousness. Biomaterials, v. 4, n. 1, p. 25–28, jan. 1983.

CARDOSO, R. G. et al. Impact of Mandibular Conventional Denture and Overdenture on Quality of Life and Masticatory Efficiency. Brazilian Oral Research, v. 30, n. 1, p. e102, 10 out. 2016.

CHEN, J. et al. Immediate versus Early or Conventional Loading Dental Implants with Fixed Prostheses: A Systematic Review and Meta-Analysis of Randomized Controlled Clinical Trials. The Journal of Prosthetic Dentistry, v. 122, n. 6, p. 516–536, dez. 2019.

CHIAPASCO, M.; GATTI, C. Implant-Retained Mandibular Overdentures with Immediate Loading: A 3- to 8-Year Prospective Study on 328 Implants. Clinical Implant Dentistry and Related Research, v. 5, n. 1, p. 29–38, 2003.

CHRCANOVIC, B. R. et al. Factors Influencing Early Dental Implant Failures. Journal of Dental Research, v. 95, n. 9, p. 995–1002, 2016.

CORDEIRO, J. M. et al. Synthesis of Biofunctional Coating for a TiZr Alloy: Surface, Electrochemical, and Biological Characterizations. Applied Surface Science, v. 452, p. 268–278, 15 set. 2018.

CORDEIRO, J. M.; BARÃO, V. A. R. Is There Scientific Evidence Favoring the Substitution of Commercially Pure Titanium with Titanium Alloys for the Manufacture of Dental Implants? Materials Science & Engineering. C, Materials for Biological Applications, v. 71, p. 1201–1215, 1 fev. 2017.

COSTA OLIVEIRA, B. E.; CURY, J. A.; RICOMINI FILHO, A. P. Biofilm Extracellular Polysaccharides Degradation during Starvation and Enamel Demineralization. PloS One, v. 12, n. 7, p. e0181168, 2017.

DERKS, J.; TOMASI, C. Peri-Implant Health and Disease. A Systematic Review of Current Epidemiology. Journal of Clinical Periodontology, v. 42 Suppl 16, p. S158-171, abr. 2015.

DOSTIE, S. et al. Chemotherapeutic Decontamination of Dental Implants Colonized by Mature Multispecies Oral Biofilm. Journal of Clinical Periodontology, v. 44, n. 4, p. 403–409, abr. 2017.

ESPOSITO, M.; GRUSOVIN, M. G.; WORTHINGTON, H. V. Interventions for Replacing Missing Teeth: Treatment of Peri-Implantitis. The Cochrane Database of Systematic Reviews, v. 1, p. CD004970, 18 jan. 2012.

FLEMMING, H.-C.; WINGENDER, J. The Biofilm Matrix. Nature Reviews. Microbiology, v. 8, n. 9, p. 623–633, set. 2010.

GALLARDO, Y. N. R. et al. A Systematic Review of Clinical Outcomes on Patients Rehabilitated with Complete-Arch Fixed Implant-Supported Prostheses According to the

Time of Loading. Journal of Prosthodontics: Official Journal of the American College of Prosthodontists, 21 ago. 2019.

GRAZIANI, F.; FIGUERO, E.; HERRERA, D. Systematic Review of Quality of Reporting, Outcome Measurements and Methods to Study Efficacy of Preventive and Therapeutic Approaches to Peri-Implant Diseases. Journal of Clinical Periodontology, v. 39 Suppl 12, p. 224–244, fev. 2012.

HENCH, L. L. The Story of Bioglass. Journal of Materials Science. Materials in Medicine, v. 17, n. 11, p. 967–978, nov. 2006.

HU, M.-L. et al. Comparison of Technical, Biological, and Esthetic Parameters of Ceramic and Metal-Ceramic Implant-Supported Fixed Dental Prostheses: A Systematic Review and Meta-Analysis. The Journal of Prosthetic Dentistry, 18 nov. 2019.

HWANG, G. et al. Nonleachable Imidazolium-Incorporated Composite for Disruption of Bacterial Clustering, Exopolysaccharide-Matrix Assembly, and Enhanced Biofilm Removal. ACS Applied Materials & Interfaces, v. 9, n. 44, p. 38270–38280, 8 nov. 2017.

JAWAD, S. et al. A Pilot Randomised Controlled Trial Evaluating Mini and Conventional Implant Retained Dentures on the Function and Quality of Life of Patients with an Edentulous Mandible. BMC oral health, v. 17, n. 1, p. 53, 15 fev. 2017.

JONES, J. R. Reprint of: Review of Bioactive Glass: From Hench to Hybrids. Acta Biomaterialia, v. 23 Suppl, p. S53-82, set. 2015.

KERN, M. et al. Survival and Complications of Single Dental Implants in the Edentulous Mandible Following Immediate or Delayed Loading: A Randomized Controlled Clinical Trial. Journal of Dental Research, v. 97, n. 2, p. 163–170, 2018.

KIM, D. et al. Bacterial-Derived Exopolysaccharides Enhance Antifungal Drug Tolerance in a Cross-Kingdom Oral Biofilm. The ISME journal, v. 12, n. 6, p. 1427–1442, 2018.

KLEIN, M. I. et al. Streptococcus Mutans-Derived Extracellular Matrix in Cariogenic Oral Biofilms. Frontiers in Cellular and Infection Microbiology, v. 5, p. 10, 2015.

KOO, H. et al. Targeting Microbial Biofilms: Current and Prospective Therapeutic Strategies. Nature Reviews. Microbiology, v. 15, n. 12, p. 740–755, dez. 2017.

KOO, H.; FALSETTA, M. L.; KLEIN, M. I. The Exopolysaccharide Matrix. Journal of Dental Research, v. 92, n. 12, p. 1065–1073, dez. 2013.

KOO, H.; YAMADA, K. M. Dynamic Cell-Matrix Interactions Modulate Microbial Biofilm and Tissue 3D Microenvironments. Current Opinion in Cell Biology, v. 42, p. 102–112, 2016.

LAM VO, T. et al. Masticatory Function and Bite Force of Mandibular Single-Implant Overdentures and Complete Dentures: A Randomized Crossover Control Study. Journal of Prosthodontic Research, v. 63, n. 4, p. 428–433, out. 2019.

LEE, C.-T. et al. Prevalences of Peri-Implantitis and Peri-Implant Mucositis: Systematic Review and Meta-Analysis. Journal of Dentistry, v. 62, p. 1–12, jul. 2017.

LOUROPOULOU, A.; SLOT, D. E.; VAN DER WEIJDEN, F. The Effects of Mechanical Instruments on Contaminated Titanium Dental Implant Surfaces: A Systematic Review. Clinical Oral Implants Research, v. 25, n. 10, p. 1149–1160, out. 2014.

MARQUES, I. da S. V. et al. Biomimetic Coatings Enhance Tribocorrosion Behavior and Cell Responses of Commercially Pure Titanium Surfaces. Biointerphases, v. 11, n. 3, p. 031008, 11 2016.

MARRA, R. et al. Rehabilitation of Full-Mouth Edentulism: Immediate Loading of Implants Inserted With Computer-Guided Flapless Surgery Versus Conventional Dentures: A 5-Year Multicenter Retrospective Analysis and OHIP Questionnaire. Implant Dentistry, v. 26, n. 1, p. 54–58, fev. 2017.

MARSH, P. D.; DEVINE, D. A. How Is the Development of Dental Biofilms Influenced by the Host? Journal of Clinical Periodontology, v. 38 Suppl 11, p. 28–35, mar. 2011.

MATHEW, M. T. et al. Influence of PH on the Tribocorrosion Behavior of CpTi in the Oral Environment: Synergistic Interactions of Wear and Corrosion. Journal of Biomedical Materials Research. Part B, Applied Biomaterials, v. 100, n. 6, p. 1662–1671, ago. 2012.

MATOS, A. O. et al. Three-Species Biofilm Model onto Plasma-Treated Titanium Implant Surface. Colloids and Surfaces. B, Biointerfaces, v. 152, p. 354–366, 1 abr. 2017.

MISHRA, S. K.; CHOWDHARY, R. Patient's Oral Health-Related Quality of Life and Satisfaction with Implant Supported Overdentures -a Systematic Review. Journal of Oral Biology and Craniofacial Research, v. 9, n. 4, p. 340–346, dez. 2019.

MOMBELLI, A.; DÉCAILLET, F. The Characteristics of Biofilms in Peri-Implant Disease. Journal of Clinical Periodontology, v. 38 Suppl 11, p. 203–213, mar. 2011.

NAGAY, B. E. et al. Visible-Light-Induced Photocatalytic and Antibacterial Activity of TiO2 Codoped with Nitrogen and Bismuth: New Perspectives to Control Implant-Biofilm-Related Diseases. ACS applied materials & interfaces, v. 11, n. 20, p. 18186–18202, 22 maio 2019.

NICOLAU, P. et al. 10-Year Outcomes with Immediate and Early Loaded Implants with a Chemically Modified SLA Surface. Quintessence International (Berlin, Germany: 1985), v. 50, n. 2, p. 114–124, 25 2019.

PANTAROTO, H. N. et al. Antibacterial Photocatalytic Activity of Different Crystalline TiO2 Phases in Oral Multispecies Biofilm. Dental Materials: Official Publication of the Academy of Dental Materials, v. 34, n. 7, p. e182–e195, 2018.

POPA, A. C. et al. Superior Biofunctionality of Dental Implant Fixtures Uniformly Coated with Durable Bioglass Films by Magnetron Sputtering. Journal of the Mechanical Behavior of Biomedical Materials, v. 51, p. 313–327, 1 nov. 2015.

REN, Z. et al. Dual-Targeting Approach Degrades Biofilm Matrix and Enhances Bacterial Killing. Journal of Dental Research, v. 98, n. 3, p. 322–330, mar. 2019.

RIZWAN, M. et al. Surface Modification of Valve Metals Using Plasma Electrolytic Oxidation for Antibacterial Applications: A Review. Journal of Biomedical Materials Research. Part A, v. 106, n. 2, p. 590–605, 2018.

ROHR, N. et al. Influence of Bioactive Glass-Coating of Zirconia Implant Surfaces on Human Osteoblast Behavior in Vitro. Dental Materials: Official Publication of the Academy of Dental Materials, v. 35, n. 6, p. 862–870, jun. 2019.

SANTOS-COQUILLAT, A. et al. Bioactive Multi-Elemental PEO-Coatings on Titanium for Dental Implant Applications. Materials Science and Engineering: C, v. 97, p. 738–752, 1 abr. 2019.

SHI, X. et al. Improved osseointegration of long-term stored SLA implant by hydrothermal sterilization. Journal of the Mechanical Behavior of Biomedical Materials, v. 53, p. 312–319, 2016.

SOARES, P. B. F. et al. Effect of Titanium Surface Functionalization with Bioactive Glass on Osseointegration: An Experimental Study in Dogs. Clinical Oral Implants Research, 28 set. 2018.

SONG, F.; KOO, H.; REN, D. Effects of Material Properties on Bacterial Adhesion and Biofilm Formation. Journal of Dental Research, v. 94, n. 8, p. 1027–1034, ago. 2015.

SPRIANO, S. et al. A Critical Review of Multifunctional Titanium Surfaces: New Frontiers for Improving Osseointegration and Host Response, Avoiding Bacteria Contamination. Acta Biomaterialia, v. 79, p. 1–22, 1 out. 2018.

WELDRICK, P. J.; HARDMAN, M. J.; PAUNOV, V. N. Enhanced Clearing of Wound-Related Pathogenic Bacterial Biofilms Using Protease-Functionalized Antibiotic Nanocarriers. ACS applied materials & interfaces, 13 nov. 2019.

XUE, B. et al. Electrophoretic Deposition and Laser Cladding of Bioglass Coating on Ti. Journal of Alloys and Compounds, v. 710, p. 663–669, 5 jul. 2017.

ANEXOS

ANEXO 1: Verificação de originalidade e prevenção de plágio

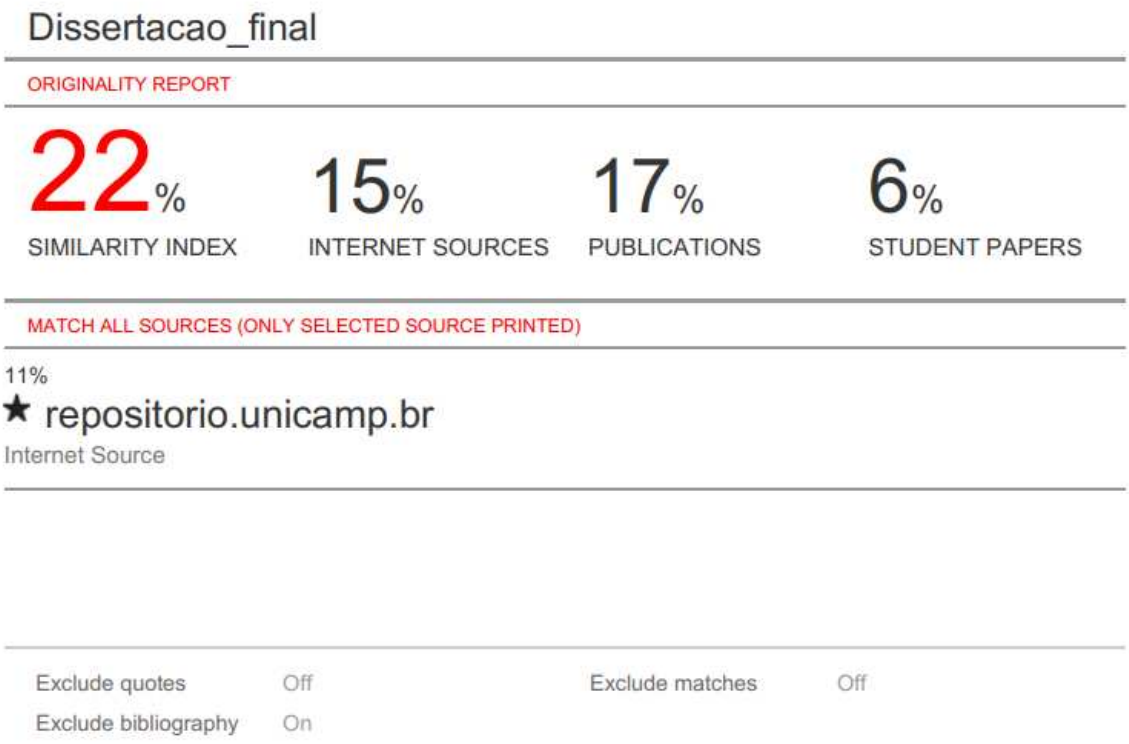

Dissertacao_final

ORIGINALITY REPORT

22%	15%	17%	6%
SIMILARITY INDEX	INTERNET SOURCES	PUBLICATIONS	STUDENT PAPERS

MATCH ALL SOURCES (ONLY SELECTED SOURCE PRINTED)

11%

★ repositorio.unicamp.br

Internet Source

Exclude quotes	Off	Exclude matches	Off
Exclude bibliography	On		

ANEXO 2: Certificado do Comitê de Ética em Pesquisa

UNICAMP - FACULDADE DE ODONTOLOGIA DE PIRACICABA DA

PARECER CONSUBSTANCIADO DO CEP

DADOS DO PROJETO DE PESQUISA

Título da Pesquisa: Síntese de filme de vidro bioativo para superfície de titânio por meio de plasma eletrolítico de oxidação: Análise eletroquímica e antimicrobiana em modelo de microcosmos

Pesquisador: Raphael Cavalcante Costa

Área Temática:

Versão: 2

CAAE: 86638918.0.0000.5418

Instituição Proponente: Faculdade de Odontologia de Piracicaba - Unicamp

Patrocinador Principal: Financiamento Próprio

DADOS DO PARECER

Número do Parecer: 2.632.919

Apresentação do Projeto:

Transcrição editada do conteúdo do registro do protocolo e dos arquivos anexados à Plataforma Brasil

Delineamento da pesquisa: Trata-se de estudo laboratorial, in vitro, que utilizará amostras de saliva de 5 participantes, com idades de 18 anos ou mais, saudáveis, que passarão pela coleta de saliva total estimulada em jejum de 90 minutos, durante três dias. Discos de Ticp (10 × 2mm) serão utilizados: usinado (grupo controle) e tratado com Bioglass45S5® (grupo experimental). A topografia dos discos será caracterizada por meio da microscopia de força atômica (MFA), microscopia eletrônica de varredura (MEV), perfilometria e energia livre de superfície. A composição e fase dos óxidos formados na superfície serão avaliadas por meio da espectroscopia de energia dispersiva (EDS), espectroscopia de fotoelétrons excitados por raios X (XPS) e da difração de raios-x (DRX). Para analisar o comportamento corrosivo do Ticp, testes eletroquímicos serão conduzidos (potencial de circuito aberto, espectroscopia de impedância eletroquímica e teste potenciodinâmico). O efeito do tratamento na adesão bacteriana e formação de biofilme na superfície será testado utilizando modelo de biofilme multi-espécies de microcosmos, tendo a saliva humana de 5 voluntários como inóculo bacteriano. Na análise quantitativa dos dados microbiológicos será avaliado o pH do biofilme e os níveis e proporções de 40 espécies bacterianas pela técnica de checkerboard DNA- DNA hybridization. MEV e microscopia confocal

Endereço: Av.Limeira 901 Caixa Postal 52
Bairro: Areião **CEP:** 13.414-903
UF: SP **Município:** PIRACICABA
Telefone: (19)2106-5349 **Fax:** (19)2106-5349 **E-mail:** cep@fop.unicamp.br

ANEXO 2: Certificado do Comitê de Ética em Pesquisa

UNICAMP - FACULDADE DE ODONTOLOGIA DE PIRACICABA DA

Continuação do Parecer: 2.632.919

Folha de Rosto	1Folhaderosto.pdf	28/03/2018 11:14:30	Raphael Cavalcante Costa	Aceito

Situação do Parecer:
Aprovado

Necessita Apreciação da CONEP:
Não

PIRACICABA, 03 de Maio de 2018

Assinado por:
jacks jorge junior
(Coordenador)

Endereço: Av.Limeira 901 Caixa Postal 52
Bairro: Areião **CEP:** 13.414-903
UF: SP **Município:** PIRACICABA
Telefone: (19)2106-5349 **Fax:** (19)2106-5349 **E-mail:** cep@fop.unicamp.br

ANEXO 3: Comprovante de submissão do artigo científico

Molecular Oral Microbiology - Manuscript ID MOM-02-20-1145 [email ref: SE-6-a]

Dear Professor Barao:

Your manuscript entitled "Extracellular biofilm matrix leads to microbial dysbiosis and reduces biofilm susceptibility to antimicrobials on titanium biomaterial" by Costa, Raphael; Souza, João Gabriel; Bertolini, Martinna; Retamal-Valdes, Belén ; Feres, Magda; Barao, Valentim, has been successfully submitted online and is presently being given full consideration for publication in Molecular Oral Microbiology.

Co-authors: Please contact the Editorial Office as soon as possible if you disagree with being listed as a co-author for this manuscript.

Your manuscript ID is MOM-02-20-1145.

Please mention the above manuscript ID in all future correspondence or when calling the office for questions. If there are any changes in your street address or e-mail address, please log in to ScholarOne Manuscripts at https://mc.manuscriptcentral.com/mom and edit your user information as appropriate.

You can also view the status of your manuscript at any time by checking your Author Center after logging in to https://mc.manuscriptcentral.com/mom.

Thank you for submitting your manuscript to Molecular Oral Microbiology.

Sincerely,
Molecular Oral Microbiology Editorial Office